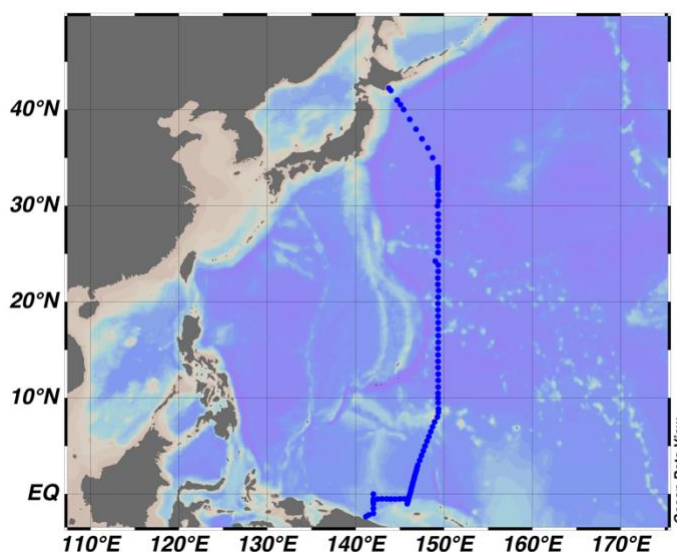


CRUISE REPORT: RF14-05, RF14-06, RF14-07

Created: January 2025



Highlights

Cruise Summary Information

Section Designation	P10
Expedition Designation (ExpoCode)	49UP20140609
Chief Scientist	RF14-05, RF14-06: Kazuhiro NEMOTO (JMA) RF14-07: Takahiro SEGAWA (JMA)
Dates	RF14-05: 9 June – 29 June 2014 RF14-06: 3 July – 21 July 2014 RF14-07: Leg 1: 28 July – 19 August 2014 Leg 2: 23 August – 16 September 2014
Ship	R/V Ryofu Maru
Ports of Call	RF14-05: Tokyo, JP – Tokyo, JP RF14-06: Tokyo, JP – Tokyo, JP RF14-07: Leg 1: Tokyo, JP – Pohnpei, JP Leg 2: Pohnpei, JP – Tokyo, JP
Geographic Boundaries	42° 25'N 141° 15'E 149° 38'E 2° 34'S
Stations	99
Floats and Drifters Deployed	RF14-05: 3 floats and 1 drifter RF14-07: 2 floats and 1 drifter
Moorings Deployed and Recovered	0

Contact Information:

Kazuhiro NEMOTO and Takahiro SEGAWA

Marine Division • Global Environment and Marine Department • Japan Meteorological Agency

Phone: +81-3-3212-8341, Ext. 5128, 4764

Email: k-nemoto@met.kishou.go.jp or tsegawa@met.kishou.go.jp

Contents:

A. Cruise narrative

B. Underway measurements

5. *Underway Chlorophyll-a*

C. Hydrographic Measurement Techniques and Calibration

1. *CTD/O₂ Measurements*

2. *Bottle Salinity*

3. *Bottle Oxygen*

4. *Nutrients*

5. *Phytopigment (Chlorophyll-a and phaeopigments)*

6. *Total Dissolved Inorganic Carbon (DIC)*

7. *Total Alkalinity (TA)*

8. *pH*

A. Cruise narrative

1. Highlights

Cruise designation: RF14-05, RF14-06 and RF14-07 (WHP-P10 revisit)

- a. EXPOCODE: 49UP20140609
- b. Chief scientist: RF14-05 Kazuhiro NEMOTO (k-nemoto@met.kishou.go.jp)
RF14-06 Kazuhiro NEMOTO (k-nemoto@met.kishou.go.jp)
RF14-07 Takahiro SEGAWA (tsegawa@met.kishou.go.jp)
Marine Division
Global Environment and Marine Department
Japan Meteorological Agency (JMA)
1-3-4, Otemachi, Chiyoda-ku, Tokyo 100-8122, JAPAN
Phone: +81-3-3212-8341 Ext. 5128, 4764
- c. Ship name: R/V Ryofu Maru
- d. Ports of call: RF14-05 : Tokyo–Tokyo
RF14-06 : Tokyo–Tokyo
RF14-07 Leg 1: Tokyo–Pohnpei
Leg 2: Pohnpei–Tokyo
- e. Cruise dates: RF14-05 : 9 June 2014–29 June 2014
RF14-06 : 3 July 2014–21 July 2014
RF14-07 Leg 1: 28 July 2014–19 August 2014
Leg 2: 23 August 2014–16 September 2014
- f. Floats and drifters deployed: RF14-05: 3 floats and 1 drifter
RF14-07: 2 floats and 1 drifter

1. Cruise Summary Information

RF14-05, RF14-06 and RF14-07 cruises were carried out during the period from June 9 to September 16, 2014. The observation line along approximately 149°E meridian was observed by Japan Agency for Marine-Earth Science and Technology (JAMSTEC), Japan in 2005, 2011 and 2012. These cruises were carried out as ‘WHP-P10’, which is a part of WOCE (World Ocean Circulation Experiment) Hydrographic Programme, CLIVAR (Climate Variability and Predictability Project) and GO-SHIP (Global Ocean Ship-based Hydrographic Investigations Program).

The stations from Stn.1 (34°00’N, 149°18’E; RF5113) to Stn.18 (42°15’N, 143°44’E; RF5130) for RF14-05 cruise, from Stn.20 (34°02’N, 149°20’E; RF5145) to Stn.44 (20°30’N, 149°20’E; RF5169) for RF14-06 cruise and from Stn.45 (20°30’N, 149°20’E; RF5171) to Stn.111 (2°20’S, 141°09’E; RF5236) for RF14-07 cruise had been designed.

A total of 111 stations was occupied using a Sea-Bird Electronics (SBE) 36 position carousel equipped with 10-liter Niskin water sample bottles, a CTD system (SBE911plus) equipped with SBE35 deep ocean standards thermometer, JFE Advantech oxygen sensor (RINKO III), Teledyne Benthos altimeter (PSA-916D), and Teledyne RD Instruments L-ADCP (300kHz). Cruise track and station location are shown in Figure 1.

At each station, full-depth CTDO₂ (temperature, conductivity (salinity) and dissolved oxygen) profile and up to 36 water samples were taken and analyzed. Water samples were obtained from 10 dbar to approximately 10 m above the bottom. In addition, surface water was sampled using a stainless steel bucket at each station. Sampling layer is designed as so-called staggered mesh as shown in Table 1 (*Swift*, 2010). The bottle depth diagram is shown in Figure 2.

Water samples were analyzed for salinity, dissolved oxygen, nutrients, dissolved inorganic carbon (DIC), total alkalinity (TA), pH, CFC-11, CFC-12 and phytopigment (chlorophyll-a and phaeopigments). Underway measurements of partial pressure of carbon dioxide (*p*CO₂), temperature, salinity, chlorophyll-a, subsurface current, bathymetry and meteorological parameters were conducted along the cruise track.

RF14-05

RF14-05 cruise was carried out during the period from June 9 to June 29, 2014. Before the observation at the first station, all watch standers were drilled in the method of sample drawing and CTD operations near Izu-Oshima (34°42’N, 139°50’E). The cruise started from Stn.19 (34°00’N, 149°18’E; RF5113) on June 12 and sailed northward to Stn.1 (42°15’N, 143°44’E; RF5130) on June 18. We skipped the Stn.7 (40°02’N, 145°26’E; RF5135) that was cross 40°N. After observation of Stn.1, we observed twelve stations at the 40°N section. Stn.7 was done while observing along 40°N on June 19. RF14-05 cruise consisted of 19 stations at the WHP-P10 section.

Three Argo floats and one drifting ocean data buoy were deployed along the cruise track. The information of deployed the float and the buoy are listed in Table 2a.

RF14-06

RF14-06 cruise was carried out during the period from July 3 to July 16, 2014. Before the observation at the first station, all watch standers were drilled in the method of sample drawing and CTD operations at the point (34°27'N, 142°59'E). The hydrographic cast of CTDO₂ was started at the first station (Stn.20 (34°02'N, 149°20'E; RF5145)) that was the same location of Stn.19 on July 5, and sailed southward to Stn.44 (20°30'N, 149°20'E; RF5169) at July 13. After observed Stn.44 she sailed toward Tokyo. RF14-06 cruise consisted of 25 stations.

RF14-07

RF14-07 cruise was carried out during the period from July 28 to September 16, 2014. Before the observation at the first station, all watch standers were drilled in the method of sample drawing and CTD operations at the point (34°44'N, 139°50'E). The hydrographic cast of CTDO₂ was started at the first station (Stn.45 (20°30'N, 149°20'E; RF5171)) that was the same station of Stn.44 on August 1. Leg 1 consisted of 43 stations from Stn.45 to Stn.87 (0°01'S, 146°09'E; RF5213). Stn.87 was finished on July 23. She called for Pohnpei (Federated States of Micronesia) on August 19 (Leg 1). She left Pohnpei on August 23, 2014. The hydrographic cast of CTDO₂ was restarted at the station (Stn.88 (0°01'N, 146°08'E; RF5214)) that was the same station of Stn.87 on August 26. We sailed westward to Stn.101 (0°30'S, 142°00'E; RF5226) at August 30 and turned southward to Stn.111 (2°20'S, 141°09'E; RF5236) Stn.111 was finished on September 1. After observation of Stn.111 she sailed northward, we observed Stn.100 (0°00', 142°00'E; RF5237) on September 2, and observed other two stations (1°N and 2°N, 142°E). She arrived at Tokyo (Japan) on September 16, 2014 (Leg 2). Leg 2 consisted of 24 stations from Stn.88 to Stn.111 at the WHP-P10 section.

Two Argo floats and one drifting ocean data buoy were deployed along the cruise track. The information of deployed the float and the buoy are listed in Table 2b.

Location data of stations is shown in Table 3.

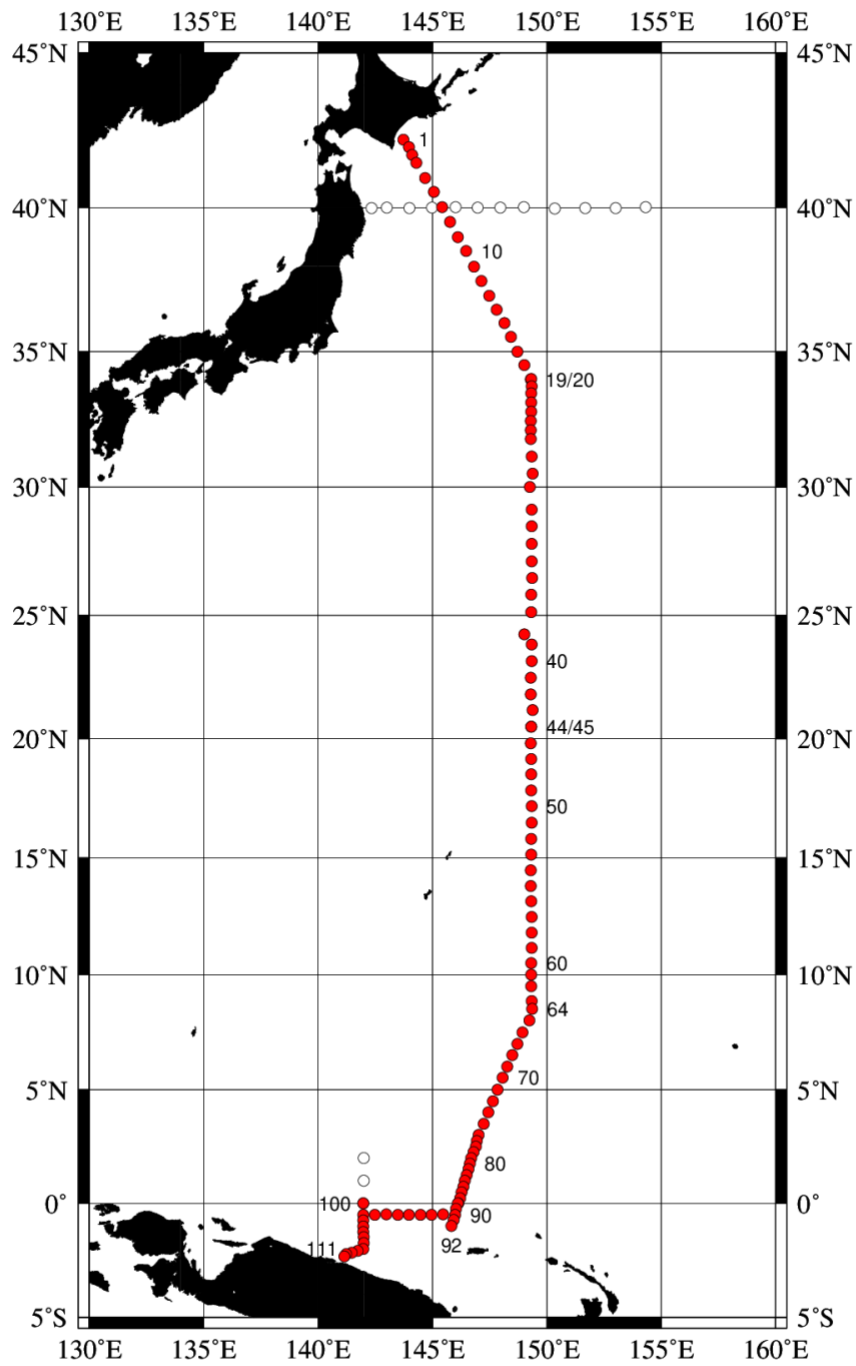


Figure 1. Cruise track of RF14-05, RF14-06 and RF14-07. Red closed circles indicate the observation stations at the WHP-P10 section. Open circles indicate the CTD stations of other section.

Bottle Depth Diagram along P10

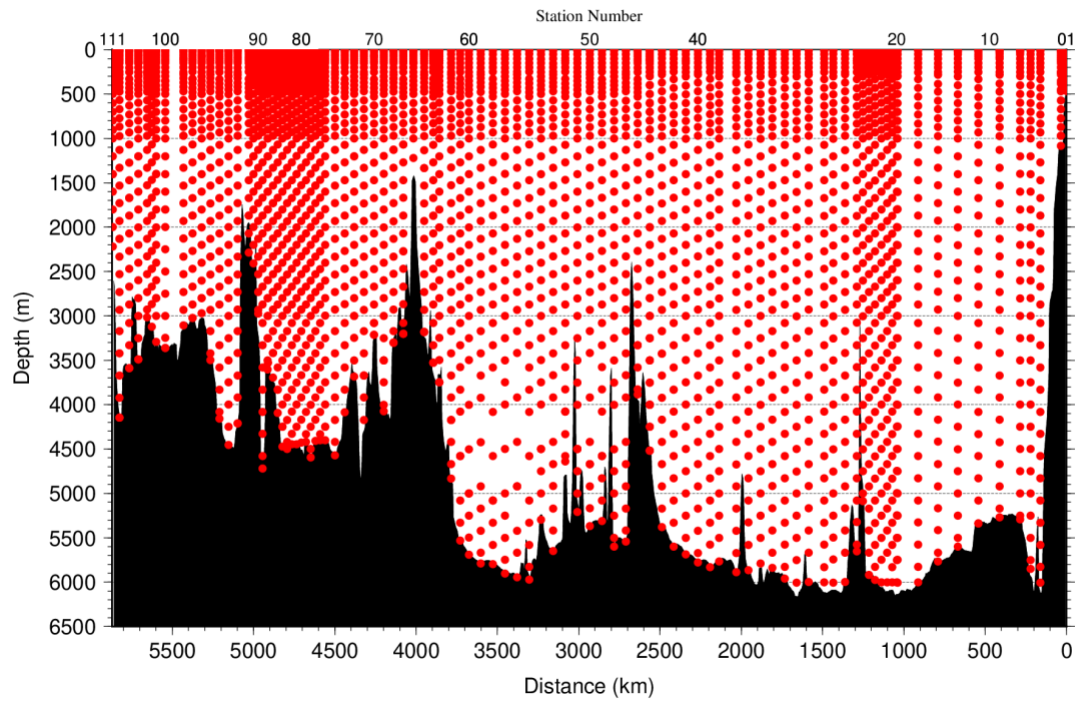


Figure 2. The bottle depth diagram for WHP-P10 revisit.

Table 1a. The scheme of sampling layer in meters (RF14-05).

<i>Bottle count</i>	<i>scheme1</i>	<i>scheme2</i>	<i>scheme3</i>
<i>1</i>	10	10	10
<i>2</i>	25	25	25
<i>3</i>	50	50	50
<i>4</i>	75	75	75
<i>5</i>	100	100	100
<i>6</i>	125	125	125
<i>7</i>	150	150	150
<i>8</i>	200	200	200
<i>9</i>	250	250	250
<i>10</i>	300	330	280
<i>11</i>	350	350	350
<i>12</i>	400	430	380
<i>13</i>	450	450	450
<i>14</i>	500	530	470
<i>15</i>	600	630	570
<i>16</i>	700	730	670
<i>17</i>	800	830	770
<i>18</i>	900	930	870
<i>19</i>	1000	1070	970
<i>20</i>	1200	1270	1130
<i>21</i>	1400	1470	1330
<i>22</i>	1600	1670	1530
<i>23</i>	1800	1870	1730
<i>24</i>	2000	2070	1930
<i>25</i>	2200	2270	2130
<i>26</i>	2400	2470	2330
<i>27</i>	2600	2670	2530
<i>28</i>	2800	2870	2730
<i>29</i>	3000	3080	2930
<i>30</i>	3250	3330	3170
<i>31</i>	3500	3580	3420
<i>32</i>	3750	3830	3670
<i>33</i>	4000	4080	3920
<i>34</i>	4250	4330	4170
<i>35</i>	4500	4580	4420
<i>36</i>	4750	4830	4670

<i>Bottle count</i>	<i>scheme1</i>	<i>scheme2</i>	<i>scheme3</i>
<i>37</i>	5000	5080	4920
<i>38</i>	5250	5330	5170
<i>39</i>	5500	5580	5420
<i>40</i>	5750	5830	5670
<i>41</i>	6000	6000	6000

Table 1b. The scheme of sampling layer in meters (RF14-06 and RF14-07).

<i>Bottle count</i>	North of 20°N (Stn.20–Stn.45)			South of 20°N (Stn.46–Stn.111)		
	<i>scheme1</i>	<i>scheme2</i>	<i>scheme3</i>	<i>scheme4</i>	<i>scheme5</i>	<i>scheme6</i>
<i>1</i>	10	10	10	10	10	10
<i>2</i>	25	25	25	25	25	25
<i>3</i>	50	50	50	50	50	50
<i>4</i>	75	75	75	75	75	75
<i>5</i>	100	100	100	100	100	100
<i>6</i>	125	125	125	125	125	125
<i>7</i>	150	150	150	150	150	150
<i>8</i>	200	200	200	200	200	200
<i>9</i>	250	250	250	250	250	250
<i>10</i>	300	330	280	300	330	280
<i>11</i>	400	430	370	350	380	320
<i>12</i>	500	530	470	400	430	370
<i>13</i>	600	630	570	450	480	420
<i>14</i>	700	730	670	500	530	470
<i>15</i>	800	830	770	600	630	570

<i>Bottle count</i>	North of 20°N (Stn.20–Stn.45)			South of 20°N (Stn.46–Stn.111)		
	<i>scheme1</i>	<i>scheme2</i>	<i>scheme3</i>	<i>scheme4</i>	<i>scheme5</i>	<i>scheme6</i>
<i>16</i>	900	930	870	700	730	670
<i>17</i>	1000	1070	970	800	830	770
<i>18</i>	1200	1270	1130	900	930	870
<i>19</i>	1400	1470	1330	1000	1070	970
<i>20</i>	1600	1670	1530	1200	1270	1130
<i>21</i>	1800	1870	1730	1400	1470	1330
<i>22</i>	2000	2070	1930	1600	1670	1530
<i>23</i>	2200	2270	2130	1800	1870	1730
<i>24</i>	2400	2470	2330	2000	2070	1930
<i>25</i>	2600	2670	2530	2200	2270	2130
<i>26</i>	2800	2870	2730	2400	2470	2330
<i>27</i>	3000	3080	2930	2600	2670	2530
<i>28</i>	3250	3330	3170	2800	2870	2730
<i>29</i>	3500	3580	3420	3000	3080	2930
<i>30</i>	3750	3830	3670	3250	3330	3170
<i>31</i>	4000	4080	3920	3500	3580	3420
<i>32</i>	4250	4330	4170	3750	3830	3670
<i>33</i>	4500	4580	4420	4000	4080	3920
<i>34</i>	4750	4830	4670	4250	4330	4170
<i>35</i>	5000	5080	4920	4500	4580	4420

Table 1. Continue.

<i>Bottle count</i>	North of 20°N (Stn.20–Stn.45)			South of 20°N (Stn.46–Stn.111)		
	<i>scheme1</i>	<i>scheme2</i>	<i>scheme3</i>	<i>scheme4</i>	<i>scheme5</i>	<i>scheme6</i>
<i>36</i>	5250	5330	5170	4750	4830	4670
<i>37</i>	5500	5580	5420	5000	5080	4920
<i>38</i>	5750	5830	5670	5250	5330	5170
<i>39</i>	6000	6000	6000	5500	5580	5420
<i>40</i>				5750	5830	5670
<i>41</i>				6000	6000	6000

Table 2a. Information of deployed float and buoy at RF14-05.

<i>Float</i>	<i>Date and Time (UTC)</i>	<i>Position of deployment</i>		<i>PI</i>	
<i>WMO number</i>	<i>of Deployment</i>	<i>Latitude</i>	<i>Longitude</i>		
2902517	2014 June 16 02:47	40-01.63 N	144-59.61 E	JMA	APEX
2902516	2014 June 19 04:23	40-01.04 N	145-25.52 E	JMA	APEX
2902522	2014 June 22 00:19	40-02.74 N	154-19.92 E	JAMSTEC	Navis
<i>Buoy</i>	<i>Date and Time (UTC)</i>	<i>Position of deployment</i>		<i>PI</i>	
<i>WMO number</i>	<i>of Deployment</i>	<i>Latitude</i>	<i>Longitude</i>		
21638	2014 June 15 23:40	39-29.37 N	145-47.08 E	JMA	YTSS-2100

APEX: Teledyne Webb Research (USA)

Navis: Sea-Bird Scientific (USA)

YTSS-2100: JVC KENWOOD Co., Japan

Table 2b. Information of deployed float and buoy at RF14-07.

<i>Float</i>	<i>Date and Time (UTC)</i>	<i>Position of deployment</i>		<i>PI</i>	
<i>WMO number</i>	<i>of Deployment</i>	<i>Latitude</i>	<i>Longitude</i>		
2902523	2014 July 30 08:00	27-31.02 N	147-09.21 E	JAMSTEC	Navis
2902524	2014 July 31 00:30	24-00.96 N	148-14.62 E	JAMSTEC	Navis
<i>Buoy</i>	<i>Date and Time (UTC)</i>	<i>Position of deployment</i>		<i>PI</i>	
<i>WMO number</i>	<i>of Deployment</i>	<i>Latitude</i>	<i>Longitude</i>		
21597	2014 Sep. 10 03:17	29-50.35 N	140-08.58 E	JMA	YTSS-2100

Navis: Sea-Bird Scientific (USA)

YTSS-2100: JVC KENWOOD Co., Japan

Table 3a. Station data of RF14-05 cruises. The ‘RF’ column indicates the JMA station identification number.

<i>Leg</i>	<i>Station</i>		<i>Position</i>	
	<i>Stn.</i>	<i>RF</i>	<i>Latitude</i>	<i>Longitude</i>
1	1	5130	42-15.03 N	143-44.19 E
1	2	5129	42-00.03 N	143-58.51 E
1	3	5128	41-45.02 N	144-07.93 E
1	4	5127	41-29.69 N	144-18.26 E
1	5	5126	40-59.64 N	144-41.77 E
1	6	5125	40-32.29 N	145-03.42 E
1	7	5135	40-01.67 N	145-25.68 E
1	8	5124	39-31.98 N	145-46.44 E
1	9	5123	39-00.87 N	146-06.67 E
1	10	5122	38-32.20 N	146-28.81 E
1	11	5121	37-59.37 N	146-49.48 E
1	12	5120	37-30.99 N	147-08.86 E
1	13	5119	36-59.01 N	147-29.97 E
1	14	5118	36-29.52 N	147-48.70 E
1	15	5117	36-01.89 N	148-09.81 E
1	16	5116	35-31.74 N	148-25.42 E
1	17	5115	35-00.94 N	148-42.14 E
1	18	5114	34-31.15 N	149-01.67 E
1	19	5113	34-00.14 N	149-17.68 E

Table 3b. Station data of RF14-06 cruises. The ‘RF’ column indicates the JMA station identification number.

<i>EXPOCODE</i>	<i>Leg</i>	<i>Station</i>		<i>Position</i>	
sub number		<i>Stn.</i>	<i>RF</i>	<i>Latitude</i>	<i>Longitude</i>
2	1	20	5145	34-01.66 N	149-19.74 E
2	1	21	5146	33-45.70 N	149-20.62 E
2	1	22	5147	33-29.03 N	149-19.89 E
2	1	23	5148	33-09.33 N	149-19.34 E
2	1	24	5149	32-49.02 N	149-19.83 E
2	1	25	5150	32-28.04 N	149-18.40 E
2	1	26	5151	32-08.21 N	149-17.57 E
2	1	27	5152	31-48.44 N	149-18.67 E
2	1	28	5153	31-09.38 N	149-20.39 E
2	1	29	5154	30-30.07 N	149-22.62 E
2	1	30	5155	30-00.27 N	149-15.18 E
2	1	31	5156	29-08.74 N	149-20.68 E
2	1	32	5157	28-29.22 N	149-20.52 E
2	1	33	5158	27-49.37 N	149-20.47 E
2	1	34	5159	27-08.57 N	149-20.13 E
2	1	35	5160	26-29.33 N	149-21.17 E
2	1	36	5161	25-49.11 N	149-19.49 E
2	1	37	5162	25-08.81 N	149-19.59 E
2	1	38	5163	24-14.83 N	149-00.98 E
2	1	39	5164	23-50.37 N	149-20.25 E
2	1	40	5165	23-10.17 N	149-20.10 E
2	1	41	5166	22-29.45 N	149-18.48 E
2	1	42	5167	21-49.24 N	149-17.72 E
2	1	43	5168	21-10.82 N	149-22.51 E
2	1	44	5169	20-30.37 N	149-19.65 E

Table 3c. Station data of RF14-07 cruises. The ‘RF’ column indicates the JMA station identification number.

<i>EXPOCODE</i>	<i>Leg</i>	<i>Station</i>		<i>Position</i>	
sub number		<i>Stn.</i>	<i>RF</i>	<i>Latitude</i>	<i>Longitude</i>
3	1	45	5171	20-30.10 N	149-19.69 E
3	1	46	5172	19-49.89 N	149-18.45 E
3	1	47	5173	19-10.43 N	149-19.32 E
3	1	48	5174	18-31.70 N	149-19.34 E
3	1	49	5175	17-51.28 N	149-19.77 E
3	1	50	5176	17-11.64 N	149-20.19 E
3	1	51	5177	16-30.13 N	149-20.46 E
3	1	52	5178	15-49.22 N	149-19.84 E
3	1	53	5179	15-09.66 N	149-19.25 E
3	1	54	5180	14-29.44 N	149-18.83 E
3	1	55	5181	13-49.67 N	149-18.58 E
3	1	56	5182	13-10.15 N	149-19.59 E
3	1	57	5183	12-29.53 N	149-20.33 E
3	1	58	5184	11-49.48 N	149-20.40 E
3	1	59	5185	11-09.20 N	149-20.46 E
3	1	60	5186	10-30.02 N	149-19.58 E
3	1	61	5187	10-00.72 N	149-19.33 E
3	1	62	5188	9-30.62 N	149-19.92 E
3	1	63	5189	8-51.10 N	149-20.91 E
3	1	64	5190	8-31.36 N	149-21.27 E
3	1	65	5191	8-01.84 N	149-14.63 E
3	1	66	5192	7-30.74 N	148-56.56 E
3	1	67	5193	7-00.56 N	148-42.74 E
3	1	68	5194	6-30.91 N	148-29.30 E
3	1	69	5195	6-00.53 N	148-16.54 E
3	1	70	5196	5-31.03 N	148-04.85 E
3	1	71	5197	4-59.79 N	147-51.09 E
3	1	72	5198	4-29.87 N	147-38.95 E
3	1	73	5199	4-00.49 N	147-26.65 E
3	1	74	5200	3-30.67 N	147-14.39 E
3	1	75	5201	3-00.93 N	147-01.28 E
3	1	76	5202	2-45.81 N	146-56.21 E
3	1	77	5203	2-30.55 N	146-53.13 E
3	1	78	5204	2-15.59 N	146-47.45 E

Table 3c. continue.

<i>EXPCODE</i>	<i>Leg</i>	<i>Station</i>		<i>Position</i>	
sub number		<i>Stn.</i>	<i>RF</i>	<i>Latitude</i>	<i>Longitude</i>
3	1	79	5205	2-00.31 N	146-42.47 E
3	1	80	5206	1-45.29 N	146-38.34 E
3	1	81	5207	1-30.57 N	146-34.26 E
3	1	82	5208	1-15.10 N	146-29.19 E
3	1	83	5209	1-00.30 N	146-25.47 E
3	1	84	5210	0-44.88 N	146-21.41 E
3	1	85	5211	0-30.18 N	146-16.15 E
3	1	86	5212	0-14.61 N	146-12.88 E
3	1	87	5213	0-00.72 S	146-08.78 E
4	2	88	5214	0-00.50 N	146-07.86 E
4	2	89	5215	0-14.93 S	146-02.90 E
4	2	90	5216	0-30.02 S	145-59.21 E
4	2	91	5217	0-44.96 S	145-55.30 E
4	2	92	5218	0-59.91 S	145-50.38 E
4	2	93	5219	0-29.85 S	145-28.77 E
4	2	94	5220	0-30.12 S	144-58.78 E
4	2	95	5221	0-30.37 S	144-28.85 E
4	2	96	5222	0-30.67 S	143-58.64 E
4	2	97	5223	0-30.24 S	143-29.52 E
4	2	98	5224	0-29.81 S	142-59.15 E
4	2	99	5225	0-30.76 S	142-29.23 E
4	2	100	5237	0-00.00 N	141-59.81 E
4	2	101	5226	0-30.38 S	141-59.69 E
4	2	102	5227	0-45.35 S	141-59.35 E
4	2	103	5228	1-00.25 S	141-59.90 E
4	2	104	5229	1-15.58 S	141-59.89 E
4	2	105	5230	1-29.96 S	142-00.33 E
4	2	106	5231	1-44.56 S	142-00.04 E
4	2	107	5232	2-00.23 S	141-59.58 E
4	2	108	5233	2-05.05 S	141-44.59 E
4	2	109	5234	2-10.14 S	141-28.66 E
4	2	110	5235	2-14.98 S	141-14.04 E
4	2	111	5236	2-20.34 S	141-09.17 E

List of Principal Investigators for all Measurements

The principal investigator (PI) and the person in charge responsible for major parameters measured on the cruise are listed in Table 4a (RF14-05), Table 4b (RF14-06) and Table 4c (RF14-07).

Table 4a. List of principal investigator and the person in charge on the ship for RF14-05.

Item	Principal Investigator (PI)	Person in charge on the ship
<u>Hydrography</u>		
CTDO ₂ / LADCP	Toshiya NAKANO	Keizo SHUTTA
Salinity	Toshiya NAKANO	Keizo SHUTTA
Dissolve oxygen	Toshiya NAKANO	Takahiro KITAGAWA
Nutrients	Toshiya NAKANO	Takahiro KITAGAWA
Phytopigment	Toshiya NAKANO	Naoshi KUBO
DIC	Toshiya NAKANO	Shu SAITO
Total Alkalinity	Toshiya NAKANO	Shu SAITO
pH	Toshiya NAKANO	Shu SAITO
CFCs	Toshiya NAKANO	Shu SAITO
<u>Underway</u>		
Meteorology	Toshiya NAKANO	Kazuhiro NEMOTO
Thermo-Salinograph	Toshiya NAKANO	Shu SAITO
pCO ₂	Toshiya NAKANO	Shu SAITO
Chlorophyll-a	Toshiya NAKANO	Naoshi KUBO
ADCP	Toshiya NAKANO	Keizo SHUTTA
Bathymetry	Toshiya NAKANO	Keizo SHUTTA
<u>Float and Buoy</u>		
Argo float (JMA)	Kazuhiro NEMOTO	Keizo SHUTTA
Argo float (JAMSTEC)	Shigeki HOSODA	Keizo SHUTTA
Buoy (JMA)	Kazuhiro NEMOTO	Keizo SHUTTA

Table 4b. List of principal investigator and the person in charge on the ship for RF14-06.

Item	Principal Investigator (PI)	Person in charge on the ship
<u>Hydrography</u>		
CTDO ₂ / LADCP	Toshiya NAKANO	Keizo SHUTTA
Salinity	Toshiya NAKANO	Keizo SHUTTA
Dissolve oxygen	Toshiya NAKANO	Sonoki IWANO
Nutrients	Toshiya NAKANO	Takahiro KITAGAWA
Phytopigment	Toshiya NAKANO	Sonoki IWANO
DIC	Toshiya NAKANO	Kazutaka ENYO
Total Alkalinity	Toshiya NAKANO	Kazutaka ENYO
pH	Toshiya NAKANO	Kazutaka ENYO
CFCs	Toshiya NAKANO	Akira WADA

Underway

Meteorology	Toshiya NAKANO	Kazuhiro NEMOTO
Thermo-Salinograph	Toshiya NAKANO	Kazutaka ENYO
<i>p</i> CO ₂	Toshiya NAKANO	Kazutaka ENYO
Chlorophyll-a	Toshiya NAKANO	Sonoki IWANO
ADCP	Toshiya NAKANO	Keizo SHUTTA
Bathymetry	Toshiya NAKANO	Keizo SHUTTA

Table 4c. List of principal investigator and the person in charge on the ship for RF14-07.

Item	Principal Investigator (PI)	Person in charge on the ship
-------------	------------------------------------	-------------------------------------

Hydrography

CTDO ₂ / LADCP	Toshiya NAKANO	Keizo SHUTTA
Salinity	Toshiya NAKANO	Keizo SHUTTA
Dissolve oxygen	Toshiya NAKANO	Sonoki IWANO
Nutrients	Toshiya NAKANO	Hiroyuki FUJIWARA
Phytopigment	Toshiya NAKANO	Sonoki IWANO
DIC	Toshiya NAKANO	Shu SAITO
Total Alkalinity	Toshiya NAKANO	Shu SAITO
pH	Toshiya NAKANO	Shu SAITO
CFCs	Toshiya NAKANO	Kazutaka ENYO

Underway

Meteorology	Toshiya NAKANO	Takahiro SEGAWA
Thermo-Salinograph	Toshiya NAKANO	Shu SAITO
<i>p</i> CO ₂	Toshiya NAKANO	Shu SAITO
Chlorophyll-a	Toshiya NAKANO	Sonoki IWANO
ADCP	Toshiya NAKANO	Keizo SHUTTA
Bathymetry	Toshiya NAKANO	Keizo SHUTTA

Float and Buoy

Argo float (JAMSTEC)	Shigeki HOSODA	Keizo SHUTTA
Buoy (JMA)	Kazuhiro NEMOTO	Keizo SHUTTA

Toshiya NAKANO (nakano_t@met.kishou.go.jp)

Marine Division, Global Environment and Marine Department, JMA
1-3-4, Otemachi, Chiyoda-ku, Tokyo 100-8122, JAPAN
Phone: +81-3-3212-8341 Ext. 5131

Kazuhiro NEMOTO (k-nemoto@met.kishou.go.jp)

Marine Division, Global Environment and Marine Department, JMA
1-3-4, Otemachi, Chiyoda-ku, Tokyo 100-8122, JAPAN
Phone: +81-3-3212-8341 Ext. 5128

Shigeki HOSODA (hosodas@jamstec.go.jp)

Ocean Circulation Research Group,
Research and Development Center for Global Change (RCGC),
Strategic Research and Development area,
Japan Agency for Marine-Earth Science and Technology (JAMSTEC)
2-15 Natsushima, Yokosuka-shi, Kanagawa 237-0061, JAPAN

Reference

Swift, J. H. (2010): Reference-quality water sample data: Notes on acquisition, record keeping, and evaluation. *IOCCP Report No.14, ICPO Pub. 134, 2010 ver.1*

5. Underway chlorophyll-*a*

17 October 2023

(1) Personnel

Chihiro KAWAMURA (GEMD/JMA)

(2) Method

The Continuous Sea Surface Water Monitoring System of fluorescence (Nippon Kaiyo, Japan) automatically had been continuously measured seawater which is pumped from a depth of about 4.5 m below the maximum load line to the laboratory. The flow rate of the surface seawater was controlled by several valves and adjusted to about 0.6 L min⁻¹. The sensor in this system is a fluorometer 10-AU (S/N: 5408, Turner Designs, United States).

(3) Observation log

The chlorophyll-*a* continuous measurements were conducted during the entire cruise; from 10 Jun. to 25 Jun., 2014 in RF14-05, 3 Jul. to 16 Jul., 2014 in RF14-06, 28 Jul. to 15 Aug., 2014 in RF14-07 Leg 1, and from 26 Aug. to 11 Sep., 2014 in RF14-07 Leg 2.

(4) Water sampling

Surface seawater was corrected from outlet of water line of the system at nominally 1 day intervals. The seawater sample was measured in the same procedure as hydrographic samples of chlorophyll-*a* (see Chapter C5 “Phytopigments”).

(5) Calibration

At the beginning and the end of legs, a raw fluorescence value of sensor was adjusted in sensitivity of the sensor using deionized water and a rhodamine 0.1ppm solution measured.

After the cruise, the fluorescence value was converted to chlorophyll-*a* concentration by programs in the system based on nearby water sampling data (chlorophyll-*a* concentration and distance from location of sensor data).

(6) Data

Underway fluorescence and chlorophyll-*a* data is distributed in JMA format in “49UP20140609_P10_underway_chl.csv”. The record structure of the format is as follows;

Column1 DATE: Date (YYYYMMDD) [JST]
Column2 TIME: Time (HHMM) [JST] (= UTC + 9h)
Column3 LATITUDE: Latitude
Column4 LONGITUDE: Longitude
Column5 FLUOR: Fluorescence value (RFU)
Column6 CHLORA: Chlorophyll-*a* concentration (µg L⁻¹)
Column7 BTLCHL: Chlorophyll-*a* concentration of water sampling (µg L⁻¹).

C. Hydrographic Measurement Techniques and Calibration

CTDO₂ Measurements

Updated 5 March 2020

(1) Personnel

RF14-05

Keizo SHUTTA (GEMD/JMA)
 Kiyoshi MURAKAMI (GEMD/JMA)
 Noriyuki OKUNO (GEMD/JMA)
 Jinya MIURA (GEMD/JMA)

RF14-06

Keizo SHUTTA (GEMD/JMA)
 Shuji TSUBAKI (GEMD/JMA)
 Atsuro ICHIMATSU (GEMD/JMA)
 Tomoyuki KITAMURA (GEMD/JMA)
 Sho HIBINO (GEMD/JMA)
 Ryoma SUZUKI (GEMD/JMA)

RF14-07

Keizo SHUTTA (GEMD/JMA)
 Noriyuki OKUNO (GEMD/JMA)
 Masahiro TANIGUCHI (GEMD/JMA)
 Jinya MIURA (GEMD/JMA)
 Atsushi KOJIMA (GEMD/JMA)

(2) CTDO₂ measurement system

(Software : SEASAVEwin32 ver7.23.2)

<i>Deck unit</i>	<i>Serial Number</i>	<i>Station</i>
SBE 11plus (SBE)	0683	RF5113 – 5237
<i>Under water unit</i>	<i>Serial Number</i>	<i>Station</i>
SBE 9plus (SBE)	69709 (Pressure: 1103)	RF5113 – 5237
<i>Temperature</i>	<i>Serial Number</i>	<i>Station</i>
SBE 3plus (SBE)	4437 (primary)	RF5113 – 5237
	4199 (secondary)	RF5113 – 5237
SBE 35 (SBE)	0069	RF5113 – 5237
<i>Conductivity</i>	<i>Serial Number</i>	<i>Station</i>
SBE 4C (SBE)	2842 (primary)	RF5113 – 5236
	2987 (secondary)	RF5113 – 5135
	3670 (secondary)	RF5171 – 5237 RF5145 – 5169
<i>Pump</i>	<i>Serial Number</i>	<i>Station</i>
SBE 5T (SBE)	6552 (primary)	RF5113 – 5237
	6021 (secondary)	RF5113 – 5237
<i>Oxygen</i>	<i>Serial Number</i>	<i>Station</i>
RINKO III (JFE)	025 (foil number:133101A)	RF5113 – 5237
	003 (foil number:160008A)	RF5113 – 5237
<i>Water sampler (36 position)</i>	<i>Serial Number</i>	<i>Station</i>
SBE 32 (SBE)	0734	RF5113 – 5237
<i>Altimeter</i>	<i>Serial Number</i>	<i>Station</i>

PSA-916D (TB)	47830	RF5113 – 5237
Water Sampling Bottle		Station
Niskin Bottle (GO)		RF5113 – 5237

SBE: Sea- Bird Electronics, Inc., USA

JFE: JFE Advantech Co., Ltd., Japan

TB: Teledyne Benthos, Inc., USA

GO: General Oceanics, Inc., USA

(3) Pre-cruise calibration

(3.1) Pressure

S/N 1103, 25 Apr. 2014

c_1	=	-4.282684e+004	t_1	=	3.006702e+001
c_2	=	5.097742e-001	t_2	=	-8.607997e-005
c_3	=	1.312000e-002	t_3	=	3.727820e-006
d_1	=	3.583800e-002	t_4	=	3.699030e-009
d_2	=	0.000000e+000	t_5	=	0.000000e+000

Formula:

$$c = c_1 + c_2 \times U + c_3 \times U^2$$

$$d = d_1 + d_2 \times U$$

$$t_0 = t_1 + t_2 \times U + t_3 \times U^2 + t_4 \times U^3 + t_5 \times U^4$$

$$U \text{ (degrees Celsius)} = M \times (\text{12-bit pressure temperature compensation word}) + B$$

U : temperature in degrees Celsius

S/N 1103 coefficients in SEASOFT (configuration sheet dated on 08 May 2017)

$$M = 1.28040e-002, B = -9.31868e+000$$

Finally, pressure is computed as

$$P(\text{psi}) = c \times (1 - t_0^2/t^2) \times \{1 - d \times (1 - t_0^2/t^2)\}$$

t : pressure period (μsec)

The drift-corrected pressure is computed as

$$\text{Drift corrected pressure (dbar)} = \text{slope} \times (\text{computed pressure in dbar}) + \text{offset}$$

$\text{Slope} = 1.00001, \text{Offset} = -0.0008$

(3.2) Temperature (ITS-90): SBE 3plus

S/N 4437(primary), 25 Apr. 2014

$g = 4.33412492\text{e-}003$	$j = 1.82723329\text{e-}006$
$h = 6.37239385\text{e-}004$	$f_0 = 1000.0$
$i = 2.11053843\text{e-}005$	

S/N 4199(secondary), 25 Apr. 2014

$g = 4.39462185\text{e-}003$	$j = 2.23960817\text{e-}006$
$h = 6.49833980\text{e-}004$	$f_0 = 1000.0$
$i = 2.39904658\text{e-}005$	

Formula:

$$\text{Temperature(ITS-90)} = \frac{1}{g + h \times \ln(f_0/f) + i \times \ln^2(f_0/f) + j \times \ln^3(f_0/f)} - 273.15$$

f : Instrument freq.[Hz]

(3.3) Deep Ocean Standards Thermometer Temperature (ITS-90): SBE 35

S/N 0069, 23 Oct. 2006

$a_0 = 4.96812728\text{e-}003$	$a_3 = -1.14827915\text{e-}005$
$a_1 = -1.39341438\text{e-}003$	$a_4 = 2.44200422\text{e-}007$
$a_2 = 2.06596098\text{e-}004$	

Formula:

$$\text{Linearized temperature(ITS-90)} = 1/\{a_0 + a_1 \times \ln(n) + a_2 \times \ln^2(n) + a_3 \times \ln^3(n) + a_4 \times \ln^4(n)\} - 273.15$$

n : instrument output

The slow time drift of the SBE 35

S/N 0069, 22 Sep. 2013 (2nd step: fixed point calibration)

$\text{Slope} = 1.000008, \text{Offset} = -0.000532$

Formula:

$$\text{Temperature(ITS-90)} = \text{slope} \times (\text{Linearized temperature}) + \text{offset}$$

(3.4) Conductivity: SBE 4C

S/N 2842(primary), 25 Apr. 2014

$g = -1.01309979\text{e+}000$	$j = 4.32083308\text{e-}005$
$h = 1.38922077\text{e+}000$	$CP_{cor} = -9.5700\text{e-}008$
$i = 3.33035740\text{e-}004$	$CT_{cor} = 3.2500\text{e-}006$

S/N 2987(secondary), 25 Apr. 2014

$g = -9.91860554\text{e+}000$	$j = 4.72455296\text{e-}004$
$h = 1.36194050\text{e+}000$	$CP_{cor} = -9.5700\text{e-}008$
$i = 5.03394089\text{e-}004$	$CT_{cor} = 3.2500\text{e-}006$

S/N 3670(secondary), 03 Jan. 2014

$g = -1.01868925\text{e+}001$	$j = 2.06528405\text{e-}004$
$h = 1.57207852\text{e+}000$	$CP_{cor} = -9.5700\text{e-}008$

$$i = -1.11066333\text{e-}003 \quad CT_{cor} = 3.2500\text{e-}006$$

Conductivity of a fluid in the cell is expressed as:

$$C(S/m) = (g + h \times f^2 + i \times f^3 + j \times f^4) / \{10 \times (1 + CT_{cor} \times t + CP_{cor} \times p)\}$$

f : instrument frequency (kHz)

t : water temperature (degrees Celsius)

p : water pressure (dbar).

(3.5) Oxygen (RINKO III)

RINKO III (JFE Advantech Co., Ltd., Japan) is based on the ability of selected substance to act as dynamic fluorescence quenchers. RINKO III model is designed to use with a CTD system which accept an auxiliary analog sensor, and is designed to operate down to 7000 m.

RINKOIII output is expressed in voltage from 0 to 5 V.

(4) Data correction and Post-cruise calibration

(4.1) Temporal change of deck pressure and Post-cruise calibration

The drift-corrected pressure of post-cruise is computed as

$$\text{Drift corrected pressure (dbar)} = \text{slope} \times (\text{computed pressure in dbar}) + \text{offset}$$

S/N 1103, 09 Oct. 2014

Slope = 1.00002, Offset = 0.0799

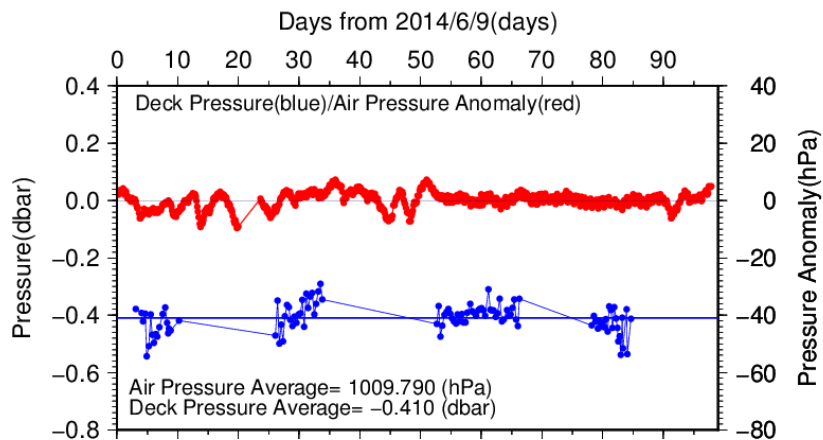


Figure C.1.1. Time series of the CTD deck pressure. Red line indicates atmospheric pressure anomaly. Blue line and dots indicate pre-cast deck pressure and average.

(4.2) Temperature sensor (SBE 3plus)

The practical corrections for CTD temperature data can be made by using a SBE 35, correcting the SBE 3plus to agree with the SBE 35 (McTaggart *et al.*, 2010; Uchida *et al.*, 2007).

CTD temperature is corrected as

$$\text{Corrected temperature} = T - (c_0 + c_1 \times P + c_2 \times P^2)$$

T : the CTD temperature (degrees Celsius), P : pressure (dbar) and c_0, c_1, c_2 : coefficients

Table C.1.1. Temperature correction summary (Pressure \geq 2000dbar). (Bold : selected sensor)

<i>S/N</i>	<i>Num</i>	$c_0(K)$	$c_1(K/dbar)$	$C_2(K/dbar^2)$	<i>Stations</i>
4437	188	6.4259848e-4	1.3309503e-7	0.0000000e+0	RF5113 – 5130
4437	460	6.8696547e-4	1.0220544e-7	0.0000000e+0	RF5145 – 5169
4437	577	3.8729702e-4	1.3163966e-7	0.0000000e+0	RF5171 – 5213
4437	168	1.6603746e-4	1.6464443e-7	0.0000000e+0	RF5214 – 5237
4199	188	1.1647193e-3	-4.1792194e-7	7.8310540e-11	RF5113 – 5130
4199	442	-4.5753635e-4	1.7899292e-7	0.0000000e+0	RF5145 – 5169
4199	579	4.1141676e-4	-9.8262538e-8	3.3459199e-11	RF5171 – 5213
4199	164	1.0457530e-4	-1.2083651e-8	3.0561553e-11	RF5214 – 5237

Table C.1.2. Temperature correction summary for S/N 4437.

Stations	Pressure < 2000dbar			Pressure \geq 2000dbar		
	Num	Average (K)	Std (K)	Num	Average (K)	Std (K)
RF5113 – 5130	315	0.0003	0.0206	188	0.0000	0.0002
RF5145 – 5169	462	0.0000	0.0063	460	0.0000	0.0001
RF5171 – 5213	979	0.0007	0.0107	577	0.0000	0.0002
RF5214 – 5237	528	0.0004	0.0115	168	0.0000	0.0002

Table C.1.3. Temperature correction summary for S/N 4199.

Stations	Pressure < 2000dbar			Pressure \geq 2000dbar		
	Num	Average (K)	Std (K)	Num	Average (K)	Std (K)
RF5113 – 5130	315	0.0001	0.0220	188	0.0000	0.0002
RF5145 – 5169	445	-0.0004	0.0078	442	0.0000	0.0003
RF5171 – 5213	979	-0.0012	0.0118	579	0.0000	0.0003
RF5214 – 5237	528	-0.0004	0.0097	164	0.0000	0.0003

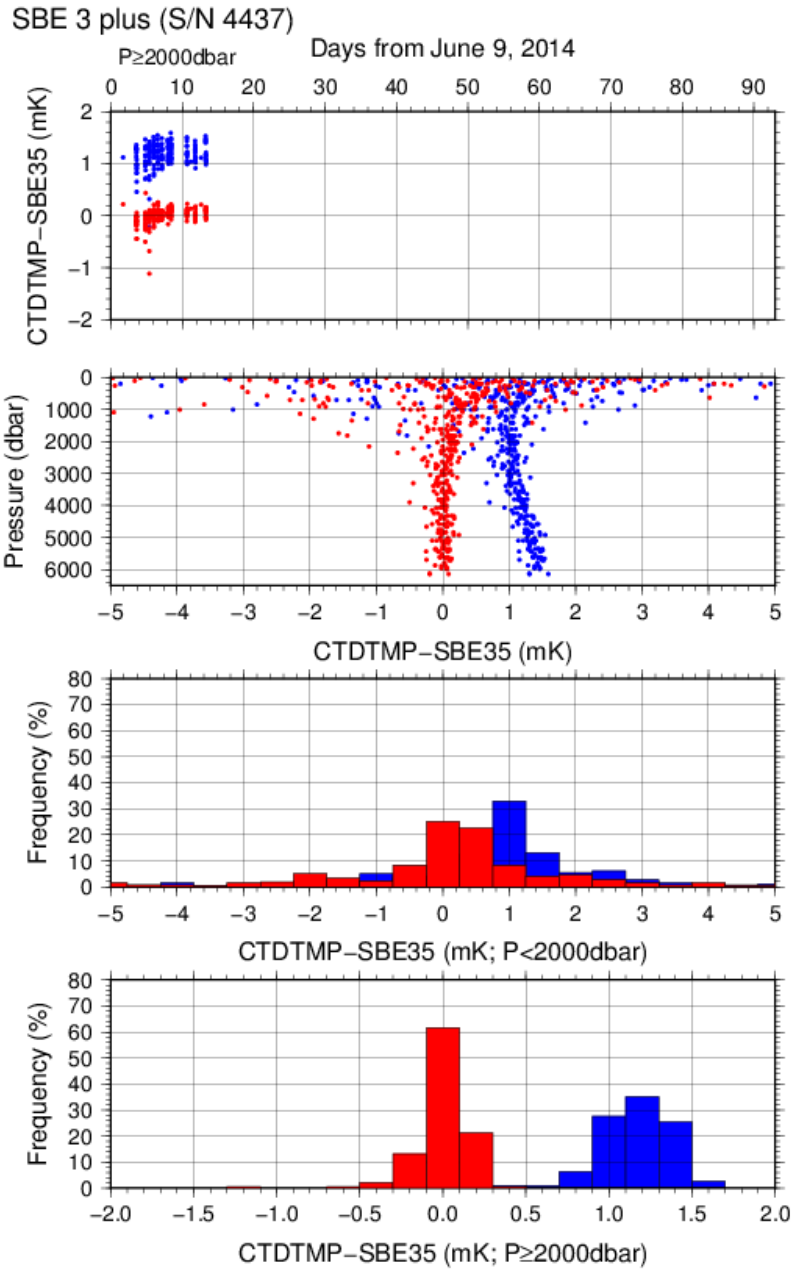


Figure C.1.2. Difference between the CTD temperature (*S/N 4437*) and the Deep Ocean Standards thermometer (SBE 35) at RF14-05. Blue and red dots indicate before and after the correction using SBE 35 data respectively. Lower two panels show histogram of the difference after correction.

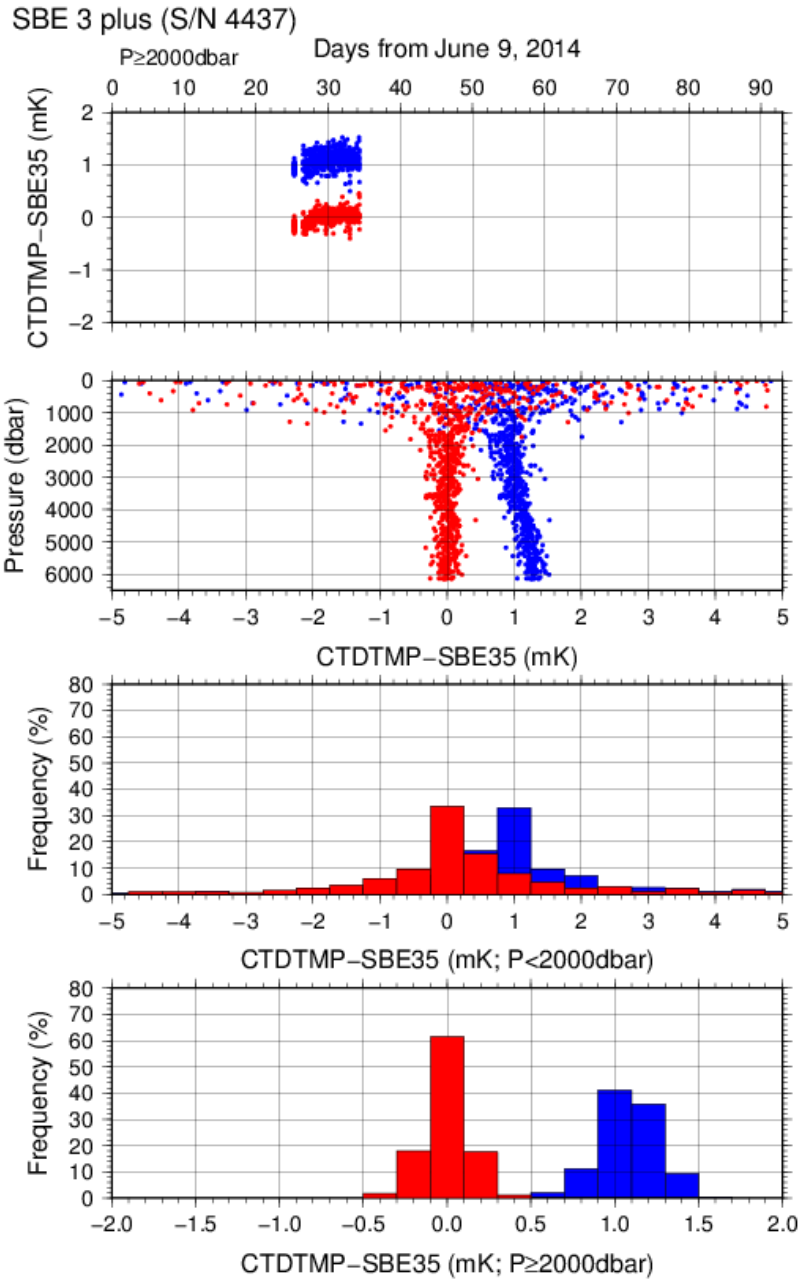


Figure C.1.3. Difference between the CTD temperature (S/N 4437) and the Deep Ocean Standards thermometer (SBE 35) at RF14-06. Blue and red dots indicate before and after the correction using SBE 35 data respectively. Lower two panels show histogram of the difference after correction.

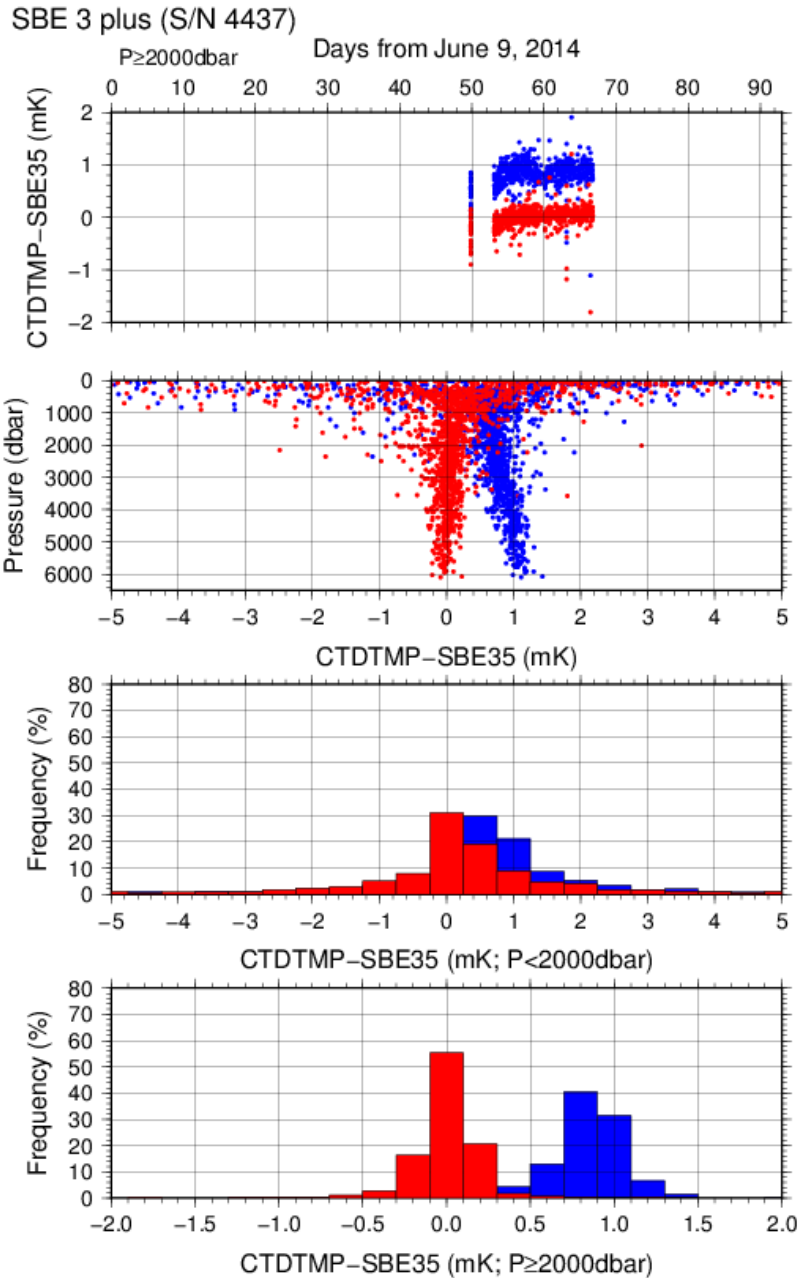


Figure C.1.4. Difference between the CTD temperature (*S/N 4437*) and the Deep Ocean Standards thermometer (SBE 35) at RF14-07 Leg 1. Blue and red dots indicate before and after the correction using SBE 35 data respectively. Lower two panels show histogram of the difference after correction.

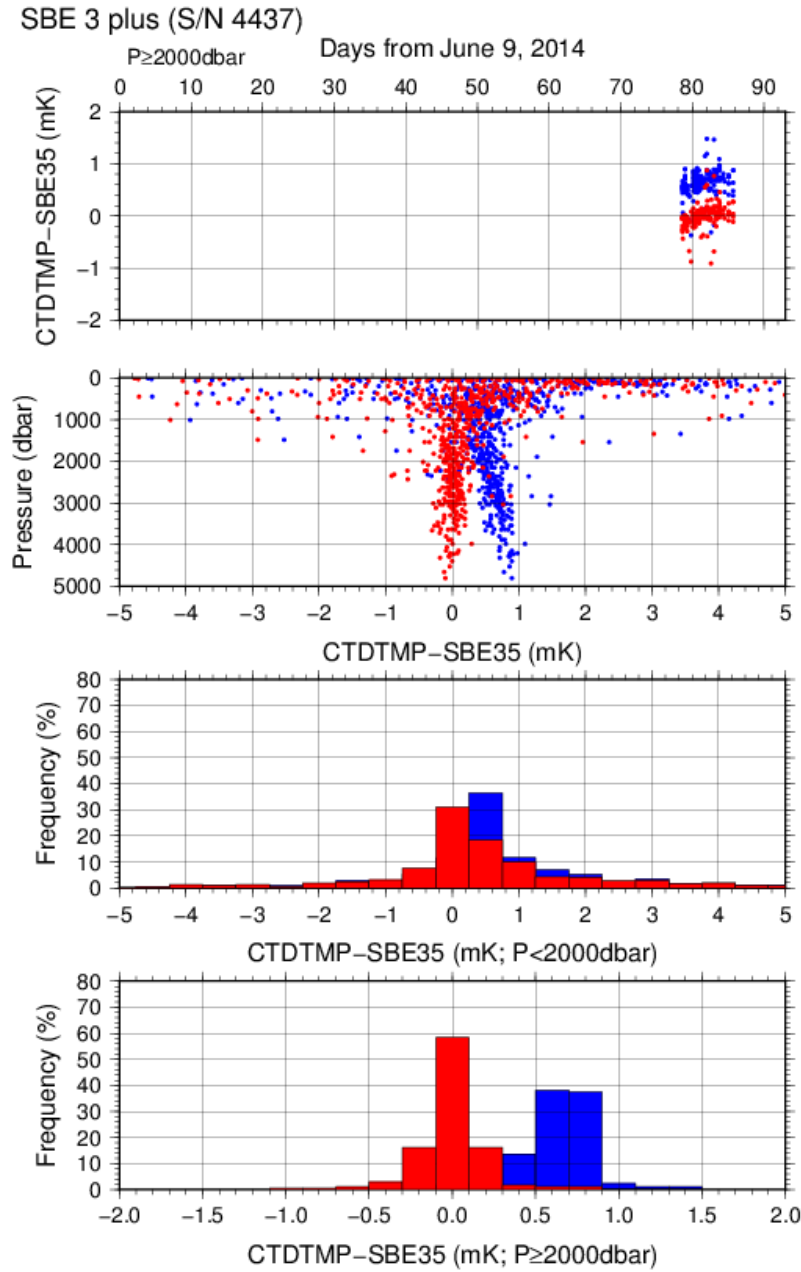


Figure C.1.5. Difference between the CTD temperature (*S/N 4437*) and the Deep Ocean Standards thermometer (SBE 35) at RF14-07 Leg 2. Blue and red dots indicate before and after the correction using SBE 35 data respectively. Lower two panels show histogram of the difference after correction.

Post-cruise sensor calibration for the SBE 3plus
S/N 4437(primary), 09 Oct. 2014

$$\begin{aligned}
 g &= 4.33422048\text{e-}003 & j &= 1.86411402\text{e-}006 \\
 h &= 6.37460951\text{e-}004 & f_0 &= 1000.0 \\
 i &= 2.12630682\text{e-}005
 \end{aligned}$$

S/N 4199(secondary), 09 Oct. 2014

$$\begin{aligned}
 g &= 4.39461305\text{e-}003 & j &= 2.23286586\text{e-}006 \\
 h &= 6.49808583\text{e-}004 & f_0 &= 1000.0 \\
 i &= 2.39650889\text{e-}005
 \end{aligned}$$

Formula:

$$\text{Temperature}(ITS - 90) = \frac{1}{g + h \times \ln(f_0/f) + i \times \ln^2(f_0/f) + j \times \ln^3(f_0/f)} - 273.15$$

f : Instrument freq.[Hz]

Post-cruise sensor calibration for the SBE 35

S/N 0069, 17 OCT. 2014 (2nd step: fixed point calibration)
Slope = 1.000012, Offset = -0.000550

Formula:

$$\text{Temperature}(ITS - 90) = \text{slope} \times (\text{Linearized temperature}) + \text{offset}$$

(4.3) Conductivity sensor (SBE 4C)

The practical corrections for CTD conductivity data can be made by using a bottle salinity data, correcting the SBE 4C to agree with measured conductivity (McTaggart et al., 2010).

CTD conductivity is corrected

$$\text{Corrected Conductivity} = C - \left(\sum_{i=0}^I c_i \times C^i + \sum_{j=1}^J p_j \times P^j \right)$$

C : CTD conductivity, c_i and p_j : calibration coefficients

i, j : determined by referring to AIC (Akaike, 1974). According to McTaggart et al. (2010), maximum of I and J are 2.

Table C.1.4. Conductivity correction coefficient summary. (Bold : selected sensor)

S/N	Num	$c_0(S/m)$	c_1	$c_2(m/S)$	Stations
			$p_1(S/m/dbar)$	$p_2(S/m/dbar^2)$	
2842	363	1.0431e-4	0.0000e+0	0.0000e+0	RF5113 – 5130
			1.0007e-7	-1.0318e-11	
2842	972	1.5142e-4	0.0000e+0	0.0000e+0	RF5145 – 5169
			8.4592e-8	-8.9893e-12	
2842	1535	-8.9599e-4	5.3434e-4	5.7987e-5	RF5171 – 5213
			6.6658e-8	-5.4330e-12	
2842	658	-4.0961e-3	2.0434e-3	2.2517e-4	RF5214 – 5237
			1.7429e-7	-2.1545e-11	
2987	335	1.3172e-4	-4.0913e-5	0.0000e+0	RF5113 – 5130
			7.8257e-8	-5.4042e-12	
3670	940	-1.5659e-3	2.9783e-4	0.0000e+0	RF5145 – 5169
			9.0534e-8	-1.0724e-11	

2987	1595	1.4342e-4	0.0000e+0	0.0000e+0	RF5171 – 5213
			7.4816e-8	5.3316e-12	
2987	662	-3.6741e-3	1.6944e-3	-2.0278e-4	RF5214 – 5237
			1.7489e-7	-1.9689e-11	

Table C.1.5. Conductivity correction and salinity summary for S/N 2842.

Stations	Pressure < 1900dbar					
	Conductivity			Salinity		
	Num	Average (S/m)	Std (S/m)	Num	Average	Std
RF5113 – 5130	164	0.0000	0.0002	164	0.0001	0.0027
RF5145 – 5169	473	0.0000	0.0003	473	0.0001	0.0026
RF5171 – 5213	908	0.0000	0.0003	908	-0.0001	0.0022
RF5214 – 5236	458	0.0000	0.0003	458	0.0000	0.0022
Stations	Pressure ≥ 1900 dbar					
	Conductivity			Salinity		
	Num	Average (S/m)	Std (S/m)	Num	Average	Std
RF5113 – 5130	199	0.0000	0.0001	199	-0.0001	0.0009
RF5145 – 5169	499	0.0000	0.0001	499	0.0000	0.0007
RF5171 – 5213	627	0.0000	0.0000	627	0.0001	0.0005
RF5214 – 5236	200	0.0000	0.0001	200	0.0001	0.0007

Table C.1.6. Conductivity correction and salinity summary for S/N 2987.

Stations	Pressure < 1900dbar					
	Conductivity			Salinity		
	Num	Average (S/m)	Std (S/m)	Num	Average	Std
RF5130 – 5113	154	0.0000	0.0003	154	0.0001	0.0029
RF5171 – 5213	952	0.0000	0.0019	952	0.0000	0.0172
RF5214 – 5236	464	0.0000	0.0003	464	0.0000	0.0025
Stations	Pressure ≥ 1900 dbar					
	Conductivity			Salinity		
	Num	Average (S/m)	Std (S/m)	Num	Average	Std
RF5130 – 5113	181	0.0000	0.0001	181	-0.0001	0.0010
RF5171 – 5213	643	0.0000	0.0001	643	0.0000	0.0006
RF5214 – 5236	198	0.0000	0.0001	198	0.0001	0.0008

Table C.1.7. Conductivity correction and salinity **summary** for S/N 3670.

Stations	Pressure < 1900dbar					
	Conductivity			Salinity		
	Num	Average (S/m)	Std (S/m)	Num	Average	Std
RF5145 – 5169	455	0.0000	0.0003	455	0.0000	0.0026
Stations	Pressure ≥ 1900 dbar					
	Conductivity			Salinity		
	Num	Average (S/m)	Std (S/m)	Num	Average	Std
RF5145 – 5169	485	0.0000	0.0001	485	0.0000	0.0010

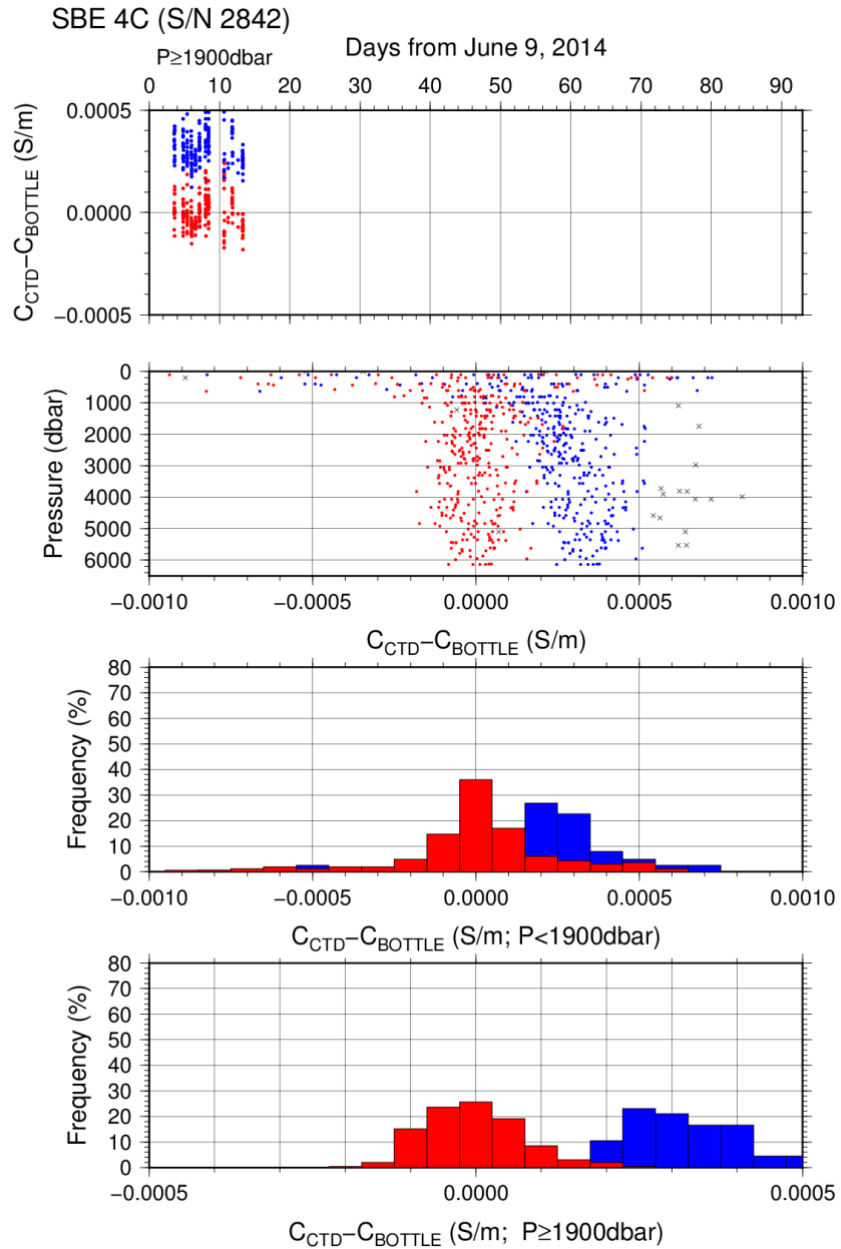


Figure C.1.6. Difference between the CTD conductivity (S/N 2842) and the bottle conductivity at RF14-05. Blue and red dots indicate before and after the calibration using bottle data respectively. Lower two panels show histogram of the difference before and after calibration.

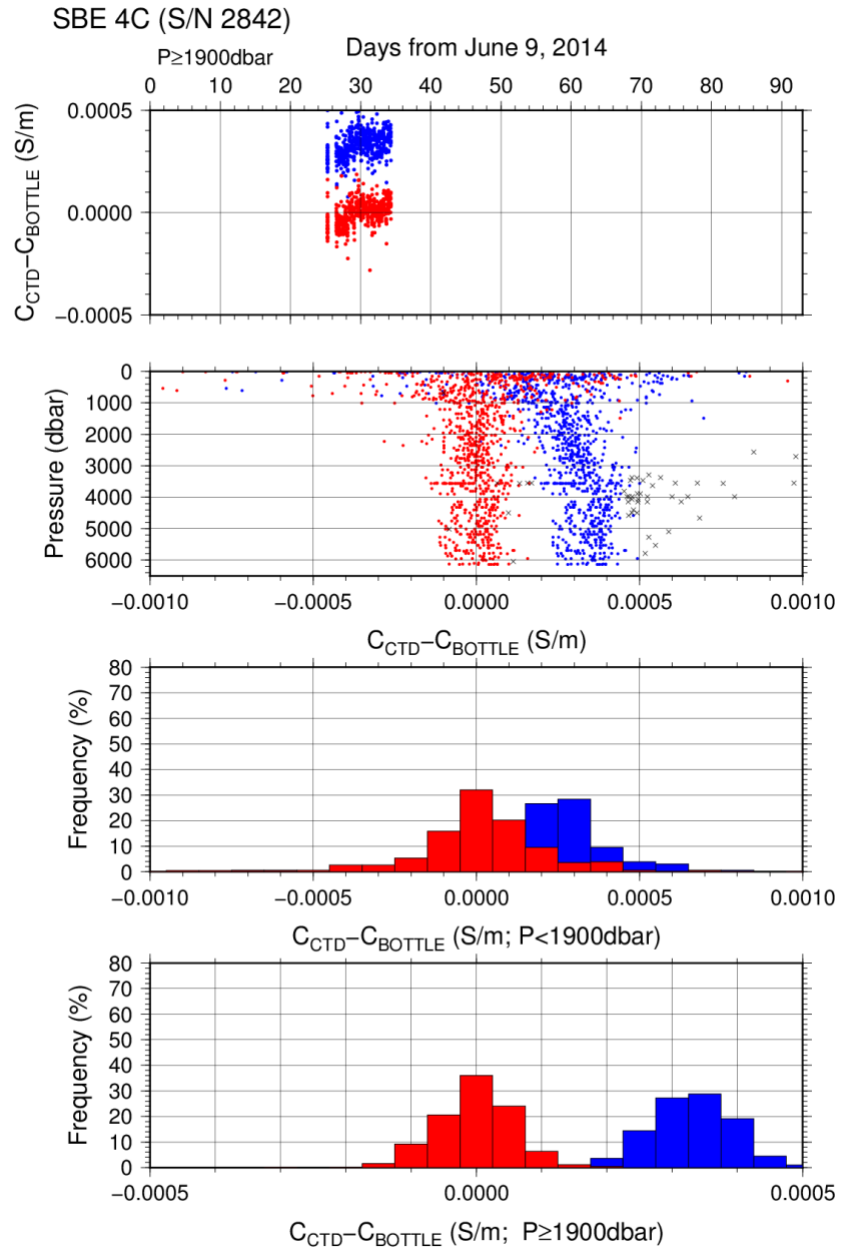


Figure C.1.7. Difference between the CTD conductivity (S/N 2842) and the bottle conductivity at RF14-06. Blue and red dots indicate before and after the calibration using bottle data respectively. Lower two panels show histogram of the difference before and after calibration.

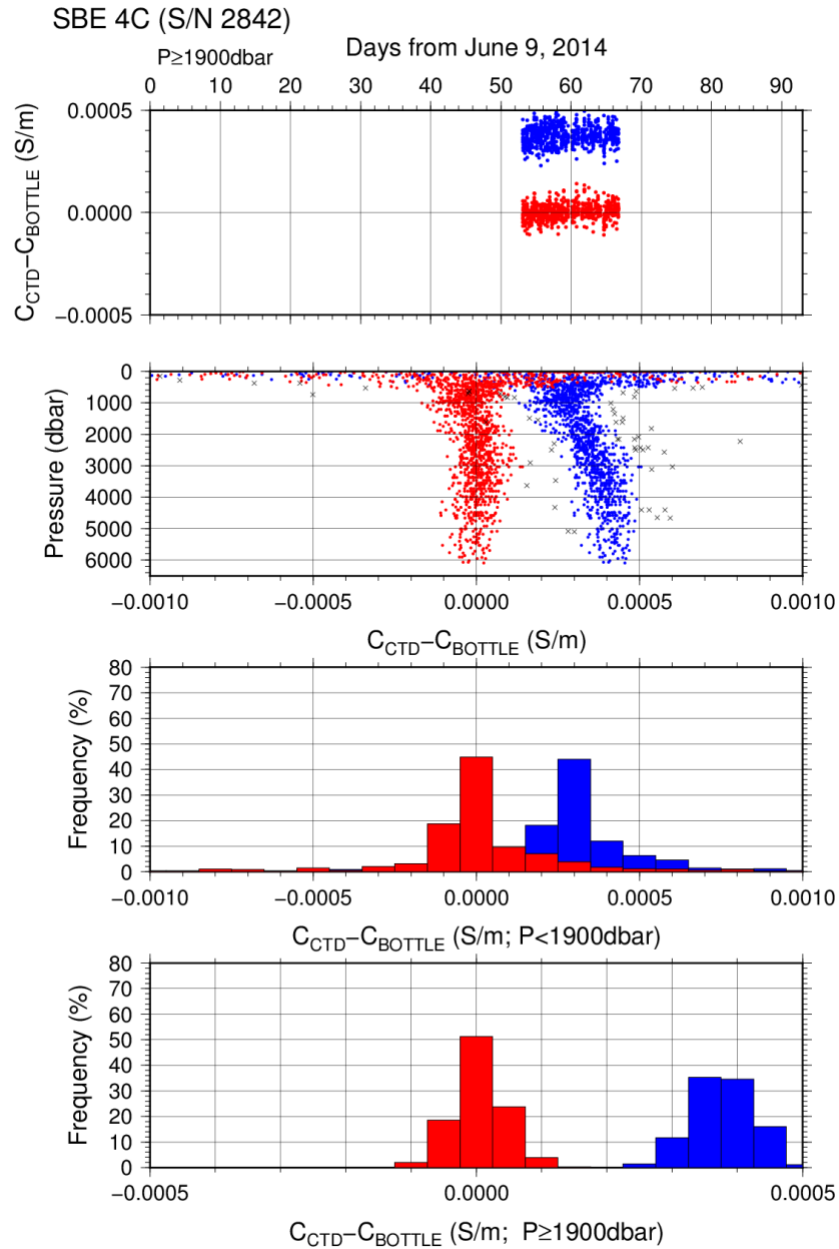


Figure C.1.8. Difference between the CTD conductivity (S/N 2842) and the bottle conductivity at RF14-07 (Leg 1). Blue and red dots indicate before and after the calibration using bottle data respectively. Lower two panels show histogram of the difference before and after calibration.

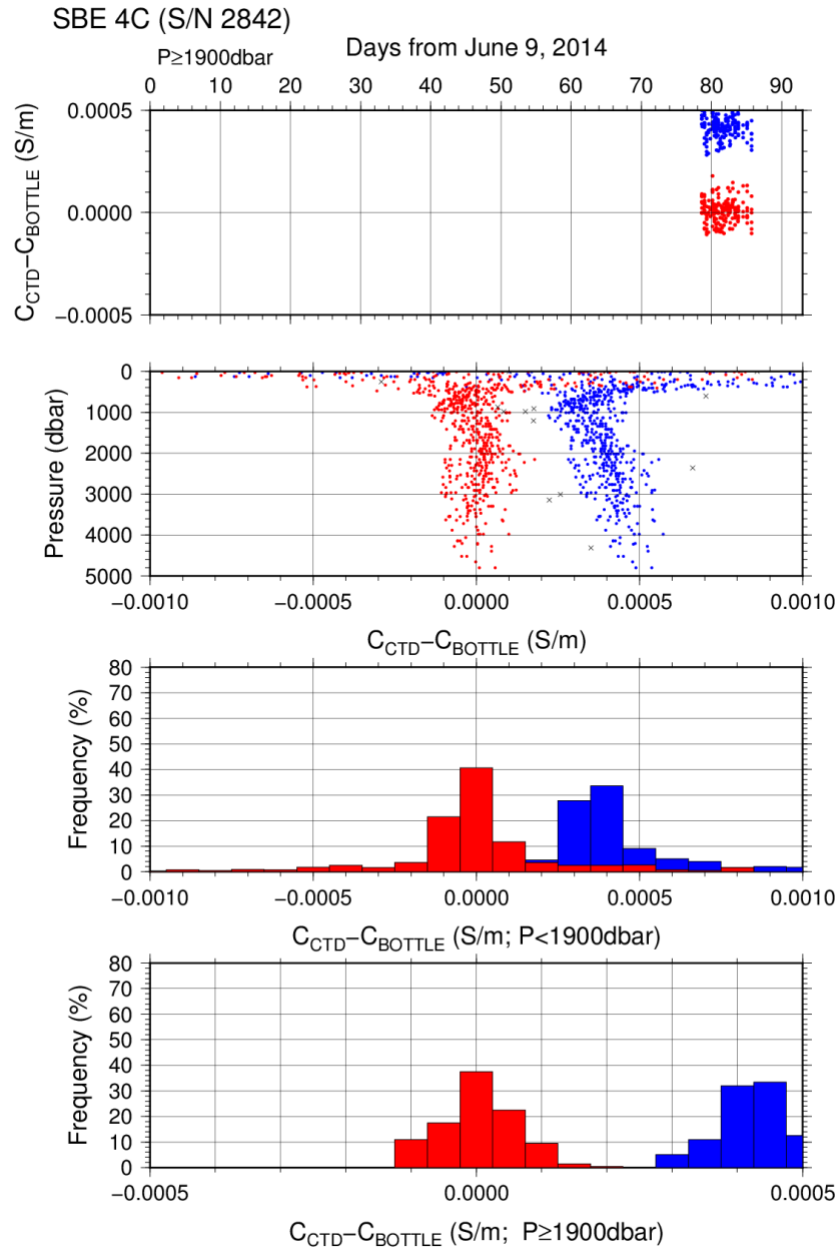


Figure C.1.9. Difference between the CTD conductivity (S/N 2842) and the bottle conductivity at RF14-07 (Leg 2). Blue and red dots indicate before and after the calibration using bottle data respectively. Lower two panels show histogram of the difference before and after calibration.

Post-cruise sensor calibration for the SBE 4C

S/N 2842(primary), 09 Oct. 2014

$$\begin{array}{ll} g = -1.01315173e+001 & j = 4.21172142e-005 \\ h = 1.38930984e+000 & CP_{cor} = -9.5700e-008 \\ i = 3.20625744e-004 & CT_{cor} = 3.2500e-006 \end{array}$$

S/N 2987(secondary), 09 Oct. 2014

$$\begin{array}{ll} g = -9.92055558e+000 & j = 5.06840801e-005 \\ h = 1.36229836e+000 & CP_{cor} = -9.5700e-008 \\ i = 4.52626817e-004 & CT_{cor} = 3.2500e-006 \end{array}$$

S/N 3670(secondary), 27 Jan. 2015

$$\begin{array}{ll} g = -1.02157134e+001 & j = 3.51876131e-004 \\ h = 1.58102504e+000 & CP_{cor} = -9.5700e-008 \\ i = -3.32850262e-003 & CT_{cor} = 3.2500e-006 \end{array}$$

Conductivity of a fluid in the cell is expressed as:

$$C(S/m) = (g + h \times f^2 + i \times f^3 + j \times f^4) / \{10 \times (1 + CT_{cor} \times t + CP_{cor} \times p)\}$$

f: instrument frequency (kHz)

t: water temperature (degrees Celsius)

p: water pressure (dbar).

(4.4) Oxygen sensor (RINKO III)

The CTD oxygen is calculated using RINKO III output (voltage) by the Stern-Volmer equation, according to a method by *Uchida et al. (2008)* and *Uchida et al. (2010)*. The pressure hysteresis for the RINKO III output (voltage) is corrected according to a method by *Sea-bird Electronics (2009)* and *Uchida et al. (2010)*. The formulas are as follows:

$$P_0 = 1.0 + c_4 \times t$$

$$P_c = c_5 + c_6 \times v + c_7 \times T + c_8 \times T \times v$$

$$K_{sv} = c_1 + c_2 \times t + c_3 \times t^2$$

$$coef = (1.0 + c_9 \times P/1000)^{1/3}$$

$$[O_2] = O_2^{sat} \times \{(P_0/P_c - 1.0)/K_{sv} \times coef\}$$

P: pressure (dbar), *t*: potential temperature, *v*: RINKO output voltage (volt)

T: elapsed time of the sensor from the beginning of first station in calculation group in day

O_2^{sat} : dissolved oxygen saturation by *Garcia and Gordon (1992)* (μmol/kg)

$[O_2]$: dissolved oxygen concentration (μmol/kg)

c_1 - c_9 : determined by minimizing difference between CTD oxygen and bottle dissolved oxygen by quasi-newton method (*Shanno, 1970*).

Table C.1.8. Dissolved oxygen correction coefficient summary. (Bold : selected sensor)

S/N	Stations	<i>c</i> ₁	<i>c</i> ₂	<i>c</i> ₃	<i>c</i> ₄	<i>c</i> ₅
		<i>c</i> ₆	<i>c</i> ₇	<i>c</i> ₈	<i>c</i> ₉	
025	RF5113 – 5130	1.59979e+0	2.91548e-2	2.64454e-4	8.75649e-4	-1.23918e-1
		3.04967e-1	-1.60558e-3	1.24424e-3	1.02659e-1	
025	RF5145 – 5169	1.57836 e+0	2.51218e-2	1.71414e-4	-1.20087e-4	-1.12771e-1
		3.04505e-1	5.55988e-4	2.64313e-4	1.107895e-1	
025	RF5171 – 5213	1.63304 e+0	2.25258e-2	1.72859e-4	-9.63090e-4	-1.12022e-1
		3.03695e-1	-4.32823e-4	6.79926e-4	1.13637e-1	
025	RF5214 – 5237	1.60853 e+0	2.35403e-2	1.53051e-4	-7.80261e-4	-1.15573e-1
		3.03759e-1	6.02594e-4	4.39747e-4	1.06033e-1	
003	RF5113 – 5130	1.60057e+0	2.97722e-2	3.06813e-4	1.27639e-3	-1.43246e-1
		3.24812e-1	-8.51485e-4	7.36341e-4	8.39722e-2	

003	RF5145 – 5169	1.57060e+0	2.47923e-2	1.80330e-4	1.38014e-4	-1.26146e-1
		3.21468e-1	4.57588e-4	7.35276e-4	8.92324e-2	
003	RF5171 – 5213	1.62351e+0	2.14343e-2	1.53758e-4	-1.07208e-3	-1.24979e-1
		3.19201e-1	-3.49798e-5	3.38168e-4	9.56222e-2	
003	RF5214 – 5237	1.59727e+0	2.45713e-2	1.27997e-4	-5.29590e-4	-1.25499e-1
		3.19388e-1	-4.54323e-5	4.06835e-4	8.81217e-2	

Table C.1.9. Dissolved oxygen correction summary for S/N 025.

Stations	Pressure < 950dbar			Pressure ≥ 950 dbar		
	Num	Average (µmol/kg)	Std (µmol/kg)	Num	Average (µmol/kg)	Std (µmol/kg)
RF5113 – 5130	243	-0.29	2.86	211	0.02	0.35
RF5145 – 5169	328	-0.04	0.72	507	0.00	0.36
RF5171 – 5213	736	0.01	0.89	755	-0.01	0.31
RF5214 – 5237	371	-0.01	0.99	270	-0.02	0.38

Table C.1.10. Dissolved oxygen correction summary for S/N 003.

Stations	Pressure < 950dbar			Pressure ≥ 950 dbar		
	Num	Average (µmol/kg)	Std (µmol/kg)	Num	Average (µmol/kg)	Std (µmol/kg)
RF5113 – 5130	243	-0.30	2.96	211	0.01	0.35
RF5145 – 5169	328	-0.04	0.73	507	0.01	0.35
RF5171 – 5213	736	0.02	0.84	755	0.00	0.27
RF5214 – 5237	399	-0.01	1.01	270	-0.02	0.36

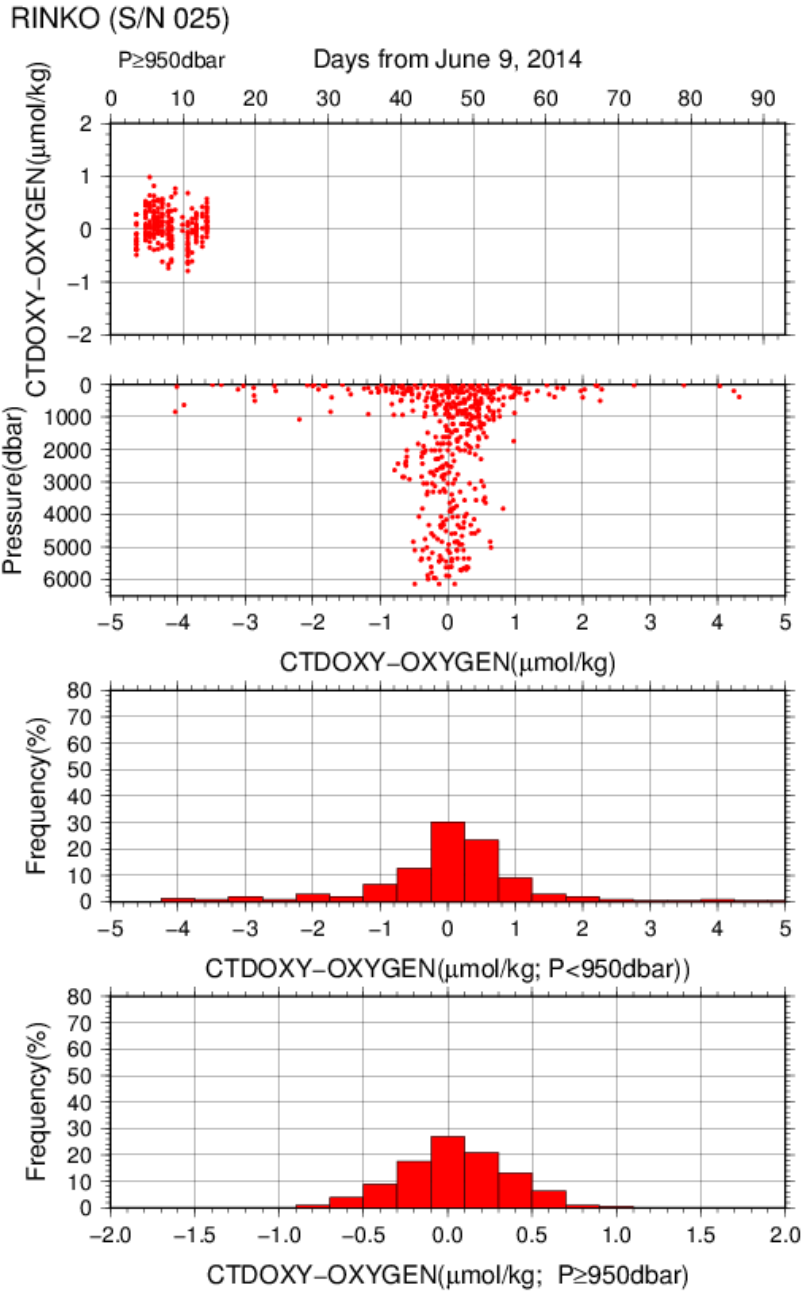


Figure C.1.10. Difference between the CTD oxygen (*S/N 025*) and bottle dissolved oxygen at RF14-05. Red dots in upper two panels indicate the result of calibration. Lower two panels show histogram of the difference between calibrated oxygen and bottle oxygen.

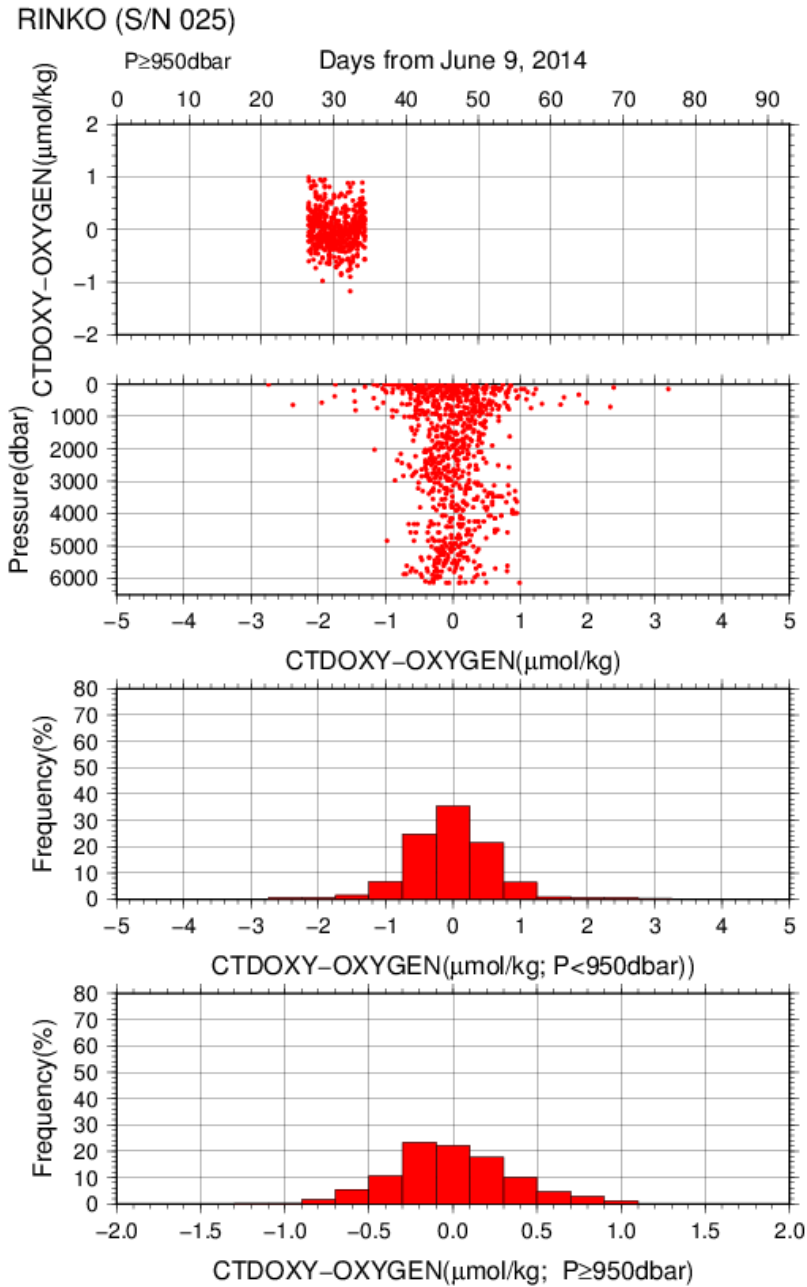


Figure C.1.11. Difference between the CTD oxygen (*S/N 025*) and bottle dissolved oxygen at RF14-06. Red dots in upper two panels indicate the result of calibration. Lower two panels show histogram of the difference between calibrated oxygen and bottle oxygen.

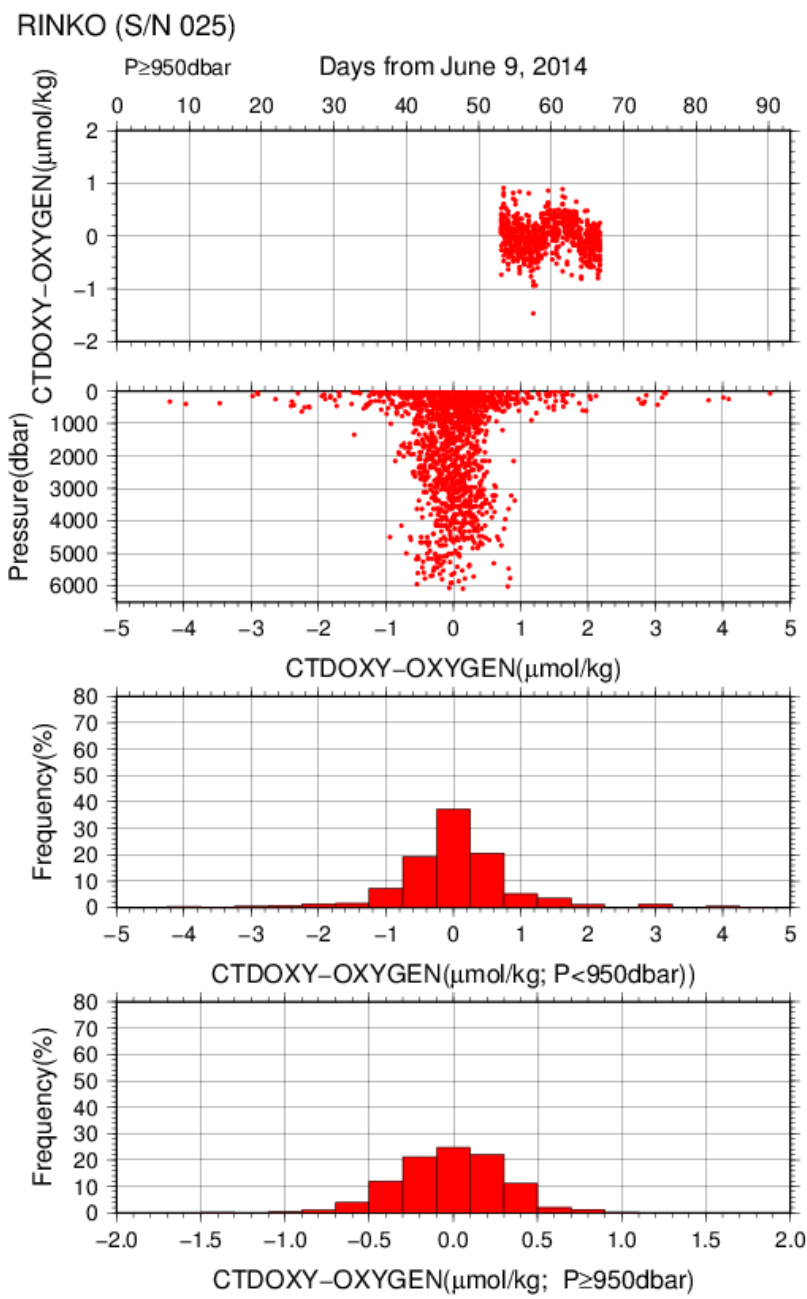


Figure C.1.12. Difference between the CTD oxygen (S/N 025) and bottle dissolved oxygen at RF14-07 (Leg 1). Red dots in upper two panels indicate the result of calibration. Lower two panels show histogram of the difference between calibrated oxygen and bottle oxygen.

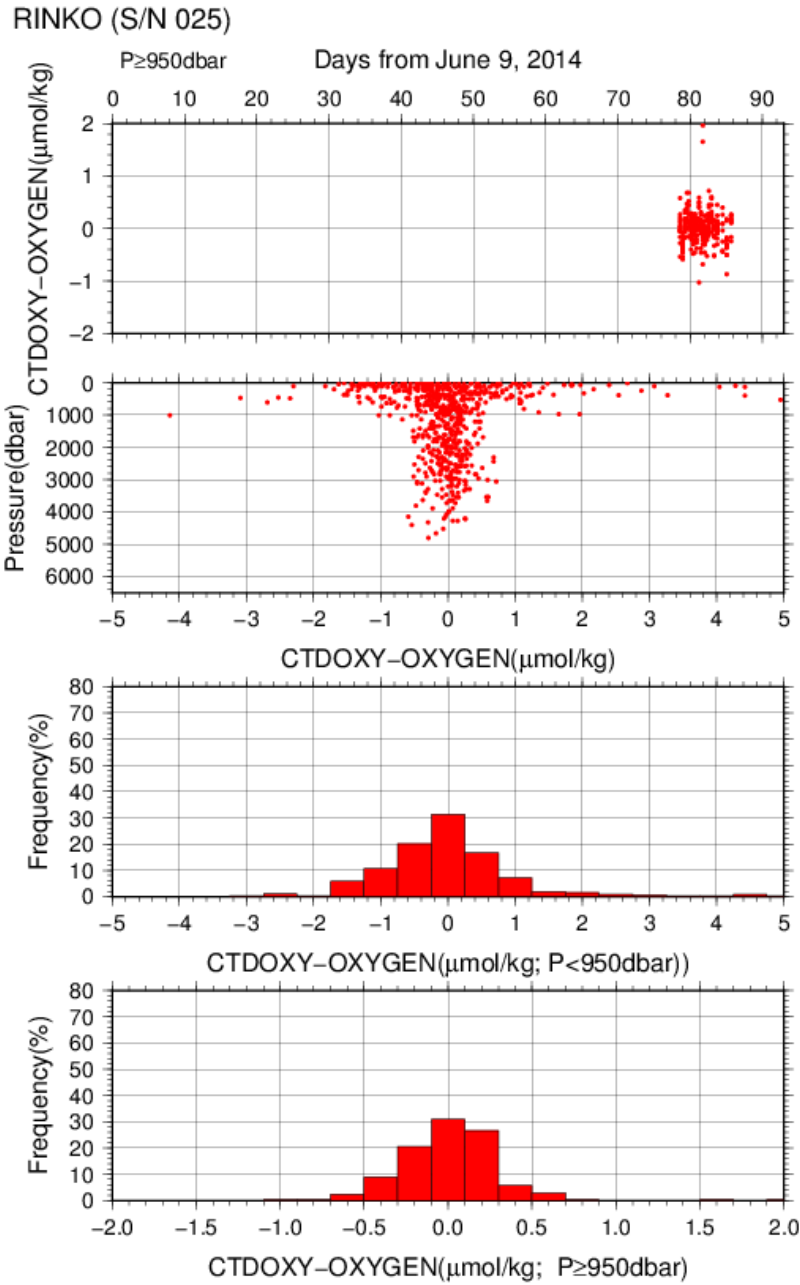


Figure C.1.13. Difference between the CTD oxygen (*S/N 025*) and bottle dissolved oxygen at RF14-07 (Leg 2). Red dots in upper two panels indicate the result of calibration. Lower two panels show histogram of the difference between calibrated oxygen and bottle oxygen.

(4.5) Results of detection of sea floor by the altimeter (PSA-916D)

The altimeter detected the sea floor at 95 of 115 stations, the average distance of beginning detecting the sea floor was 31.7m, and that of final detection of sea floor was 13.2m. The summary of detection of PSA-916D was shown in Figure C.1.8.

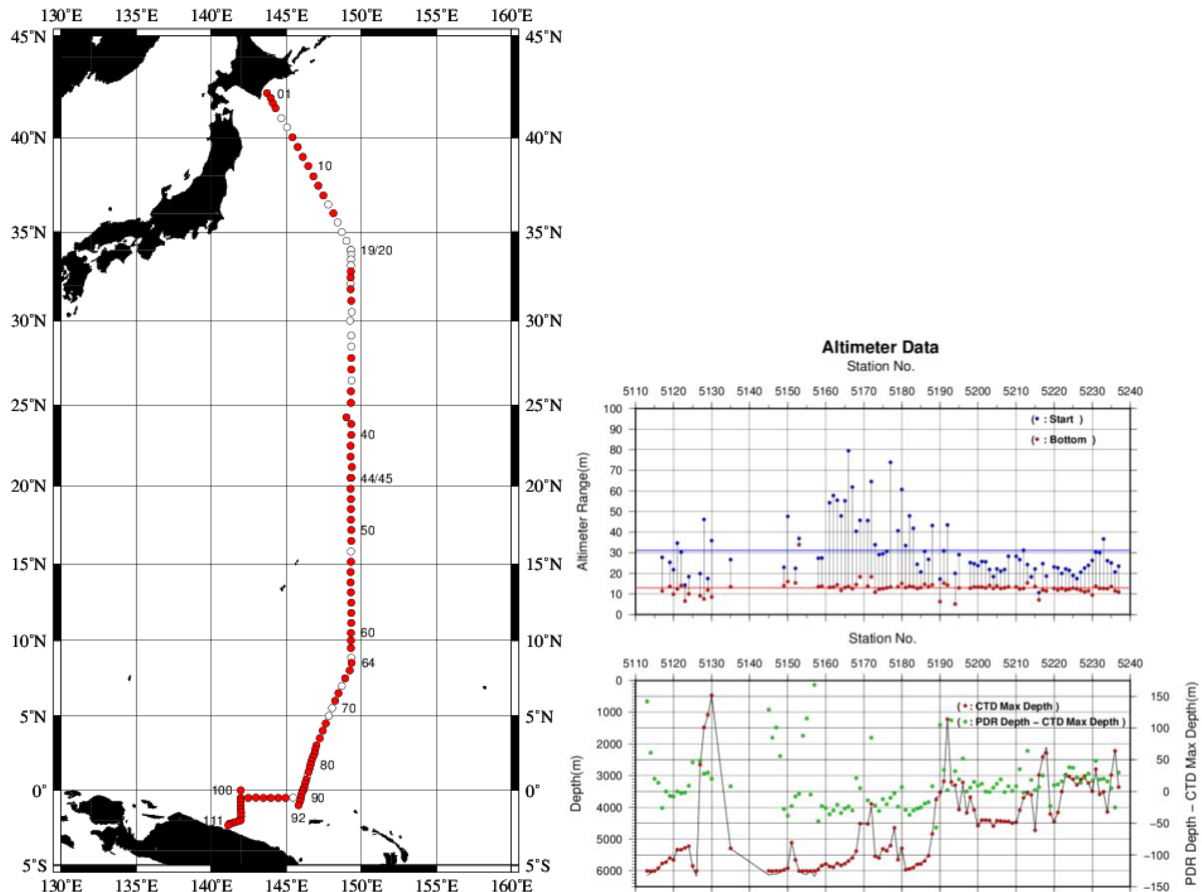


Figure C.1.14. The summary of detection of PSA-916D. The left panel shows the stations of detection, the right panel shows the relationship among PSA-916D, bathymetry and CTD depth. In the left panel, closed and open circles indicate react and no-react stations, respectively.

References

- Akaike, H. (1974): A new look at the statistical model identification. *IEEE Transactions on Automatic Control*, **19**:716–722.
- García, H. E., and L. I. Gordon (1992): Oxygen solubility in seawater: Better fitting equations. *Limnol. Oceanogr.*, **37**, 1307–1312.
- McTaggart, K. E., G. C. Johnson, M. C. Johnson, F. M. Delahoyde, and J. H. Swift (2010): The GO-SHIP Repeat Hydrography Manual: A Collection of Expert Reports and guidelines. IOCCP Report No **14**, ICPO Publication Series No. 134, version 1, 2010.
- Sea-Bird Electronics (2009): SBE 43 dissolved oxygen (DO) sensor – hysteresis corrections, *Application note no. 64-3*, 7 pp.
- Shanno, David F. (1970): Conditioning of quasi-Newton methods for function minimization. *Math. Comput.* **24**, 647–656. MR 42 #8905.
- Uchida, H., G. C. Johnson, McTaggart, K. E. (2010): CTD oxygen sensor calibration procedures. In: The GO-SHIP repeat hydrography manual: A Collection of Expert Reports and guidelines. IOCCP Report No **14**, ICPO Publication Series No. 134, version 1, 2010.
- Uchida, H., K. Ohyama, S. Ozawa, and M. Fukasawa (2007): In-situ calibration of the Sea-Bird 9plus CTD thermometer. *J. Atmos. Oceanic Technol.*, **24**, 1961–1967.
- Uchida, H., T. Kawano, I. Kaneko, and M. Fukasawa (2008): In-situ calibration of optode-based oxygen sensors. *J. Atmos. Oceanic Technol.*, **25**, 2271–2281.

Bottle Salinity

1 November 2019

(1) Personnel

RF14-05

Keizo SHUTTA (GEMD/JMA)

Kiyoshi MURAKAMI (GEMD/JMA)

Noriyuki OKUNO (GEMD/JMA)

Jinya MIURA (GEMD/JMA)

RF14-06

Keizo SHUTTA (GEMD/JMA)

Shuji TSUBAKI (GEMD/JMA)

Atsuro ICHIMATSU (GEMD/JMA)

Tomoyuki KITAMURA (GEMD/JMA)

Sho HIBINO (GEMD/JMA)

Ryoma SUZUKI (GEMD/JMA)

RF14-07

Keizo SHUTTA (GEMD/JMA)

Noriyuki OKUNO (GEMD/JMA)

Masahiro TANIGUCHI (GEMD/JMA)

Jinya MIURA (GEMD/JMA)

Atsushi KOJIMA (GEMD/JMA)

(2) Salinity measurement

Salinometer: AUTOSAL 8400B (S/N68614; Guildline Instruments Ltd., Canada)

Thermometer: Guildline platinum thermometers model 9450 (to monitor an ambient temperature and bath temperature)

IAPSO Standard Sea Water: P156 (K15=0.99984)

(3) Sampling and measurement

The measurement system was almost same as *Kawano* (2010).

Algorithm for practical salinity scale, 1978 (PSS-78; *UNESCO*, 1981) was employed to convert the conductivity ratios to salinities.

(4) Station occupied

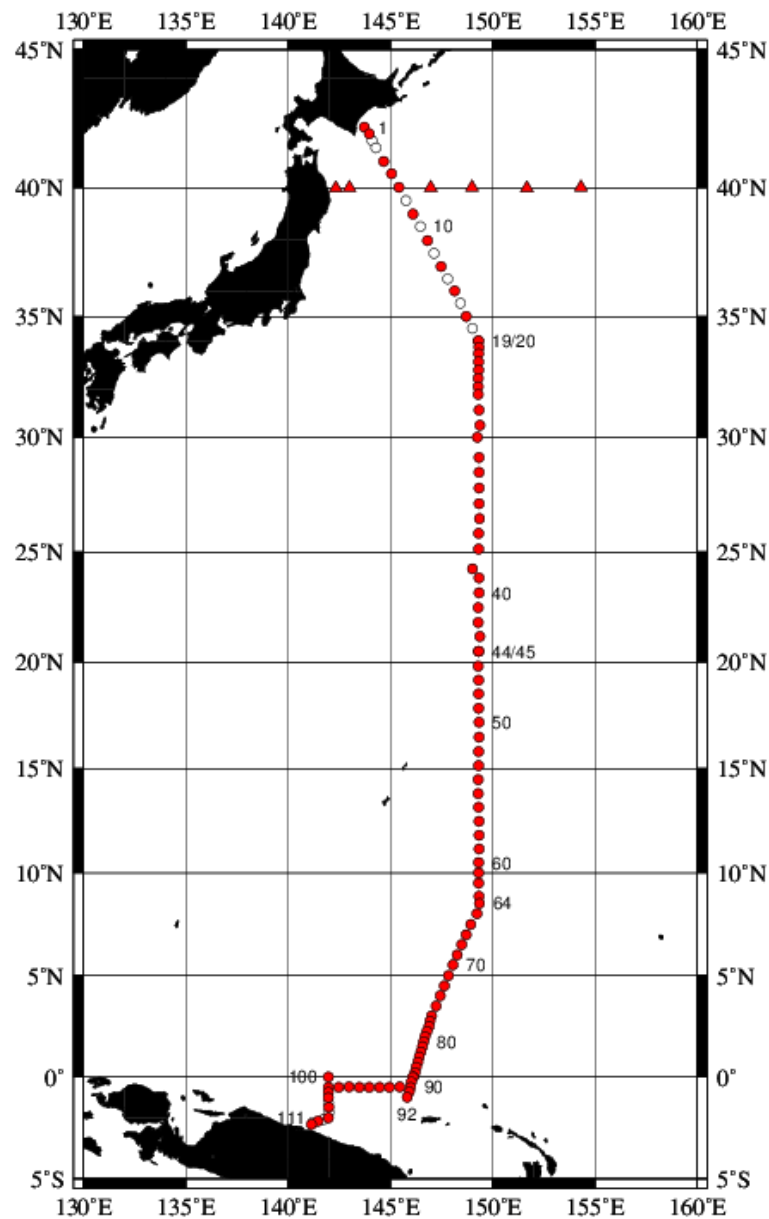


Figure C.2.1. Location of observation stations of bottle salinity. Closed and open circles indicate sampling and no-sampling station, respectively. Triangle shows a sampling station which is not reported in the bottle data file but is used for calibration for conductivity sensors.

Bottle Depth Diagram along P10

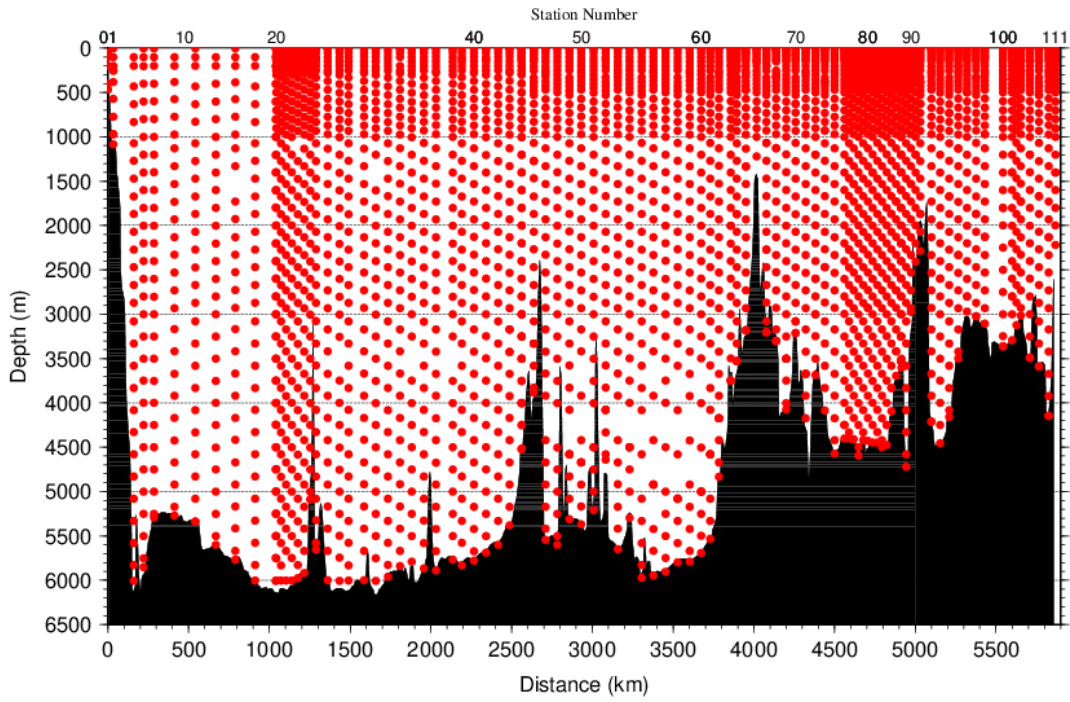


Figure C.2.2. Distance-depth distribution of sampling layers of bottle salinity.

(5) Result

(5.1) Ambient temperature, bath temperature and SSW measurements

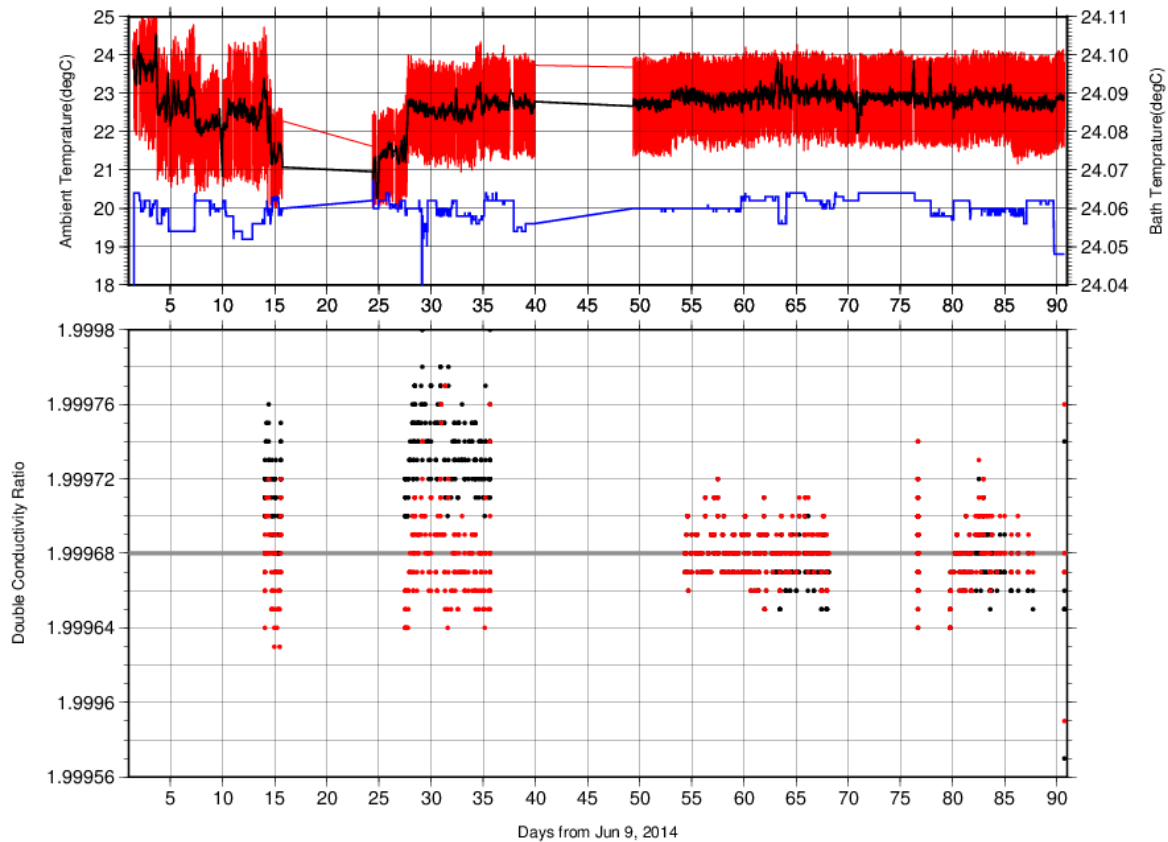


Figure C.2.3. The upper panel, red line, black line and blue line indicate time-series of ambient temperature, ambient temperature average and bath temperature during cruise. The lower panel, black dots and red dots indicate raw and corrected time-series of the double conductivity ratio of the standard sea water (P156).

(5.2) Replicate and Duplicate Samples

We took replicate (pair of water samples taken from a single Niskin bottle) and duplicate (pair of water samples taken from different Niskin bottles closed at the same depth) samples of bottle salinity through the cruise. Results of the analyses are summarized in Table C.2.1. Detailed results of them are shown in Figure C.2.4. The calculation of the standard deviation from the difference of sets was based on a procedure (SOP 23) in *DOE* (1994).

Table C.2.1. Summary of replicate and duplicate analyses.

Measurement	Ave. \pm S.D.
Replicate	0.0003 \pm 0.0003 (N=337)
Duplicate	0.0006 \pm 0.0005 (N=126)

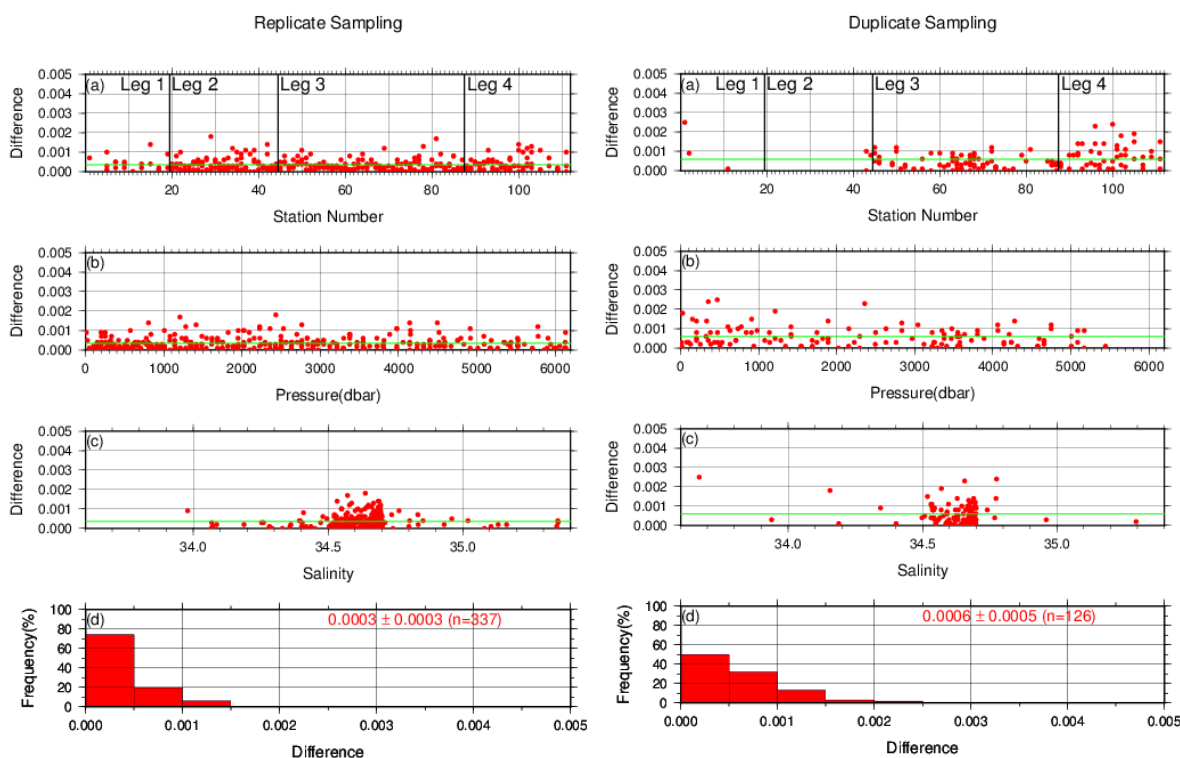


Figure C.2.4. Result of (left) replicate and (right) duplicate analyses during the cruise against (a) station number, (b) pressure and (c) salinity, and (d) histogram of the measurements. Green line indicates the mean of the differences of salinity of replicate/duplicate.

(5.3) Summary of assigned quality control flags

Table C.2.2. Summary of assigned quality control flags

Flag	Definition	Salinity
2	Good	2688
3	Questionable	0
4	Bad (Faulty)	317
6	Replicate measurements	351
Total number of samples		3356

References

- DOE (1994), Handbook of methods for the analysis of the various parameters of the carbon dioxide system in sea water; version 2. *A.G. Dickson and C. Goyet (eds), ORNL/CDIAC-74.*
- Kawano (2010), The GO-SHIP Repeat Hydrography Manual: A Collection of Expert Reports and Guidelines. *IOCCP Report No. 14, ICPO Publication Series No. 134, Version 1.*
- UNESCO (1981), Tenth report of the Joint Panel on Oceanographic Tables and Standards. *UNESCO Tech. Papers in Mar. Sci., 36, 25 pp.*

Bottle Oxygen

Updated 17 October 2023

(1) Personnel

RF14-05

Naoshi KUBO (GEMD/JMA)

Takahiro KITAGAWA (GEMD/JMA)

Chihiro KAWAMURA (GEMD/JMA)

RF14-06

Sonoki IWANO (GEMD/JMA)

Sho SHIMAMURA (GEMD/JMA)

Chihiro KAWAMURA (GEMD/JMA)

RF14-07

Sonoki IWANO (GEMD/JMA)

Hiroyuki FUJIWARA (GEMD/JMA)

Chihiro KAWAMURA (GEMD/JMA)

(2) Station occupied

A total of 107 stations (RF14-05: 17, RF14-06: 26, RF14-07 Leg 1: 43, Leg 2: 21) were occupied for dissolved oxygen measurements. Station location and sampling layers of bottle oxygen are shown in Figures C.3.1 and C.3.2, respectively.

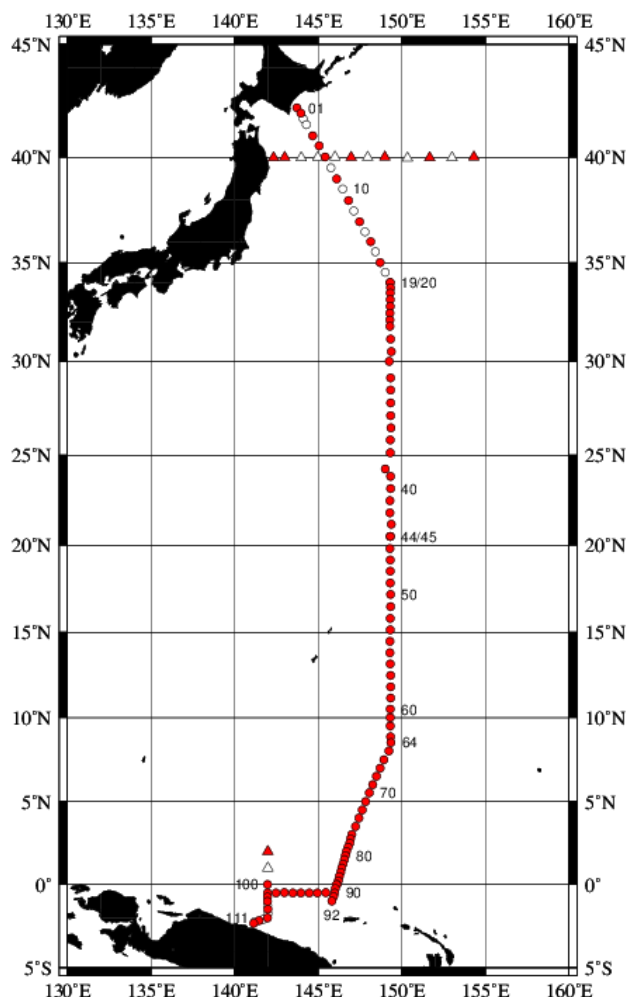


Figure C.3.1. Location of observation stations of bottle oxygen. Closed and open circles indicate sampling and no-sampling stations, respectively. Triangles show sampling station which is not reported in the bottle data file, but the data at closed triangle is used for quality control of dissolved oxygen. These data are available from the JMA (https://www.data.jma.go.jp/gmd/kaiyou/db/vessel_obs/data-report/html/ship/ship_e.php?year=2014&season=spring and https://www.data.jma.go.jp/gmd/kaiyou/db/vessel_obs/data-report/html/ship/ship_e.php?year=2014&season=summer).

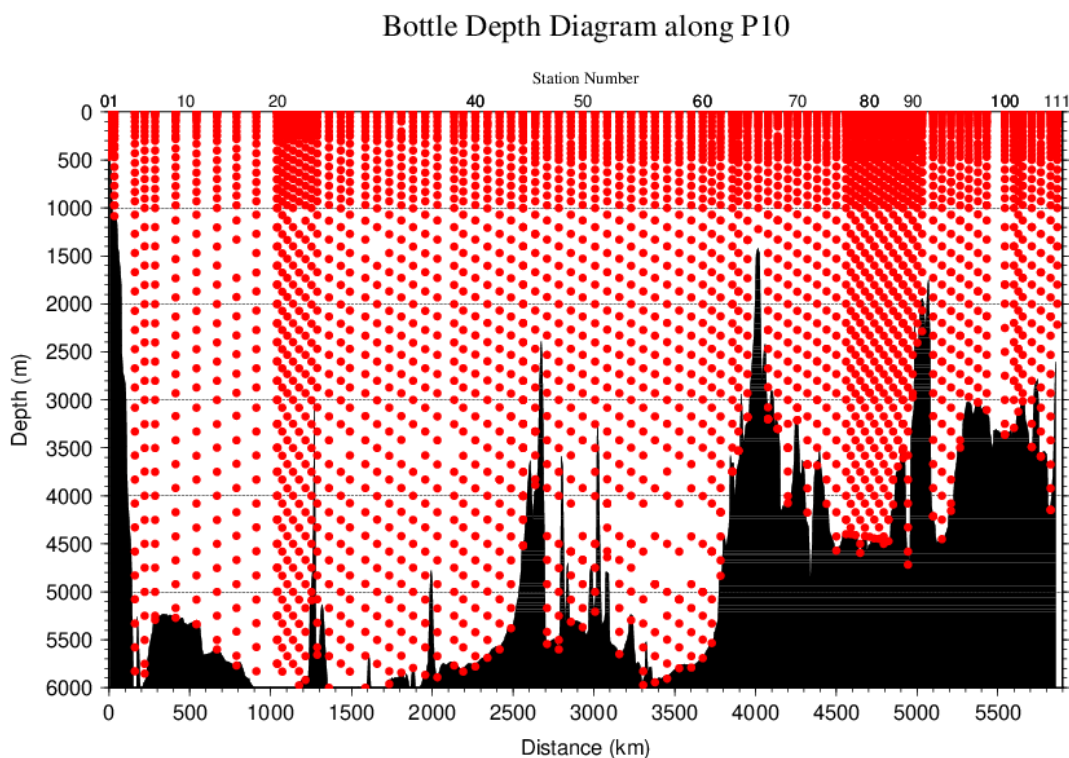


Figure C.3.2. Distance-depth distribution of sampling layers of bottle oxygen.

(3) Instrument

Detector: DOT-01X (Kimoto Electronic, Japan)

Burette: APB-510 (Kyoto Electronic, Japan)

(4) Sampling and measurement

Methods of seawater sampling, measurement, and calculation of dissolved oxygen concentration were based on IOCCP Report (Langdon, 2010). Details of the methods are shown in Appendix A1.

The reagents for the measurement were prepared according to recipes described in Appendix A2. It is noted that standard KIO_3 solutions were prepared gravimetrically using the highest purity standard substance KIO_3 (Lot. No. TLG0272, Wako Pure Chemical, Japan). Batch list of prepared standard KIO_3 solutions is shown in Table C.3.1.

Table C.3.1. Batch list of the standard KIO_3 solutions.

KIO_3 batch	Concentration and uncertainty (k=2) at 20°C. Unit is normality (N).	Purpose of use
20140313	0.010000±0.000004	Standardization (main use)
20140218-1	0.009997±0.000004	Mutual comparison

(5) Standardization

Concentration of $\text{Na}_2\text{S}_2\text{O}_3$ titrant was determined with the standard KIO_3 solution “20140313”, based on the methods of IOCCP Report (Langdon, 2010). The results of standardization during the cruise are shown in Figure C.3.3. Standard deviation of its concentration at 20°C determined through standardization was used in calculation of an uncertainty.

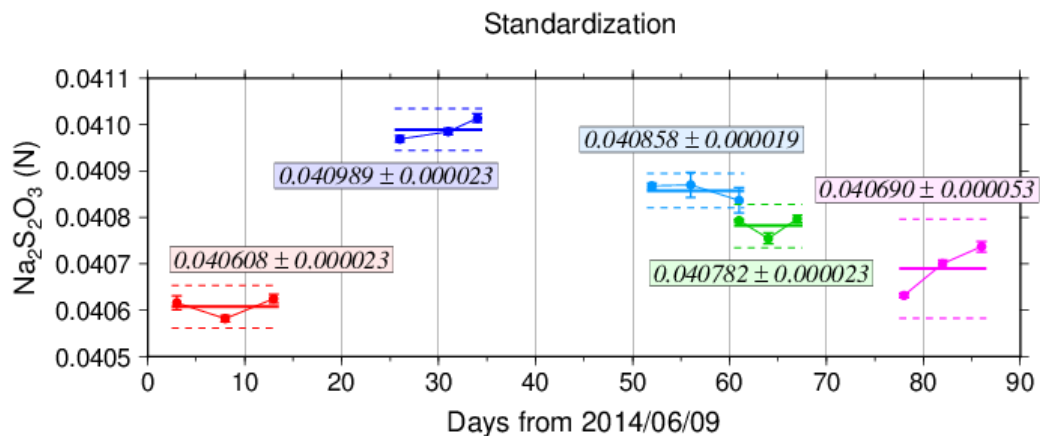


Figure C.3.3. Calculated concentration of $\text{Na}_2\text{S}_2\text{O}_3$ solution at 20°C in standardization during the cruise. Different colors of plots indicate different batches of $\text{Na}_2\text{S}_2\text{O}_3$ solution. Error bars of plots show standard deviation of concentration of $\text{Na}_2\text{S}_2\text{O}_3$ in the measurement. Thick and dashed lines denote the mean and 2 times of standard deviations for the batch measurements, respectively.

(6) Blank

(6.1) Reagent blank

Blank in oxygen measurement (reagent blank; $V_{\text{blk}, \text{dw}}$) can be represented as follows;

$$V_{\text{blk}, \text{dw}} = V_{\text{blk}, \text{ep}} + V_{\text{blk}, \text{reg}} \quad (\text{C3.1})$$

where $V_{\text{blk}, \text{ep}}$ represents a blank due to differences between the measured end-point and the equivalence point, and $V_{\text{blk}, \text{reg}}$ a blank associated with oxidants or reductants in the reagent. The reagent blank $V_{\text{blk}, \text{dw}}$ was determined by the methods described in IOCCP Report (Langdon, 2010). Because we used two sets (set A and B) of pickling reagent-I and -II, the blanks in each set were determined (Figure C.3.4).

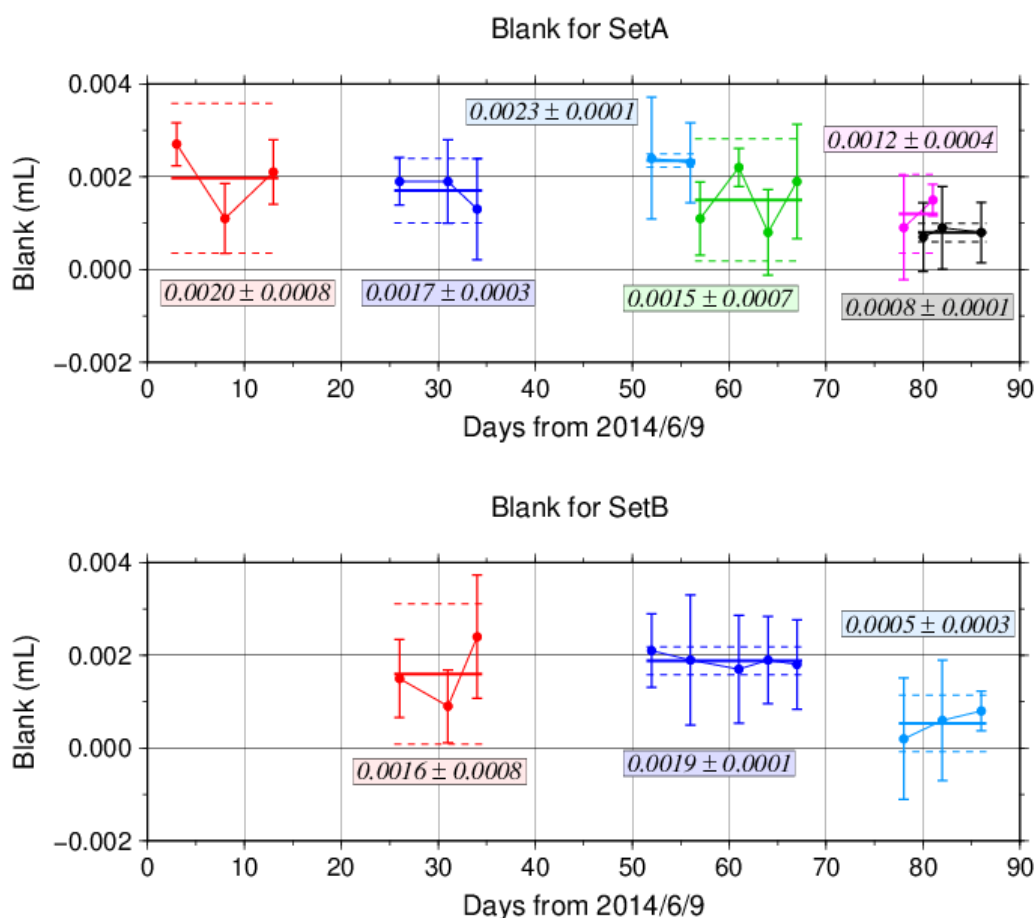


Figure C.3.4. Reagent blank ($V_{\text{blk}, \text{dw}}$) determination for set A (top) and set B (bottom). Error bars of plots show standard deviation of the measurement. Thick and dashed lines denote the mean and 2 times of standard deviations for the batch measurement, respectively.

(6.2) Other blanks

We also determined two other blanks related to oxygen measurement; the blank $V_{\text{blk}, \text{reg}}$ and the seawater blank ($V_{\text{blk}, \text{sw}}$). Details are described in Appendix A3.

(7) Quality Control

(7.1) Replicate and duplicate analyses

We took replicate (pair of water samples taken from a single Niskin bottle) and duplicate (pair of water samples taken from different Niskin bottles closed at the same depth) samples of dissolved oxygen through the cruise. Results of the analyses are summarized in Table C.3.2. Detailed results of them are shown in Figure C.3.5. The calculation of the standard deviation from the difference of sets was based on a procedure (SOP 23) in DOE (1994).

Table C.3.2. Summary of replicate and duplicate measurements.

Measurement	Ave. \pm S.D. ($\mu\text{mol kg}^{-1}$)
Replicate	0.19 ± 0.18 (N=369)
Duplicate	0.24 ± 0.24 (N=149)

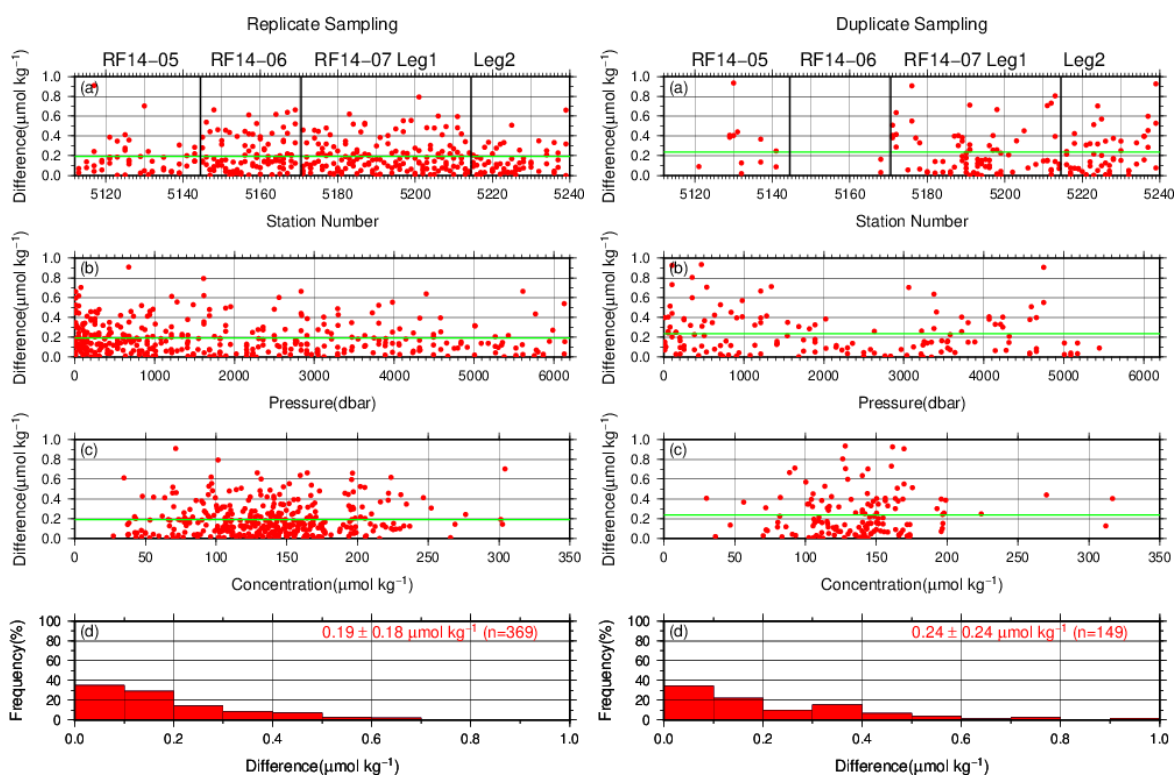


Figure C.3.5. Results of (left) replicate and (right) duplicate measurements during the cruise against (a) station number, (b) pressure and (c) concentration of dissolved oxygen. Green line denotes the average of the measurements. Bottom panels (d) show histogram of the measurements.

(7.2) Mutual comparison between each standard KIO₃ solution

During the cruise, mutual comparison between different lots of standard KIO₃ solution was performed to confirm the accuracy of our oxygen measurement and the bias of a standard KIO₃ solution. A concentration of the standard KIO₃ solution “20140218-1” was determined using Na₂S₂O₃ solution standardized with the KIO₃ solution “20140313”, and the difference between measurement value and theoretical one. A good agreement among two standards confirmed that there was no systematic shift in our oxygen measurements during the cruise (Figure C.3.6).

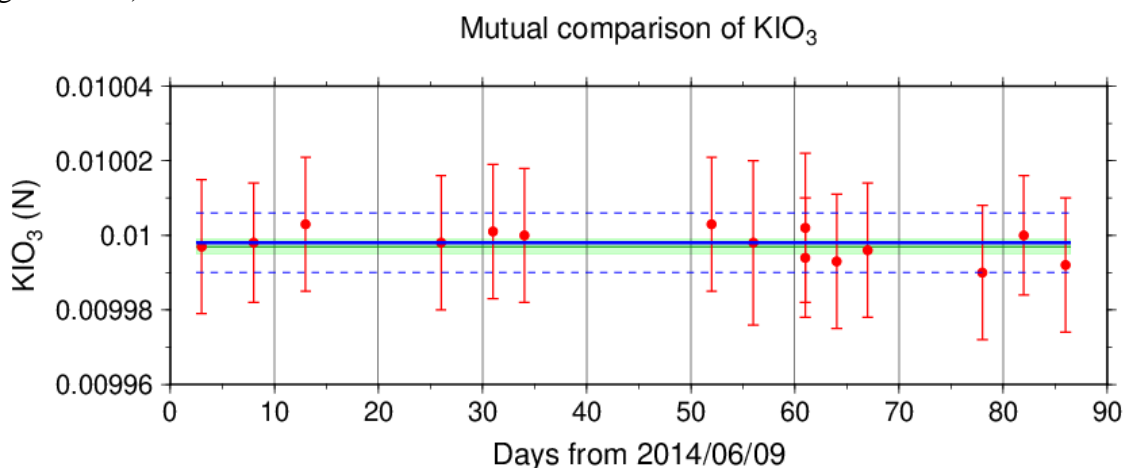


Figure C.3.6. Result of mutual comparison of standard KIO₃ solutions. Circles and error bars show mean of the measurement value and its uncertainty (k=2), respectively. Thick and dashed lines in blue denote the mean and 2 times of standard deviations, respectively, for the measurement through the cruise. Green thin line and light green thick line denote nominal concentration and its uncertainty (k=2) of standard KIO₃ solution “20140218-1”.

(7.3) Quality control flag assignment

Quality flag value was assigned to oxygen measurements as shown in Table C.3.3, using the code defined in IOCCP Report No.14 (Swift, 2010).

Table C.3.3. Summary of assigned quality control flags.

Flag	Definition	Number of samples
2	Good	3104
3	Questionable	49
4	Bad (Faulty)	32
5	Not reported	1
6	Replicate measurements	349
Total number of samples		3535

(8) Uncertainty

Oxygen measurement involves various uncertainties; determination of glass bottles volume, repeatability and systematic error of burette discharge, repeatability of pickling reagents discharge, determination of reagent blank, standardization of $\text{Na}_2\text{S}_2\text{O}_3$ solution, and uncertainty of KIO_3 concentration. Considering evaluable uncertainties as above, expanded uncertainty of bottle oxygen concentration ($T=20$, $S=34.5$) was estimated as shown in Table C.3.4. However, it is difficult to determine a strict uncertainty for oxygen concentration because there is no reference material for oxygen measurement.

Table C.3.4 Expanded uncertainty ($k=2$) of bottle oxygen in the cruise.

O ₂ conc. ($\mu\text{mol kg}^{-1}$)	Uncertainty ($\mu\text{mol kg}^{-1}$)
20	0.27
30	0.28
50	0.32
70	0.36
100	0.43
150	0.58
200	0.73
250	0.89
300	1.06
400	1.39

Appendix

A1. Methods

(A1.1) Seawater sampling

Following procedure is based on a determination method in IOCCP Report (Langdon, 2010). Seawater samples were collected from 10-liters Niskin bottles attached the CTD-system and a stainless steel bucket for the surface. Seawater for bottle oxygen measurement was transferred from the Niskin bottle and a stainless steel bucket to a volumetrically calibrated dry glass bottles. At least three times the glass volume water was overflowed. Then, pickling reagent-I 1 mL and reagent-II 1 mL were added immediately, and sample temperature was measured using a thermometer. After a stopper was inserted carefully into the glass, it was shaken vigorously to mix the content and to disperse the precipitate finely. After the precipitate has settled at least halfway down the glass, the glass was shaken again. The sample glasses containing pickled samples were stored in a laboratory until they were titrated. To prevent air from entering the glass, deionized water (DW) was added to its neck after sampling.

(A1.2) Sample measurement

At least 15 minutes after the re-shaking, the samples were measured on board. Added 1 mL H₂SO₄ solution and a magnetic stirrer bar into the sample glass, samples were titrated with Na₂S₂O₃ solution whose molarity was determined with KIO₃ solution. During the titration, the absorbance of iodine in the solution was monitored using a detector. Also, temperature of Na₂S₂O₃ solution during the titration was recorded using a thermometer. Dissolved oxygen concentration ($\mu\text{mol kg}^{-1}$) was calculated from sample temperature at the fixation, CTD salinity, glass volume, and titrated volume of the Na₂S₂O₃ solution, and oxygen in the pickling reagents-I (1 mL) and II (1 mL) (7.6×10^{-8} mol; Murray *et al.*, 1968).

A2. Reagents recipes

Pickling reagent-I; Manganous chloride solution (3 mol L⁻¹)

Dissolve 600 g of MnCl₂·4H₂O in DW, then dilute the solution with DW to a final volume of 1 L.

Pickling reagent-II; Sodium hydroxide (8 mol L⁻¹) / sodium iodide solution (4 mol L⁻¹)

Dissolve 320 g of NaOH in about 500 mL of DW, allow to cool, then add 600 g NaI and dilute with DW to a final volume of 1 L.

H₂SO₄ solution; Sulfuric acid solution (5 mol L⁻¹)

Slowly add 280 mL concentrated H₂SO₄ to roughly 500 mL of DW. After cooling the final volume should be 1 L.

Na₂S₂O₃ solution; Sodium thiosulfate solution (0.04 mol L⁻¹)

Dissolve 50 g of Na₂S₂O₃·5H₂O and 0.4 g of Na₂CO₃ in DW, then dilute the solution with DW to a final volume of 5 L.

KIO₃ solution; Potassium iodate solution (0.001667 mol L⁻¹)

Dry high purity KIO_3 for two hours in an oven at 130°C . After weight out accurately KIO_3 , dissolve it in DW in a 5 L flask. Concentration of potassium iodate is determined by a gravimetric method.

A3. Other blanks in oxygen measurement

(A3.1) Blank associated with oxidants or reductants in the reagents

The blank $V_{\text{blk, reg}}$, associated with oxidants or reductants in the reagent, was determined as follows. Using a calibrated pipette, 1 mL of the standard KIO_3 solution and 100 mL of DW were added to two glasses each. Then, 1 mL H_2SO_4 solution, 1 mL of pickling reagent-II and 1 mL reagent-I were added in sequence into the first glass. Next, added two times volume of the reagents (2 mL of H_2SO_4 solution, pickling reagent-II and I each) into the second one. After that, the sample was titrated to the end-point with $\text{Na}_2\text{S}_2\text{O}_3$ solution. $V_{\text{blk, reg}}$ was determined with difference of titrated volume of $\text{Na}_2\text{S}_2\text{O}_3$ between the first (total reagents volume is 3 mL) and the second (total reagents volume is 6 mL) one, also, experiments for three times and four times volume of them were carried out. The results are shown in Figure C.3.A1.

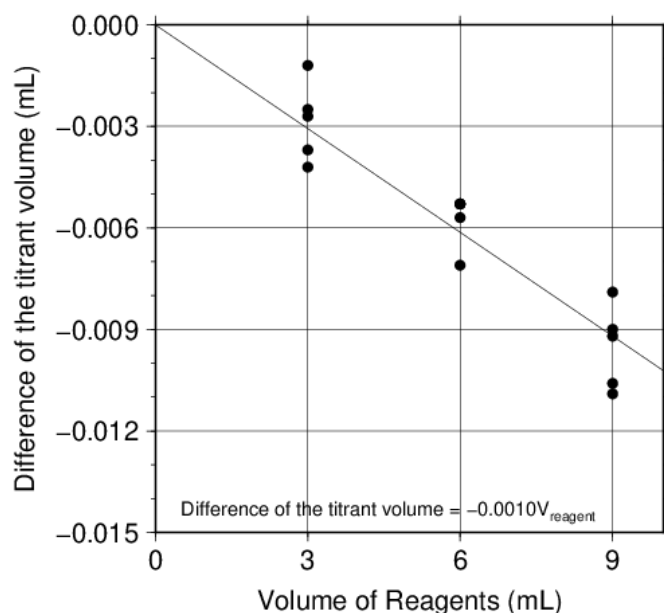


Figure C.3.A1. Blank (mL) due to redox species other than oxygen in the reagents.

The relation between difference of the titrant volume and the reagents of the volume (V_{reg}) is expressed as follows;

$$\text{Difference of the titrant volume} = -0.0010 V_{\text{reg}}. \quad (\text{C3.A1})$$

Therefore, $V_{\text{blk, reg}}$ was estimated to be about +0.004 mL.

(A3.2) Sample blank ($V_{\text{blk, spl}}$)

Blank due to redox species other than oxygen in the sample ($V_{\text{blk, spl}}$) can be a potential source of measurement error. Total blank during seawater measurement, seawater blank ($V_{\text{blk, sw}}$), can be represented as follows;

$$V_{\text{blk, sw}} = V_{\text{blk, spl}} + V_{\text{blk, dw}}. \quad (\text{C3.A2})$$

If the $V_{\text{blk, dw}}$ determined in eq. (C3.1) is identical both in seawater and in pure water, the difference between the seawater and reagent blanks gives the $V_{\text{blk, spl}}$.

Here, $V_{\text{blk, spl}}$ was determined by following procedure. Seawater was collected in the calibrated volumetric glass without the pickling solution. Then 1 mL of the standard KIO_3 solution, H_2SO_4 solution, and reagent solution-II and I each were added in sequence into the glass. After that, the sample was titrated to the end-point by $\text{Na}_2\text{S}_2\text{O}_3$ solution. Similarly, a glass contained 100 mL of DW added with 1 mL of the standard KIO_3 solution, H_2SO_4 solution, pickling reagent solution-II and I were titrated with $\text{Na}_2\text{S}_2\text{O}_3$ solution. The difference of the titrant volume of the seawater and DW glasses gave $V_{\text{blk, spl}}$.

The sample blank has been reported from 0.4 to 0.8 $\mu\text{mol kg}^{-1}$ in the previous study (Culberson *et al.*, 1991). Additionally, these errors are expected to be the same to all investigators and not to affect the comparison of results from different investigators (Culberson, 1994). However, the magnitude and variability of the seawater blank have not yet been documented. We believe that understanding of the magnitude and variability may be important to evaluate comparability of computed oxygen concentrations with other groups. The determined sample blanks are shown in Table C.3.A1.

Table C.3.A1. Results of the sample blank determinations.

Station: RF5113 34°-00'N/149°-18'E		Station: RF5126 41°-00'N/144°-42'E		Station: RF5143 40°-01'N/154°-20'E	
Depth (m)	Blank ($\mu\text{mol kg}^{-1}$)	Depth (m)	Blank ($\mu\text{mol kg}^{-1}$)	Depth (m)	Blank ($\mu\text{mol kg}^{-1}$)
11	0.50	50	0.58	26	0.51
251	0.71	331	0.87	26	0.52
602	0.69	832	0.74	401	0.52
1001	0.66	832	0.66	901	0.51
1798	0.63	1270	0.74	1400	0.62
1798	0.64	2071	0.67	2250	0.60
2598	0.57	3080	0.80	2751	0.60
3252	0.76	3830	0.83	3502	0.75
4247	0.78	4831	0.76	4501	0.93
5000	0.73	4831	0.74	5250	0.89
5748	0.67	5581	0.77	5250	0.60
5748	0.84	6005	0.74	5540	0.96

Table C.3.A1. (continued)

Station: RF5154 30°-30'N/149°-23'E		Station: RF5169 20°-30'N/149°-20'E		Station: RF5200 3°-31'N/147°-14'E	
Depth (m)	Blank ($\mu\text{mol kg}^{-1}$)	Depth (m)	Blank ($\mu\text{mol kg}^{-1}$)	Depth (m)	Blank ($\mu\text{mol kg}^{-1}$)
49	0.75	103	0.24	101	0.78
152	0.71	498	0.81	101	0.72
152	0.74	498	0.74	151	0.78
403	0.74	702	0.80	320	0.64
803	0.70	1003	0.71	670	0.83
1405	0.81	1602	0.78	1131	0.87
2206	0.74	2402	0.85	1931	0.93
3006	0.85	2800	0.83	2532	0.84
3999	0.81	3002	0.80	3171	0.92
5000	0.74	3251	0.81	3921	0.88
5000	0.85	3251	0.82	3921	0.84
5498	0.83	3500	0.90	4571	0.88
		3500	0.77		
		3751	1.17		
		3751	1.05		
		4517	0.76		

Table C.3.A1. (continued)

Station: RF5213 0°-01'S/146°-09'E				Station: RF5234 2°-10'S/141°-29'E		Station: RF5239 2°-00'N/142°-01'E	
Depth (m)	Blank ($\mu\text{mol kg}^{-1}$)	Depth (m)	Blank ($\mu\text{mol kg}^{-1}$)	Depth (m)	Blank ($\mu\text{mol kg}^{-1}$)	Depth (m)	Blank ($\mu\text{mol kg}^{-1}$)
11	0.51	800	0.74	10	0.57	11	0.47
26	0.48	900	0.86	25	0.61	26	0.49
50	0.51	1001	0.73	50	0.62	52	0.46
74	0.64	1201	0.79	74	0.69	75	0.52
74	0.64	1401	0.76	100	0.76	101	0.57
100	0.75	1600	0.79	125	0.67	126	0.62
125	0.67	1800	0.69	125	0.65	151	0.73
150	0.80	1800	0.80	149	0.67	202	0.71
150	0.69	2000	0.76	200	0.74	202	0.65
201	0.74	2201	0.82	250	0.76	251	0.69
250	0.79	2401	0.70	280	0.75	301	0.81
299	0.75	2600	0.81	321	0.78	351	0.69
350	0.82	2800	0.79	422	0.76	401	0.72
400	0.79	3001	0.76	869	0.74	451	0.62
449	0.81	3250	0.77	1532	0.78	701	0.70
501	0.70	3527	0.67	2131	0.78	1002	0.63
600	0.81	3527	0.86	2131	0.73		
700	0.73	-	-	2932	0.83		
				3672	0.79		
				4146	0.76		

Reference

- Culberson, A.H. (1994) Dissolved oxygen, in WHPO Pub. 91-1 Rev. 1, November 1994, Woods Hole, Mass., USA.
- Culberson, A.H., G. Knapp, M.C. Stalcup, R.T. Williams, and F. Zemlyak (1991) A comparison of methods for the determination of dissolved oxygen in seawater, WHPO Pub. 91-2, August 1991, Woods Hole, Mass., USA.
- DOE (1994), Handbook of methods for the analysis of the various parameters of the carbon dioxide system in sea water; version 2. *A.G. Dickson and C. Goyet (eds), ORNL/CDIAC-74.*
- Langdon, C. (2010), Determination of dissolved oxygen in seawater by Winkler titration using the amperometric technique, *IOCCP Report No.14, ICPO Pub. 134, 2010 ver.1*
- Murray, C. N., J. P. Riley and T. R. S. Wilson (1968), The solubility of oxygen in Winkler reagents used for the determination of dissolved oxygen. *Deep-Sea Res.* 15, 237–238.
- Swift, J. H. (2010), Reference-quality water sample data: Notes on acquisition, record keeping, and evaluation. *IOCCP Report No.14, ICPO Pub. 134, 2010 ver.1.*

Nutrients

Updated 17 October 2023

(1) Personnel

RF14-05

Naoshi KUBO (GEMD/JMA)

Takahiro KITAGAWA (GEMD/JMA)

Chihiro KAWAMURA (GEMD/JMA)

RF14-06

Takahiro KITAGAWA (GEMD/JMA)

Minoru HAMANA (GEMD/JMA)

Chihiro KAWAMURA (GEMD/JMA)

RF14-07

Hiroyuki FUJIWARA (GEMD/JMA)

Tomohiro UEHARA (GEMD/JMA)

Minoru HAMANA (GEMD/JMA)

(2) Station occupied

A total of 107 stations (RF14-05: 17, RF14-06: 26, RF14-07 Leg 1: 43, Leg 2: 21) were occupied for nutrients measurements. Station location and sampling layers of nutrients are shown in Figures C.4.1 and C.4.2.

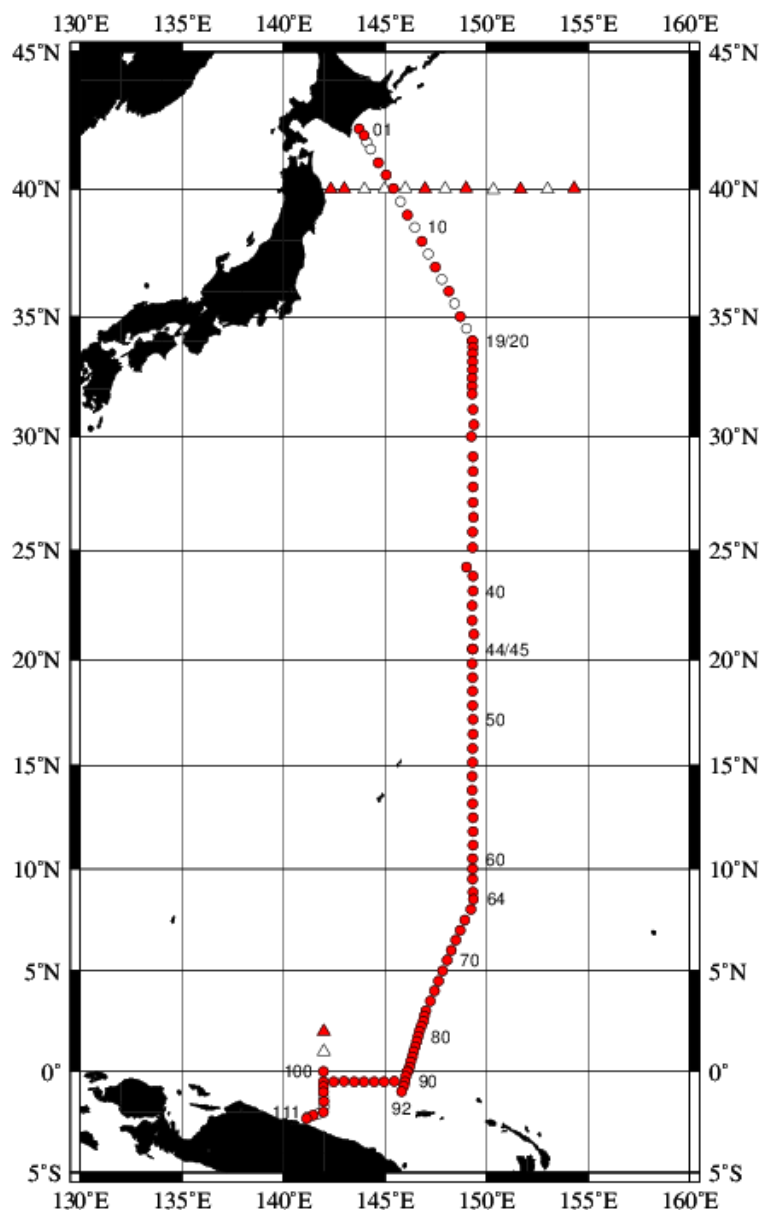


Figure C.4.1. Location of observation stations of nutrients. Closed and open circles indicate sampling and no-sampling stations, respectively. Triangles show sampling station which is not reported in the bottle data file, but the data at closed triangle is used for quality control of nutrient. These data are available from the JMA(https://www.data.jma.go.jp/gmd/kaiyou/db/vessel_obs/data-report/html/ship/ship_e.php?year=2014&season=spring and https://www.data.jma.go.jp/gmd/kaiyou/db/vessel_obs/data-report/html/ship/ship_e.php?year=2014&season=summer).

Bottle Depth Diagram along P10

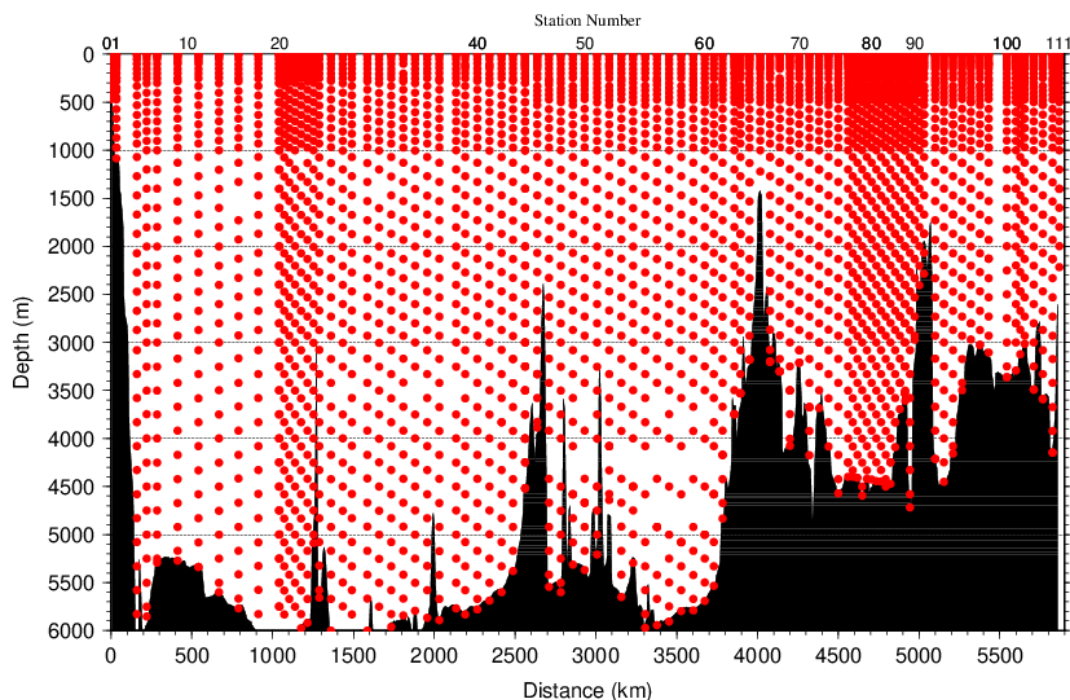


Figure C.4.2. Distance-depth distributions of sampling layers of nutrients.

(3) Instrument

The nutrients analysis was carried out on 4-channel Auto Analyzer III (BL TEC K.K., Japan) for 4 parameters; nitrate+nitrite, nitrite, phosphate, and silicate.

(4) Sampling and measurement

Methods of seawater sampling, measurement, and data processing of nutrient concentration were described in Appendixes A1, A2, and A3, respectively. The reagents for the measurement were prepared according to recipes shown in Appendix A4.

(5) Nutrients standards

(5.1) Volumetric laboratory ware of in-house standards

All volumetric wares were gravimetrically calibrated. The weights obtained in the calibration weighing were corrected for the density of water and for air buoyancy. Polymethylpenten volumetric flasks were gravimetrically calibrated at the temperature of use within 4–6 °C. All pipettes have nominal calibration tolerances of 0.1 % or better. These were gravimetrically calibrated in order to verify and improve upon this nominal tolerance.

(5.2) Reagents of standard

The batches of the reagents used for standard are listed in Table C.4.1.

Table C.4.1. List of reagents of standard used in the cruise.

	Name	CAS No	Lot. No	Industries
Nitrate	potassium nitrate 99.995 suprapur®	7757-79-1	B0771365	Merck KGaA
Nitrite	sodium nitrite GR for analysis ACS, Reag. Ph Eur	7632-00-0	A0544949	Merck KGaA
Phosphate	potassium dihydrogen phosphate anhydrous 99.995 suprapur®	7778-77-0	B0960508	Merck KGaA
Silicate	Silicon standard solution 1000 mg/l Si*	-	HC247279	Merck KGaA

* Traceable to NIST-SRM3150

(5.3) Low nutrient seawater (LNSW)

Surface water with sufficiently low nutrient concentration was taken and filtered using 10 µm pore size membrane filter in our previous cruise. This water was stored in 20 liter flexible container with paper box.

(5.4) In-house standard solutions

Nutrient concentrations for A, B and C standards were set as shown in Table C.4.2. A and B standards were prepared with deionized water (DW). C standard (full scale of working standard) was mixture of B-1 and B-2 standards, and was prepared with LNSW. C-1 standard, whose concentrations of nutrient were nearly zero, was prepared as LNSW slightly added with DW to be equal with mixing ratio of LNSW and DW in C standard. The C-2 to -5 standards were prepared with mixture of C-1 and C standards in stages as 1/4, 2/4, 3/4, and 4/4 (i.e., pure “C standard”) concentration for full scale, respectively. The actual concentration of nutrients in each standard was calculated based on the solution temperature and factors of volumetric laboratory wares calibrated prior to use. Nominal zero concentration of nutrient was determined in measurement of DW after refraction error correction. The calibration curves for each run were obtained using 5 levels of C-1 to -5 standards. These standard solutions were periodically renewed as shown in Table C.4.3.

Table C.4.2. Nominal concentrations of nutrients for A, B, and C standards at 20°C. Unit is $\mu\text{mol L}^{-1}$.

	A	B	C
Nitrate	27470	550	43.7
Nitrite	12460	250	2.0
Phosphate	2150	43	3.42
Silicate	35680	2130	170

Table C.4.3. Schedule of renewal of in-house standards.

Standard	Renewal
A-1 std. (NO_3)	No renewal
A-2 std. (NO_2)	No renewal
A-3 std. (PO_4)	No renewal
A-4 std. (Si)	Commercial prepared solution
B-1 std. (mixture of A-1, A-3, and A-4 stds.)	Maximum 8 days
B-2 std. (diluted A-2 std.)	Maximum 15 days
C-std. (mixture of B-1 and B-2 stds.)	Every measurement
C-1 to -5 stds.	Every measurement

(6) Certified reference material

Certified reference material (CRM) and reference material (RM) for nutrients in seawater, which were prepared by the General Environmental Technos (KANSO Technos, Japan), was used every analysis at each hydrographic station. Using CRMs and RMs for the analysis of seawater, stable comparability and uncertainty of our data are secured.

CRMs and RMs used in the cruise are shown in Table C.4.4.

Table C.4.4. Certified concentration and uncertainty ($k=2$) of CRMs. Unit is $\mu\text{mol kg}^{-1}$.

	Nitrate	Nitrite	Phosphate	Silicate
CRM-BY	0.024±0.019*	0.019±0.0085*	0.039±0.010*	1.763±0.063
RM-BT	18.15±0.24	0.471±0.011	1.296±0.027	42.02±0.64
CRM-BV	35.36±0.35	0.047±0.0073	2.498±0.023	102.2±1.1
CRM-BX	43.00±0.45	0.034±0.0035	2.906±0.064	136.1±1.5

* Reference value because concentration is under limit of quantitation

The CRM-BY and -BV were analyzed every runs using newly opened bottle at each hydrographic station. The RM-BT and CRM-BX were also analyzed every runs but were newly opened every 2 or 3 runs. Although this usage of CRM might be less common, we have confirmed a stability of the opened bottles to be tolerance in our observation. The CRM and RM bottles were stored at a laboratory in the ship, where the temperature was maintained around 25°C.

It is noted that nutrient data in our report are calibrated not on CRM and RM but on in-house standard solutions. Therefore, to calculate data based on CRM and RM, it is necessary that values of nutrient concentration in our report are correlated with CRM and RM values measured in the same analysis run. The result of CRM and RM measurements is attached as 49UP20140609_P10_nut_CRM_measurement.csv.

(7) Quality Control

(7.1) Replicate and duplicate analyses

We took replicate (pair of water samples taken from a single Niskin bottle) and duplicate (pair of water samples taken from different Niskin bottles closed at the same depth) samples of nutrient through the cruise. Results of the analyses are summarized in Table C.4.5. Detailed results of them are shown in Figures C.4.3–C.4.5. The calculation of the standard deviation from the difference of sets was based on a procedure (SOP 23) in DOE (1994).

Table C.4.5. Average and standard deviation of difference of replicate and duplicate measurements through the cruise. Unit is $\mu\text{mol kg}^{-1}$.

Measurement	Nitrate+nitrite	Phosphate	Silicate
Replicate	0.033±0.032 (N=375)	0.002±0.002 (N=368)	0.093±0.092 (N=372)
Duplicate	0.045±0.044 (N=151)	0.003±0.003 (N=144)	0.121±0.109 (N=151)

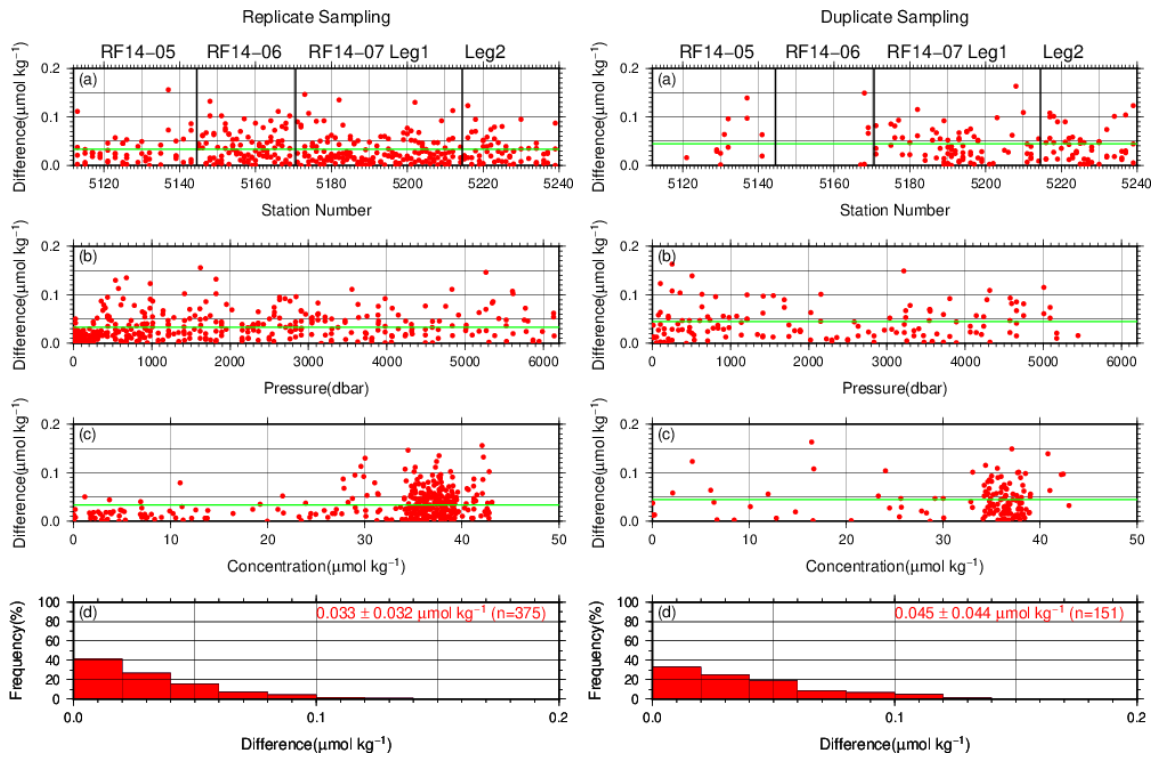


Figure C.4.3. Result of (left) replicate and (right) duplicate measurements of nitrate+nitrite through the cruise versus (a) station number, (b) sampling pressure, (c) concentration, and (d) histogram of the measurements. Green line indicates the mean of the differences of concentration of replicate/duplicate analyses.

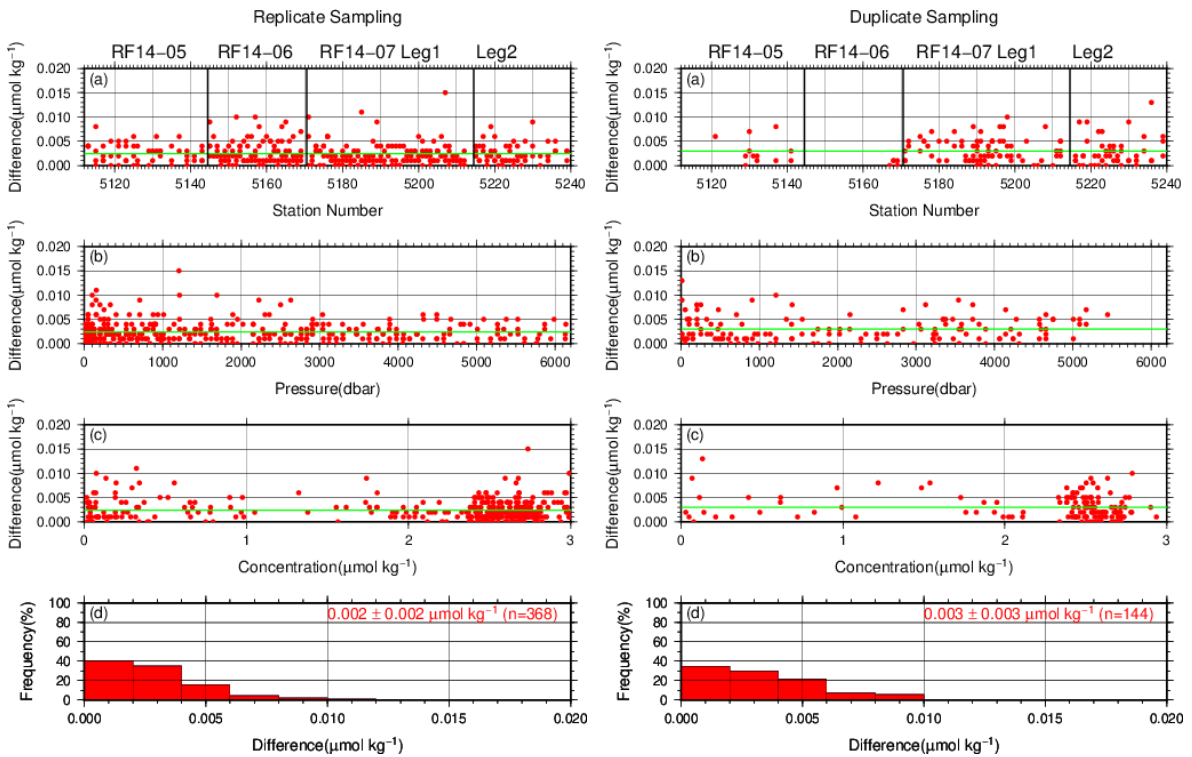


Figure C.4.4. Same as Figure C.4.3 but for phosphate.

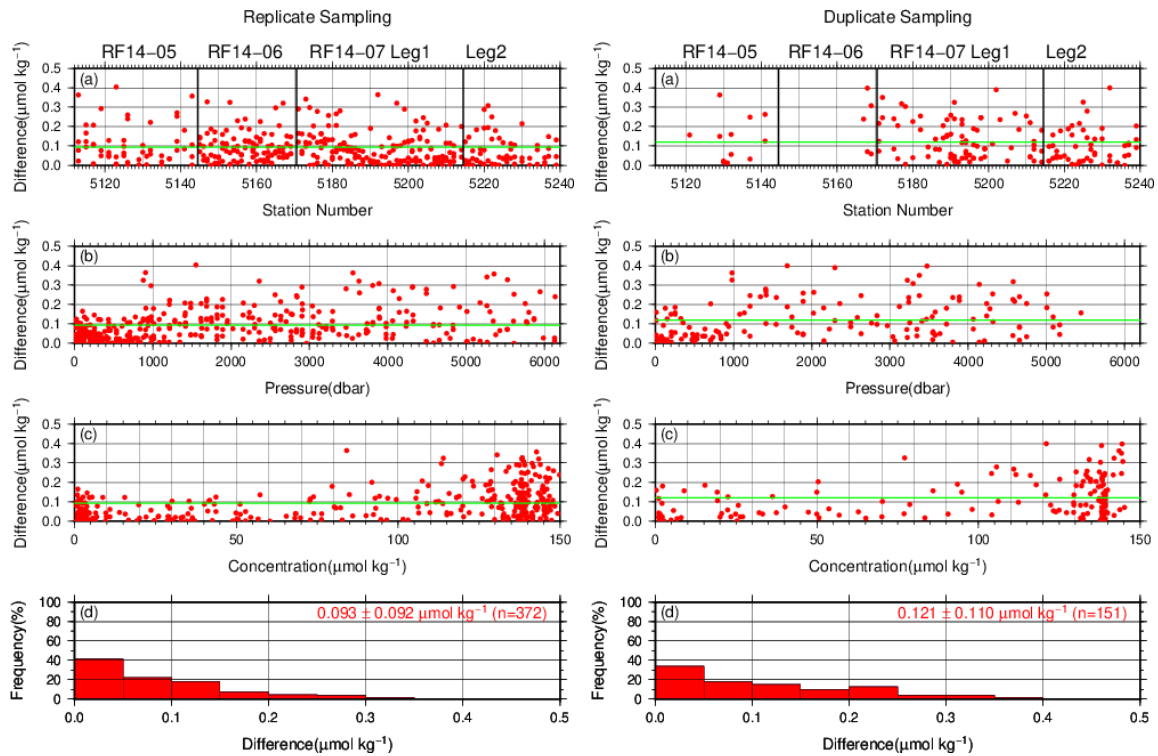


Figure C.4.5. Same as Figure C.4.3 but for silicate.

(7.2) Measurement of CRMs and RMs

CRM and RM measurements during the cruise are summarized in Table C.4.6, whose concentrations were assigned with in-house standard solutions. The measured concentrations of CRM-BX through the cruise are shown in Figures C.4.6–C.4.9.

Table C.4.6. Summary of (upper) mean concentration and its standard deviation (unit: $\mu\text{mol kg}^{-1}$), (middle) coefficient of variation (%), and (lower) total number of CRMs and RMs measurements through the cruise.

	Nitrate+nitrite	Nitrite	Phosphate	Silicate
CRM-BY	0.046 ± 0.030	0.021 ± 0.002	0.037 ± 0.004	1.70 ± 0.07
	65.47%	9.95%	10.92%	4.30%
	(N=231)	(N=230)	(N=229)	(N=233)
RM-BT	18.59 ± 0.04	0.470 ± 0.003	1.29 ± 0.01	41.93 ± 0.14
	0.24%	0.61%	0.54%	0.35%
	(N=166)	(N=168)	(N=164)	(N=168)
CRM-BV	35.33 ± 0.06	0.057 ± 0.125	2.50 ± 0.01	102.16 ± 0.29
	0.18%	2.19%	0.27%	0.28%
	(N=232)	(N=234)	(N=230)	(N=234)
CRM-BX	43.13 ± 0.08	0.036 ± 0.002	2.88 ± 0.01	137.93 ± 0.24
	0.18%	5.00%	0.25%	0.17%
	(N=166)	(N=168)	(N=164)	(N=167)

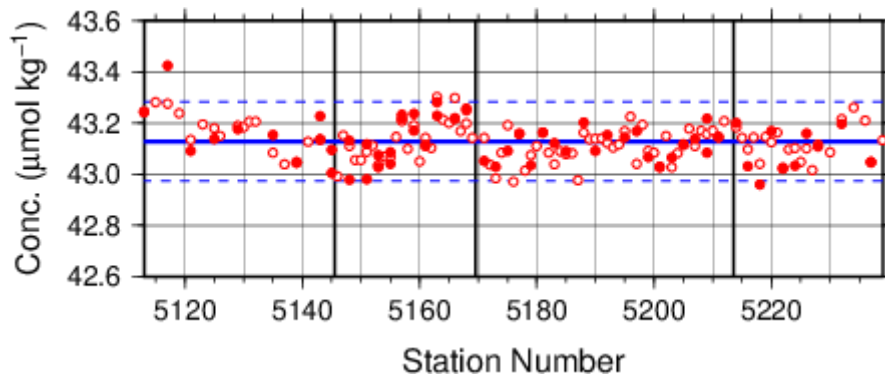


Figure C.4.6. Time-series of measured concentration of nitrate+nitrite of CRM-BX through the cruise. Closed and open circles indicate the newly and previously opened bottle, respectively. Thick and dashed lines denote the mean and 2 times of standard deviations of the measurements through the cruise, respectively.

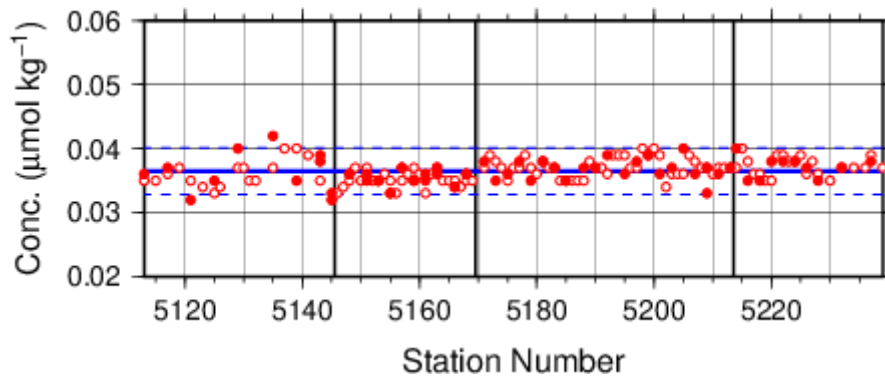


Figure C.4.7. Same as Figure C.4.6 but for nitrite.

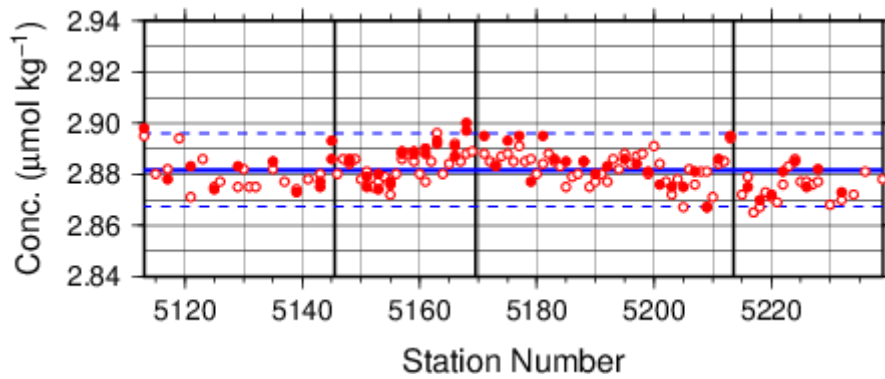


Figure C.4.8. Same as Figure C.4.6 but for phosphate.

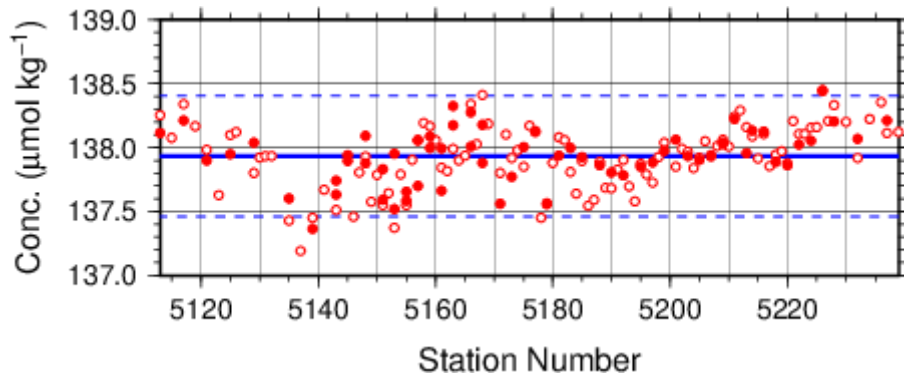


Figure C.4.9. Same as Figure C.4.6 but for silicate.

(7.3) Precision of analysis in a run

To monitor precision of analysis, the same samples were repeatedly measured in a sample array in a run. For this, C-5 standard solutions were randomly arrayed in every 2–10 samples as “check standard” (the number of the standard is about 8–9) in the run. The precision was estimated as coefficient of variation of the measurements. The results are summarized in Table C.4.7. The time series are shown in Figures C.4.10–C.4.13.

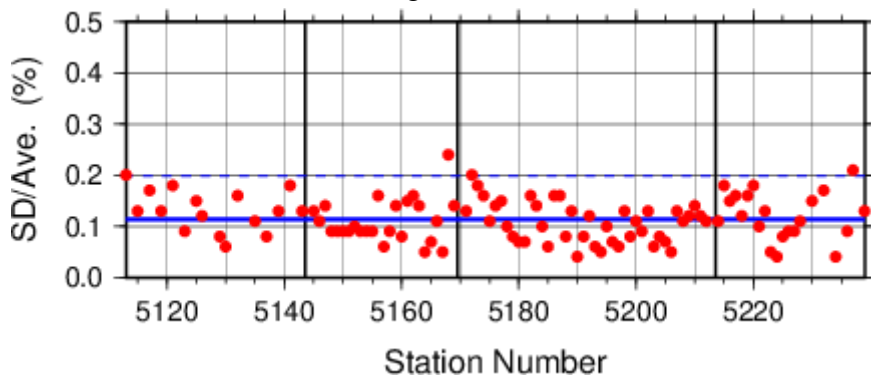


Figure C.4.10. Time-series of coefficient of variation of “check standard” measurement of nitrate+nitrite through the cruise. Thick and dashed lines denote the mean and 2 times of standard deviations of the measurements through the cruise, respectively.

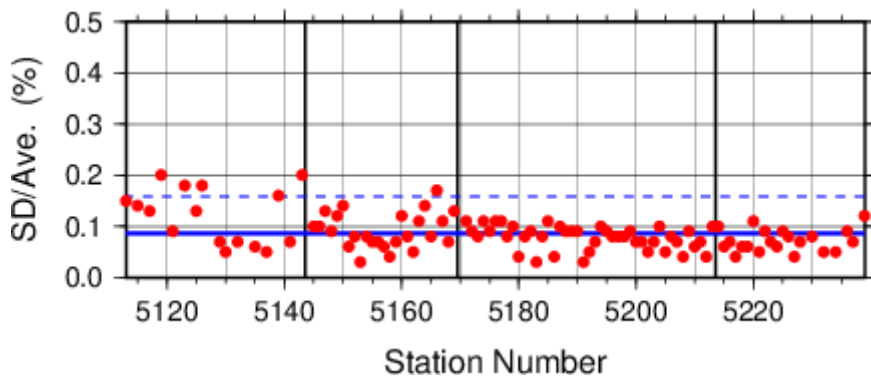


Figure C.4.11. Same as Figure C.4.10 but for nitrite.

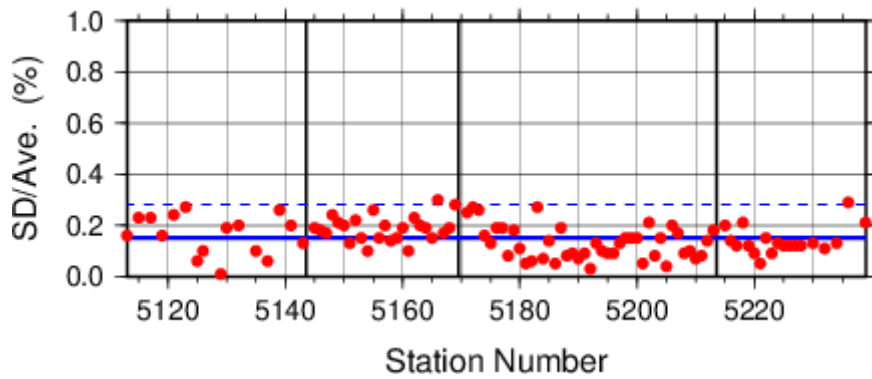


Figure C.4.12. Same as Figure C.4.10 but for phosphate.

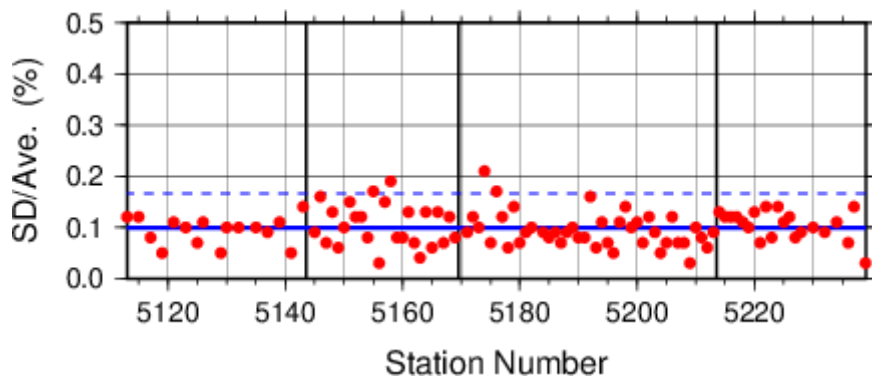


Figure C.4.13. Same as Figure C.4.10 but for silicate.

Table C.4.7. Summary of precisions during the cruise.

	Nitrate+nitrite	Nitrite	Phosphate	Silicate
Median	0.11%	0.08%	0.15%	0.10%
Mean	0.11%	0.09%	0.15%	0.10%
Minimum	0.04%	0.03%	0.01%	0.03%
Maximum	0.24%	0.20%	0.30%	0.21%
Number	104	105	103	104

(7.4) Carryover

Carryover coefficients were determined in each analysis run, using C-5 standard (high standard) followed by two C-1 standards (low standard). Time series of the carryover coefficients are shown in Figures C.4.14–17.

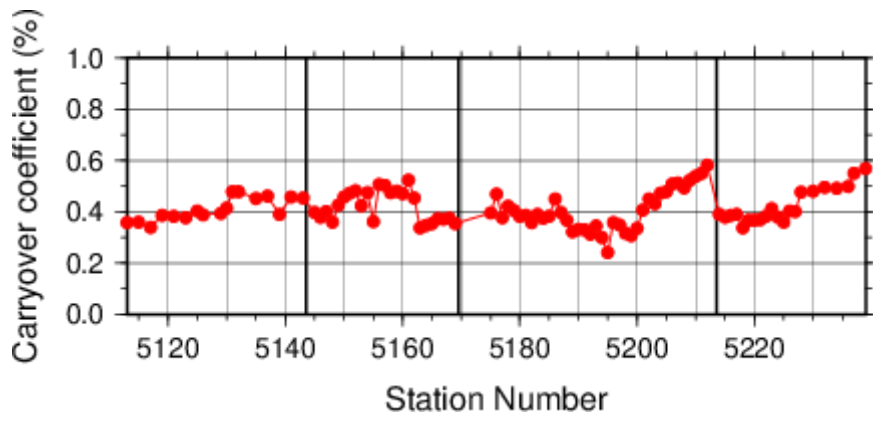


Figure C.4.14. Time-series of carryover coefficients in measurement of nitrate+nitrite through the cruise.

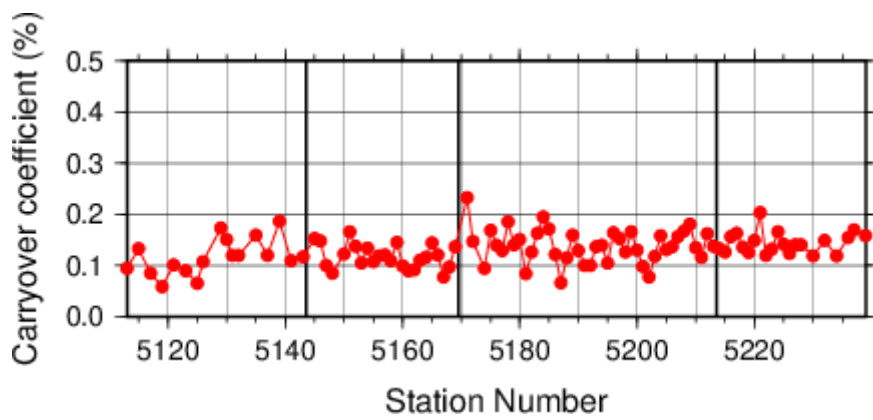


Figure C.4.15. Same as Figure C.4.14 but for nitrite.

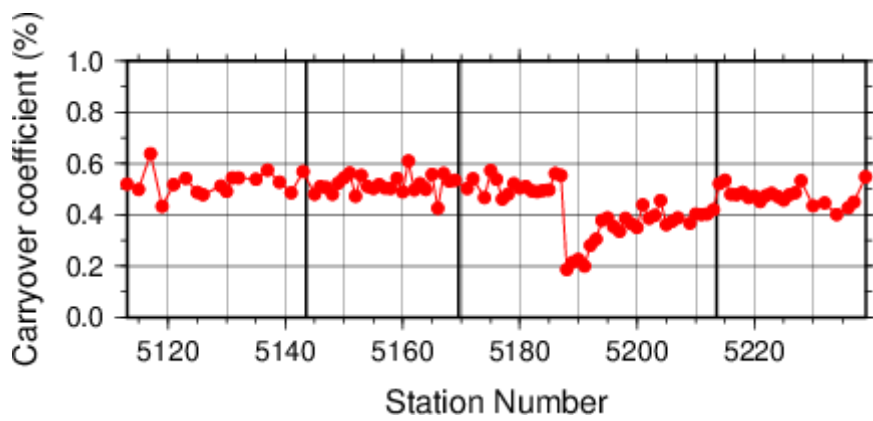


Figure C.4.16. Same as Figure C.4.14 but for phosphate.

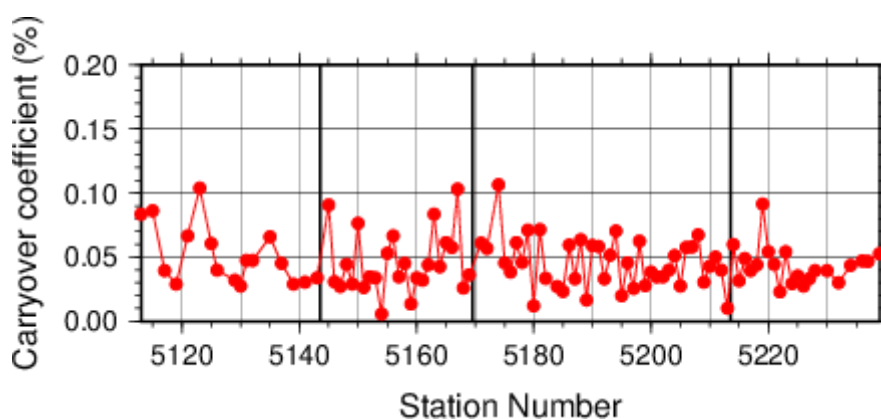


Figure C.4.17. Same as Figure C.4.14 but for silicate.

(7.5) Limit of detection/quantitation of measurement

Limit of detection (LOD) and quantitation (LOQ) of nutrient measurement were estimated from standard deviation (σ) of repeated measurements of nutrients concentration in C-1 standard as 3σ and 10σ , respectively. Summary of LOD and LOQ are shown in Table C.4.8.

Table C.4.8. Limit of detection (LOD) and quantitation (LOQ) of nutrient measurement in the cruise. Unit is $\mu\text{mol kg}^{-1}$.

	LOD	LOQ
Nitrate+nitrite	0.036	0.121
Nitrite	0.002	0.005
Phosphate	0.013	0.044
Silicate	0.088	0.294

(7.6) Quality control flag assignment

Quality flag value was assigned to nutrient measurements as shown in Table C.4.9, using the code defined in IOCCP Report No.14 (Swift, 2010).

Table C.4.9. Summary of assigned quality control flags.

Flag	Definition	Nitrate+nitrite	Nitrite	Phosphate	Silicate
2	Good	3111	3157	3087	3142
3	Questionable	14	0	7	19
4	Bad (Faulty)	55	17	87	16
5	Not reported	0	0	0	0
6	Replicate measurements	355	361	354	358
Total number of samples		3535	3535	3535	3535

(8) Uncertainty

(8.1) Uncertainty associated with concentration level: U_c

Generally, an uncertainty of nutrient measurement is expressed as a function of its concentration level which reflects that some components of uncertainty are relatively large in low concentration. Empirically, the uncertainty associated with concentrations level (U_c) can be expressed as follows;

$$U_c (\%) = a + b \cdot (1/C_x) + c \cdot (1/C_x)^2, \quad (C4.1)$$

where C_x is the concentration of sample for parameter X.

Using the coefficients of variation of the CRM measurements throughout the cruise, uncertainty associated with concentrations of nitrate+nitrite, phosphate, and silicate were determined as follows:

$$U_{c-no3} (\%) = 0.130 + 2.002 \times (1/C_n) + 0.045 \times (1/C_n)^2 \quad (C4.2)$$

$$U_{c-po4} (\%) = 0.002 + 0.696 \times (1/C_p) - 0.011 \times (1/C_p)^2 \quad (C4.3)$$

$$U_{c-sil} (\%) = 0.130 + 5.400 \times (1/C_s) + 2.822 \times (1/C_s)^2, \quad (C4.4)$$

where C_n , C_p , and C_s represent concentrations of nitrate+nitrite, phosphate, and silicate, respectively, in $\mu\text{mol kg}^{-1}$. Figures C.4.18–C.4.20 show the calculated uncertainty graphically.

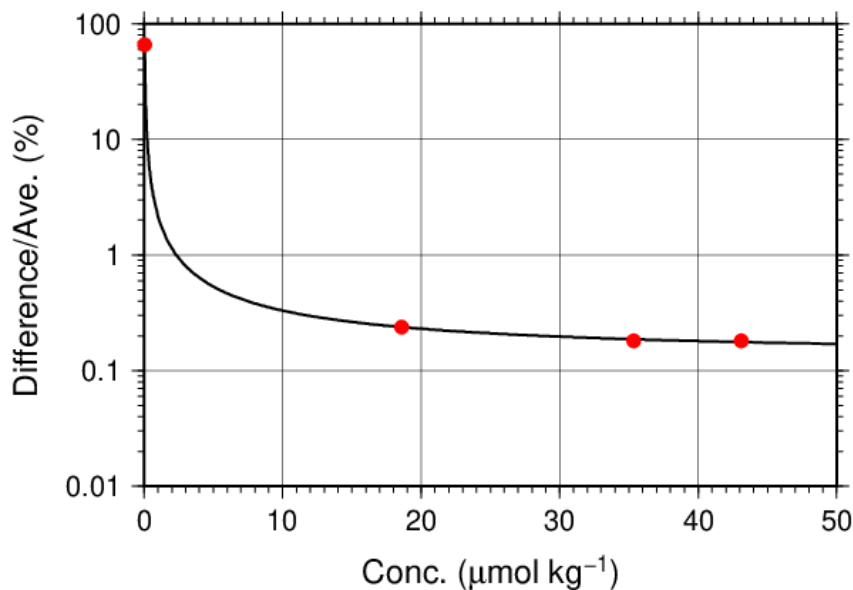


Figure C.4.18. Uncertainty of nitrate+nitrite associated with concentration level.

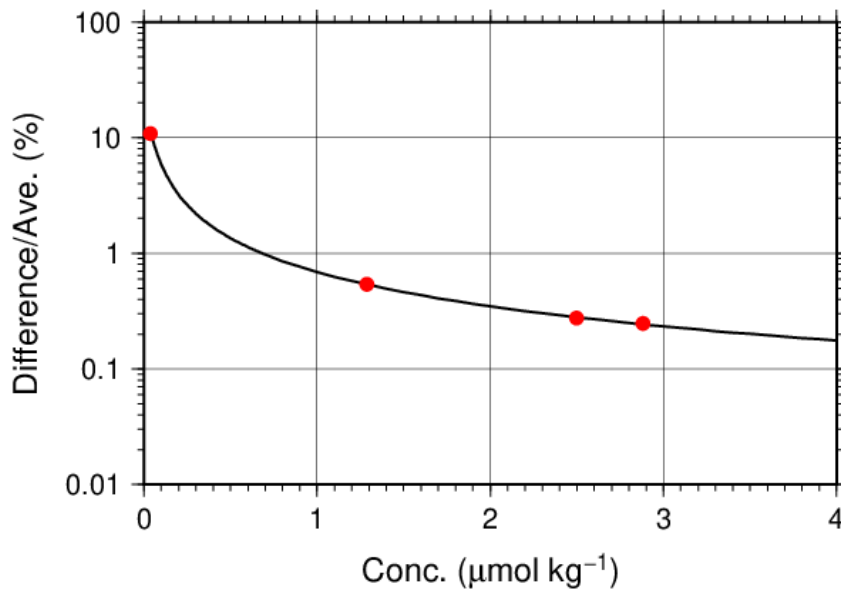


Figure C.4.19. Same as Figure C.4.18 but for phosphate.

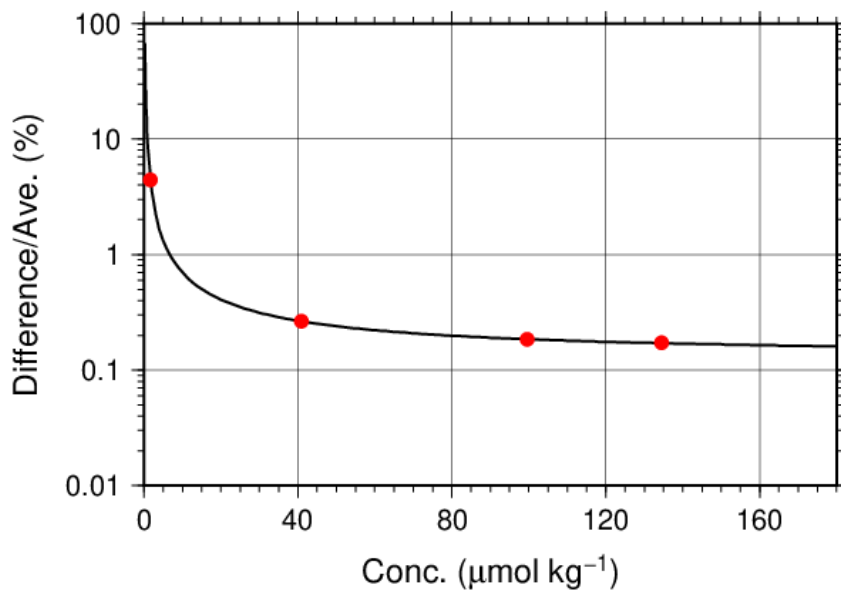


Figure C.4.20. Same as Figure C.4.A18 but for silicate.

(8.2) Uncertainty of analysis between runs: U_s

Uncertainty of analysis among runs (U_s) was evaluated based on the coefficient of variation of measured concentrations of CRM-BX with the highest concentration among the CRM lots throughout the cruise, as shown in subsection (7.2). The reason for using the CRM lot BX to state U_s is to exclude the effect of uncertainty associated with lower concentration described previously. As is clear from the definition of U_c , U_s is equal to U_c at nutrients concentrations of lot BX. It is important to note that U_s includes all of uncertainties during the measurements

throughout stations, namely uncertainties of concentrations of in-house standard solutions prepared for each run, uncertainties of slopes and intercepts of the calibration curve in each run if first order calibration curve applied, precision of measurement in a run (U_a), and between-bottle homogeneity of the CRM.

(8.3) Uncertainty of analysis in a run: U_a

Uncertainty of analysis in a run (U_a) was evaluated based on the coefficient of variation of repeated measurements of the “check standard” solution, as shown in subsection (7.3). The U_a reflects the conditions associated with chemistry of colorimetric measurement of nutrients, and stability of electronic and optical parts of the instrument throughout a run. Under a well-controlled condition of the measurements, U_a might show Poisson distribution with a mean as shown in Figures C.4.10–C.4.13 and Table C.4.7 and treated as a precision of measurement. U_a is a part of U_c at the concentration as stated in a previous section for U_c .

However, U_a may show larger value which was not expected from Poisson distribution of U_a due to the malfunction of the instruments, larger ambient temperature change, human errors in handling samples and chemistries and contaminations of samples in a run. In the cruise, we observed that U_a of our measurement was usually small and well-controlled in most runs as shown in Figures C.4.10–C.4.13 and Table C.4.7. However, in a few runs, U_a showed high values which were over the mean \pm twice the standard deviations of U_a , suggesting that the measurement system might have some problems.

(8.4) Uncertainty of CRM concentration: U_r

In the certification of CRM, the uncertainty of CRM concentrations (U_r) was stated by the manufacturer (Table C.4.4) as expanded uncertainty at $k=2$. This expanded uncertainty reflects the uncertainty of the Japan Calibration Service System (JCSS) solutions, characterization in assignment, between-bottle homogeneity, and long term stability. We have ensured comparability between cruises by ensuring that at least two lots of CRMs overlap between cruises. In comparison of nutrient concentrations between cruises using KANSO CRMs in an organization, it was not necessary to include U_r in the conclusive uncertainty of concentration of measured samples because comparability of measurements was ensured in an organization as stated previously.

(8.5) Conclusive uncertainty of nutrient measurements of samples: U

To determine the conclusive uncertainty of nutrient measurements of samples (U), we use two functions depending on U_a value acquired at each run as follows:

When U_a was small and measurement was well-controlled condition, the conclusive uncertainty of nutrient measurements of samples, U , might be as below:

$$U = U_c. \quad (C4.5)$$

When U_a was relative large and the measurement might have some problems, the conclusive uncertainty of nutrient measurements of samples, U , can be expanded as below:

$$U = \sqrt{U_c^2 + U_a^2}. \quad (\text{C4.6})$$

When U_a was relative large and the measurement might have some problems, the equation of U is defined as to include U_a to evaluate U , although U_a partly overlaps with U_c . It means that the equation overestimates the conclusive uncertainty of samples. On the other hand, for low concentration there is a possibility that the equation not only overestimates but also underestimates the conclusive uncertainty because the functional shape of U_c in lower concentration might not be the same and cannot be verified. However, we believe that the applying the above function might be better way to evaluate the conclusive uncertainty of nutrient measurements of samples because we can do realistic evaluation of uncertainties of nutrient concentrations of samples which were obtained under relatively unstable conditions, larger U_a as well as the evaluation of them under normal and good conditions of measurements of nutrients.

Appendix

A1. Seawater sampling

Seawater samples were collected from 10-liters Niskin bottle attached CTD-system and a stainless steel bucket for the surface. Samples were drawn into 10 mL polymethylpenten vials using sample drawing tubes. The vials were rinsed three times before water filling and were capped immediately after the drawing.

No transfer was made and the vials were set on an auto sampler tray directly. Samples were analyzed immediately after collection.

A2. Measurement

(A2.1) General

Auto Analyzer III is based on Continuous Flow Analysis method and consists of sampler, pump, manifolds, and colorimeters. As a baseline, we used artificial seawater (ASW).

(A2.2) Nitrate+nitrite and nitrite

Nitrate+nitrite and nitrite were analyzed according to the modification method of Armstrong (1967). The sample nitrate was reduced to nitrite in a glass tube which was filled with granular cadmium coated with copper. The sample stream with its equivalent nitrite was treated with an acidic, sulfanilamide reagent and the nitrite forms nitrous acid which reacts with the sulfanilamide to produce a diazonium ion. N-1-naphthylethylene-diamine was added to the sample stream then coupled with the diazonium ion to produce a red, azo dye. With reduction of the nitrate to nitrite, sum of nitrate and nitrite were measured; without reduction, only nitrite was measured. Thus, for the nitrite analysis, no reduction was performed and the alkaline buffer was not necessary. The flow diagrams for each parameter are shown in Figures C.4.A1 and C.4.A2. If the reduction efficiency of the cadmium column became lower than 95 %, the column was replaced.

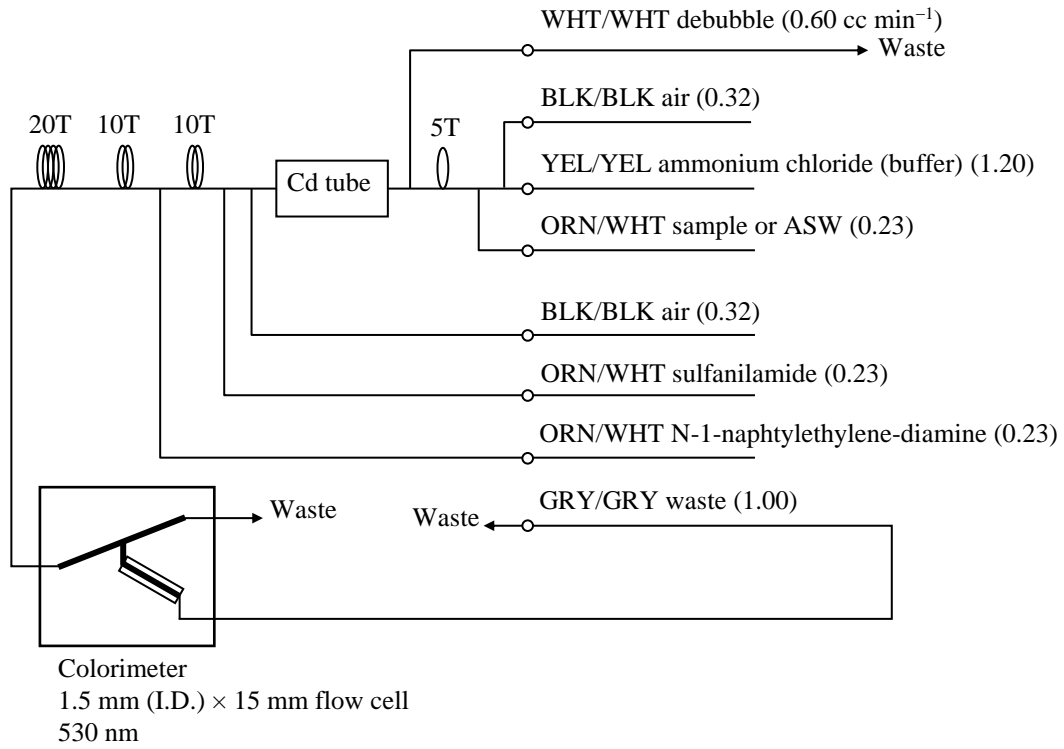


Figure C.4.A1. Nitrate+nitrite (1ch.) flow diagram.

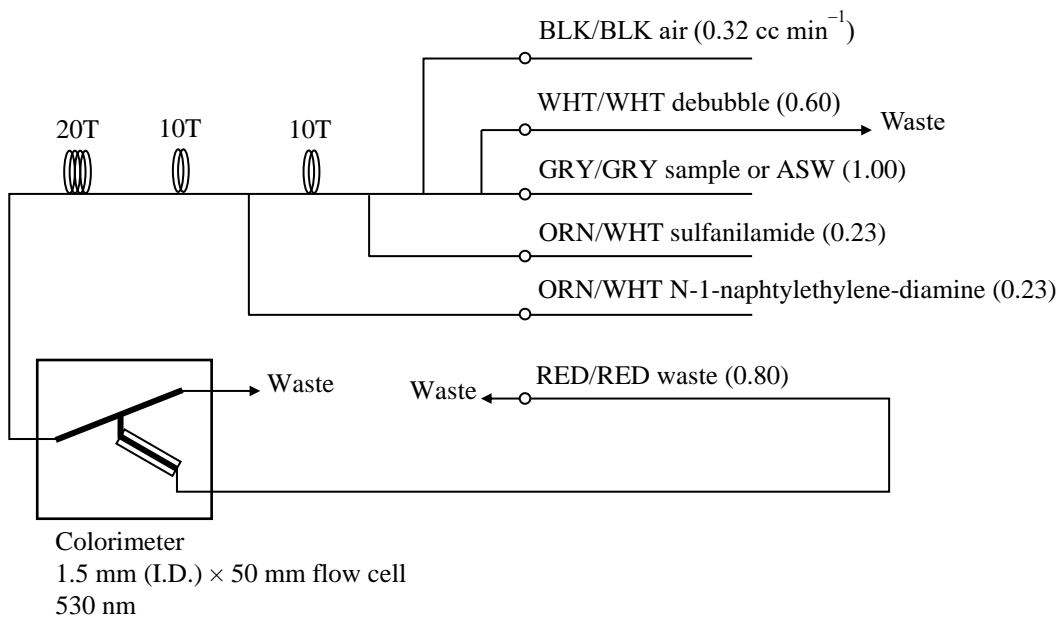


Figure C.4.A2. Nitrite (2ch.) flow diagram.

(A2.3) Phosphate

The phosphate analysis was a modification of the procedure of Murphy and Riley (1962). Molybdic acid was added to the seawater sample to form phosphomolybdic acid which was in turn reduced to phosphomolybdous acid using L-ascorbic acid as the reductant. The flow diagram for phosphate is shown in Figure C.4.A3.

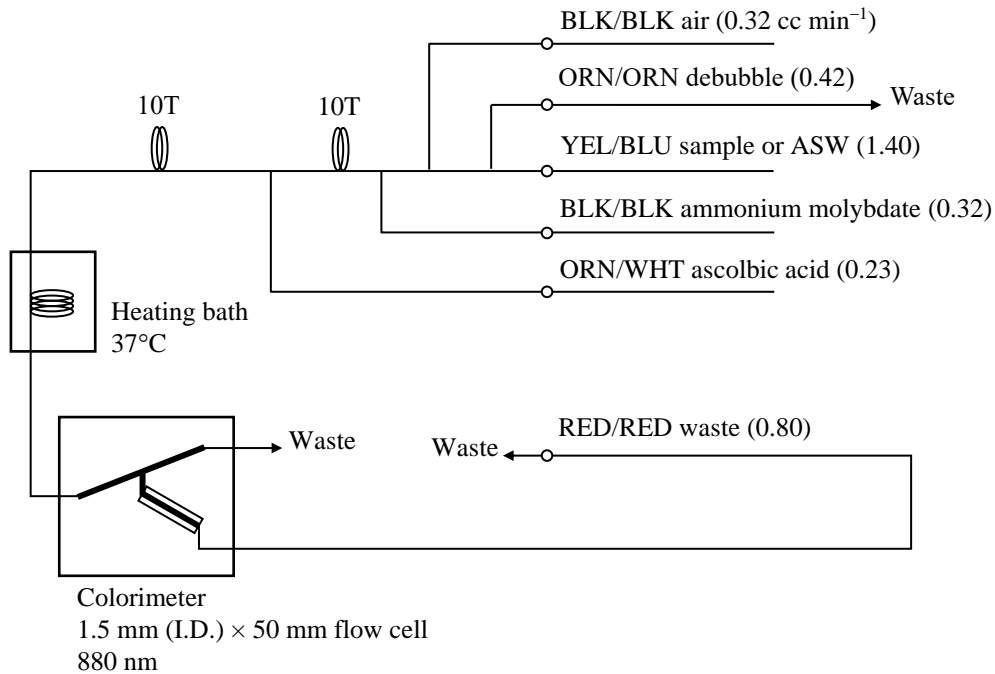


Figure C.4.A3. Phosphate (3ch.) flow diagram.

(A2.4) Silicate

The silicate was analyzed according to the modification method of Grasshoff *et al.* (1983), wherein silicomolybdic acid was first formed from the silicate in the sample and added molybdic acid, then the silicomolybdic acid was reduced to silicomolybdous acid, or "molybdenum blue," using L-ascorbic acid as the reductant. The flow diagram for silicate is shown in Figure C.4.A4.

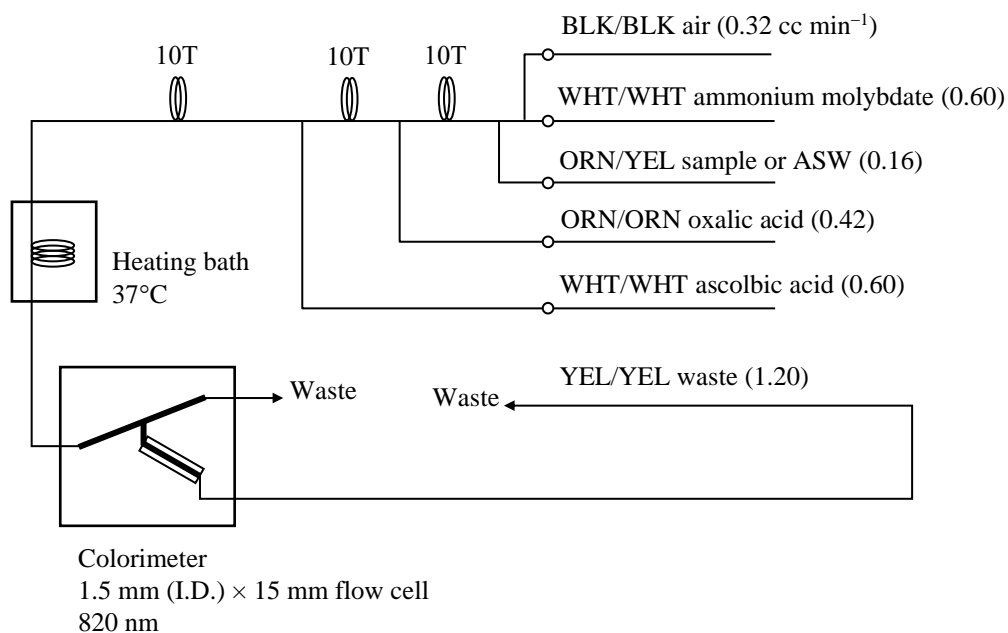


Figure C.4.A4. Silicate (4ch.) flow diagram.

A3. Data processing

Raw data from Auto Analyzer III were recorded at 1-second interval and were treated as follows;

- Check the shape of each peak and position of peak values taken, and then change the positions of peak values taken if necessary.
- Baseline correction was done basically using liner regression.
- Reagent blank correction was done basically using liner regression.
- Carryover correction was applied to peak heights of each sample.
- Sensitivity correction was applied to peak heights of each sample.
- Refraction error correction was applied to peak heights of each seawater sample.
- Calibration curves to get nutrients concentration were assumed quadratic expression.
- Concentrations were converted from $\mu\text{mol L}^{-1}$ to $\mu\text{mol kg}^{-1}$ using seawater density.

A4. Reagents recipes

(A4.1) Nitrate+nitrite

Ammonium chloride (buffer), $0.7 \mu\text{mol L}^{-1}$ (0.04 % w/v);

Dissolve 190 g ammonium chloride, NH_4Cl , in ca. 5 L of DW, add about 5 mL ammonia(aq) to adjust pH of 8.2–8.5.

Sulfanilamide, $0.06 \mu\text{mol L}^{-1}$ (1 % w/v);

Dissolve 5 g sulfanilamide, $4\text{-NH}_2\text{C}_6\text{H}_4\text{SO}_3\text{H}$, in 430 mL DW, add 70 mL concentrated HCl. After mixing, add 1 mL Brij-35 (22 % w/w).

N-1-naphtylethylene-diamine dihydrochloride (NEDA), $0.004 \mu\text{mol L}^{-1}$ (0.1 % w/v);

Dissolve 0.5 g NEDA, $\text{C}_{10}\text{H}_7\text{NH}_2\text{CH}_2\text{CH}_2\text{NH}_2 \cdot 2\text{HCl}$, in 500 mL DW.

(A4.2) Nitrite

Sulfanilamide, $0.06 \mu\text{mol L}^{-1}$ (1 % w/v); Shared from nitrate reagent.

N-1-naphtylethylene-diamine dihydrochloride (NEDA), $0.004 \mu\text{mol L}^{-1}$ (0.1 % w/v); Shared from nitrate reagent.

(A4.3) Phosphate

Ammonium molybdate, $0.005 \mu\text{mol L}^{-1}$ (0.6 % w/v);

Dissolve 3 g ammonium molybdate(VI) tetrahydrate, $(\text{NH}_4)_6\text{Mo}_7\text{O}_{24} \cdot 4\text{H}_2\text{O}$, and 0.05 g potassium antimonyl tartrate, $\text{C}_8\text{H}_4\text{K}_2\text{O}_{12}\text{Sb}_2 \cdot 3\text{H}_2\text{O}$, in 400 mL DW and add 40 mL concentrated H_2SO_4 . After mixing, dilute the solution with DW to final volume of 500 mL and add 2 mL sodium dodecyl sulfate (15 % solution in water).

L(+)-ascorbic acid, $0.08 \mu\text{mol L}^{-1}$ (1.5 % w/v);

Dissolve 4.5 g L(+)-ascorbic acid, $\text{C}_6\text{H}_8\text{O}_6$, in 300 mL DW. After mixing, add 10 mL acetone. This reagent was freshly prepared before every measurement.

(A4.4) Silicate

Ammonium molybdate, $0.005 \mu\text{mol L}^{-1}$ (0.6 % w/v);

Dissolve 3 g ammonium molybdate(VI) tetrahydrate, $(\text{NH}_4)_6\text{Mo}_7\text{O}_{24} \cdot 4\text{H}_2\text{O}$, in 500 mL DW and added concentrated 2 mL H_2SO_4 . After mixing, add 2 mL sodium dodecyl sulfate (15 % solution in water).

Oxalic acid, $0.4 \mu\text{mol L}^{-1}$ (5 % w/v);

Dissolve 25 g oxalic acid dihydrate, $(\text{COOH})_2 \cdot 2\text{H}_2\text{O}$, in 500 mL DW.

L(+)-ascorbic acid, $0.08 \mu\text{mol L}^{-1}$ (1.5 % w/v); Shared from phosphate reagent.

(A4.5) Baseline

Artificial seawater (salinity is ~34.7);

Dissolve 160.6 g sodium chloride, NaCl , 35.6 g magnesium sulfate heptahydrate, $\text{MgSO}_4 \cdot 7\text{H}_2\text{O}$, and 0.84 g sodium hydrogen carbonate, NaHCO_3 , in 5 L DW.

References

- Armstrong, F. A. J., C. R. Stearns and J. D. H. Strickland (1967), The measurement of upwelling and subsequent biological processes by means of the Technicon TM Autoanalyzer TM and associated equipment, *Deep-Sea Res.*, 14(3), 381–389.
- DOE (1994), Handbook of methods for the analysis of the various parameters of the carbon dioxide system in sea water; version 2. *A.G. Dickson and C. Goyet (eds), ORNL/CDIAC-74.*
- Grasshoff, K., Ehrhardt, M., Kremling K. et al. (1983), Methods of seawater analysis. 2nd rev, *Weinheim: Verlag Chemie, Germany, West.*
- Murphy, J. and Riley, J.P. (1962), *Analytica chimica Acta*, 27, 31-36.
- Swift, J. H. (2010), Reference-quality water sample data: Notes on acquisition, record keeping, and evaluation. *IOCCP Report No.14, ICPO Pub. 134, 2010 ver.1.*

*Phytopigments (chlorophyll-*a* and phaeopigment)*

1 November 2019

(1) Personnel

Naoshi KUBO (GEMD/JMA)

Chihiro KAWAMURA (GEMD/JMA)

(2) Station occupied

A total of 60 stations (RF14-05: 17, RF14-06: 12, RF14-07 Leg 1: 20, Leg 2: 11) were occupied for phytopigment measurements. Station location and sampling layers of phytopigment are shown in Figures C.5.1 and C.5.2.

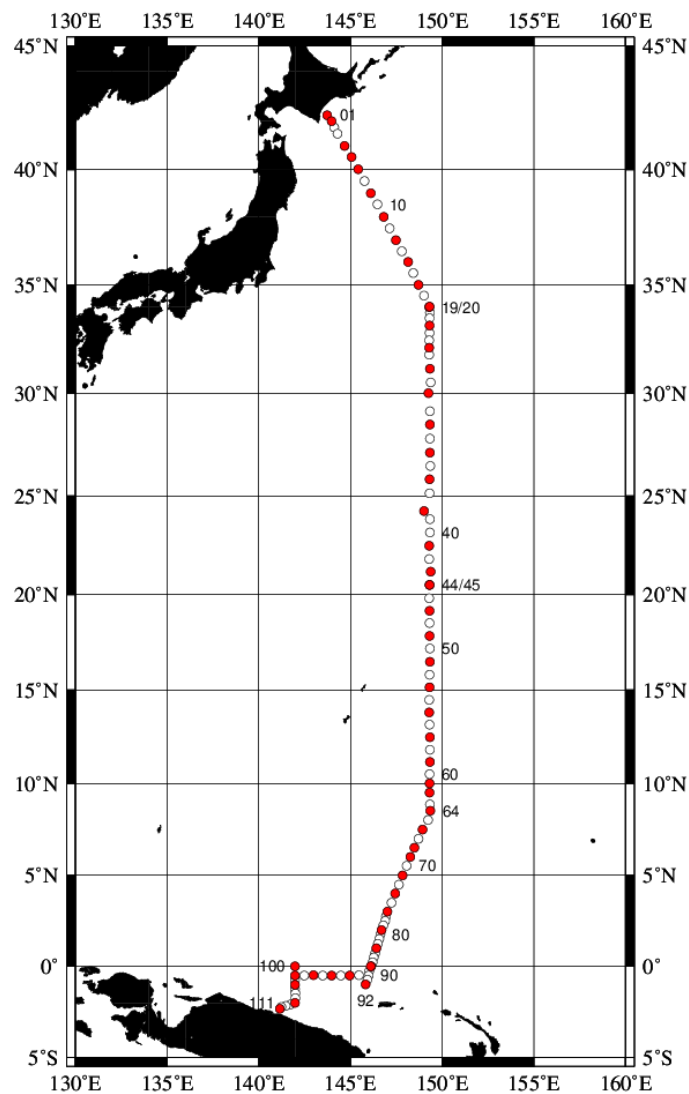


Figure C.5.1. Location of observation stations of chlorophyll-*a*. Closed and open circles indicate sampling and no-sampling stations, respectively.

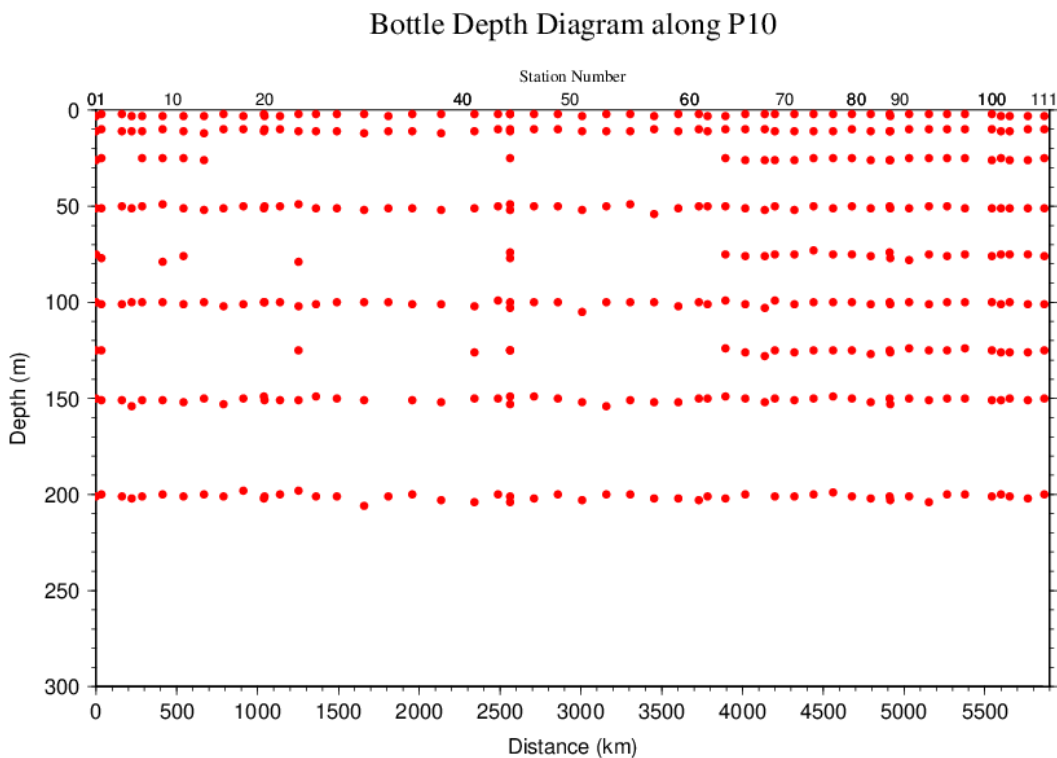


Figure C.5.2. Distance-depth distribution of sampling layers of chlorophyll-*a*.

(3) Reagents

N,N-dimethylformamide (DMF)

Hydrochloric acid (HCl), 0.5 mol L⁻¹

Chlorophyll-*a* standard from *Anacystis nidulans* algae (Sigma-Aldrich, United States)

Rhodamine WT (Turner Designs, United States)

(4) Instruments

Fluorometer: 10-AU (Turner Designs, United States)

Spectrophotometer: UV-1800 (Shimadzu, Japan)

(5) Standardization

(5.1) Determination of chlorophyll-*a* concentration of standard solution

To prepare the pure chlorophyll-*a* standard solution, reagent powder of chlorophyll-*a* standard was dissolved in DMF. A concentration of the chlorophyll-*a* solution was determined with the spectrophotometer as follows:

$$\text{chl } a \text{ concentration } (\mu\text{g mL}^{-1}) = A_{\text{chl}} / a_{\text{phy}}^* \quad (\text{C5.1})$$

where A_{chl} is the difference between absorbance at 663.8 nm and 750 nm, and a_{phy}^* is specific absorption coefficient (UNESCO, 1994). The specific absorption coefficient is 88.74 L g⁻¹ cm⁻¹ (Porra *et al.*, 1989).

(5.2) Determination of R and f_{ph}

Before measurements, sensitivity of the fluorometer was calibrated with pure DMF and a rhodamine 1 ppm solution (diluted with deionized water).

The chlorophyll-*a* standard solution, whose concentration was precisely determined in subsection (5.1), was measured with the fluorometer, and after acidified with 1–2 drops 0.5 mol L⁻¹ HCl the solution was also measured. The acidification coefficient (R) of the fluorometer was also calculated as the ratio of the unacidified and acidified readings of chlorophyll-*a* standard solution. The linear calibration factor (f_{ph}) of the fluorometer was calculated as the slope of the acidified reading against chlorophyll-*a* concentration. The R and f_{ph} in the cruise are shown in Table C.5.1.

Table C.5.1. R and f_{ph} in the cruises.

Cruise number	RF14-05	RF14-06	RF14-07
Acidification coefficient (R)	1.942	1.919	1.904
Linear calibration factor (f_{ph})	5.3974	5.4389	6.4657

(6) Seawater sampling and measurement

Water samples were collected from 10-liters Niskin bottle attached the CTD-system and a stainless steel bucket for the surface. A 200 mL seawater sample was immediately filtered through 25 mm GF/F filters by low vacuum pressure below 15 cmHg, the particulate matter collected on the filter. Phytopigments were extracted in vial with 9 mL of DMF. The extracts were stored for 24 hours in the refrigerator at -30 °C until analysis.

After the extracts were put on the room temperature for at least one hour in the dark, the extracts were decanted from the vial to the cuvette. Fluorometer readings for each cuvette were taken before and after acidification with 1–2 drops 0.5 mol L⁻¹ HCl. Chlorophyll-*a* and phaeopigment concentrations ($\mu\text{g mL}^{-1}$) in the sample are calculated as follows:

$$\text{chl } a \text{ conc.} = \frac{F_0 - F_a}{f_{ph} \cdot (R - 1)} \cdot \frac{v}{V} \quad (\text{C5.2})$$

$$\text{phaeo. conc.} = \frac{R \cdot F_0 - F_a}{f_{ph} \cdot (R - 1)} \cdot \frac{v}{V} \quad (\text{C5.3})$$

F_0 : reading before acidification

F_a : reading after acidification

R: acidification coefficient (F_0/F_a) for pure chlorophyll-*a*

f_{ph} : linear calibration factor

v: extraction volume

V: sample volume.

(7) Quality control flag assignment

Quality flag value was assigned to oxygen measurements as shown in Table C.5.2, using the code defined in IOCCP Report No.14 (Swift, 2010).

Table C.5.2. Summary of assigned quality control flags.

Flag	Definition	Chl <i>a</i>	Phaeo.
2	Good	392	392
3	Questionable	0	0
4	Bad (Faulty)	4	4
5	Not reported	0	0
Total number		396	396

References

- Porra, R. J., W. A. Thompson and P. E. Kriedemann (1989), Determination of accurate coefficients and simultaneous equations for assaying chlorophylls *a* and *b* extracted with four different solvents: verification of the concentration of chlorophyll standards by atomic absorption spectroscopy. *Biochem. Biophys. Acta*, 975, 384-394.
- Swift, J. H. (2010), Reference-quality water sample data: Notes on acquisition, record keeping, and evaluation. *IOCCP Report No.14, ICPO Pub. 134, 2010 ver.1.*
- UNESCO (1994), Protocols for the joint global ocean flux study (JGOFS) core measurements: Measurement of chlorophyll *a* and phaeopigments by fluorometric analysis, *IOC manuals and guides 29, Chapter 14.*

6. *Total Dissolved Inorganic Carbon (DIC)*

17 October 2023

(1) Personnel

ONO Etsuro	(RF14-05)
SAITO Shu	(RF14-05, RF14-07)
SAKAMOTO Naoaki	(RF14-05)
ENYO Kazutaka	(RF14-06, RF14-07)
HIRAISHI Naotaka	(RF14-06)
KAWAHARA Kyouichi	(RF14-06)
ONO Hisashi	(RF14-07)

(2) Station occupied

A total of 50 stations (RF14-05: 8, RF14-06: 12, RF14-07 Leg 1: 20, RF14-07 Leg 2: 10) were occupied for total dissolved inorganic carbon (DIC). Station location and sampling layers of them are shown in Figures C.6.1 and C.6.2, respectively.

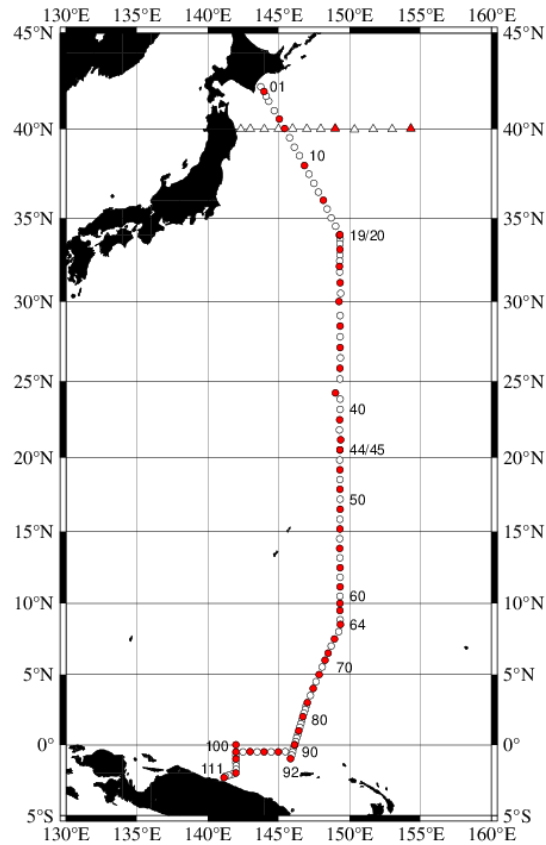


Figure C.6.1. Location of observation stations of DIC. Closed and open circles indicate sampling and no-sampling stations, respectively. Triangles show sampling station which are not reported in the bottle data file, but the data at closed triangles are used for quality control of DIC. These data are available from the JMA (https://www.data.jma.go.jp/gmd/kaiyou/db/vessel_obs/data-report/html/ship/ship_e.php?year=2014&season=spring).

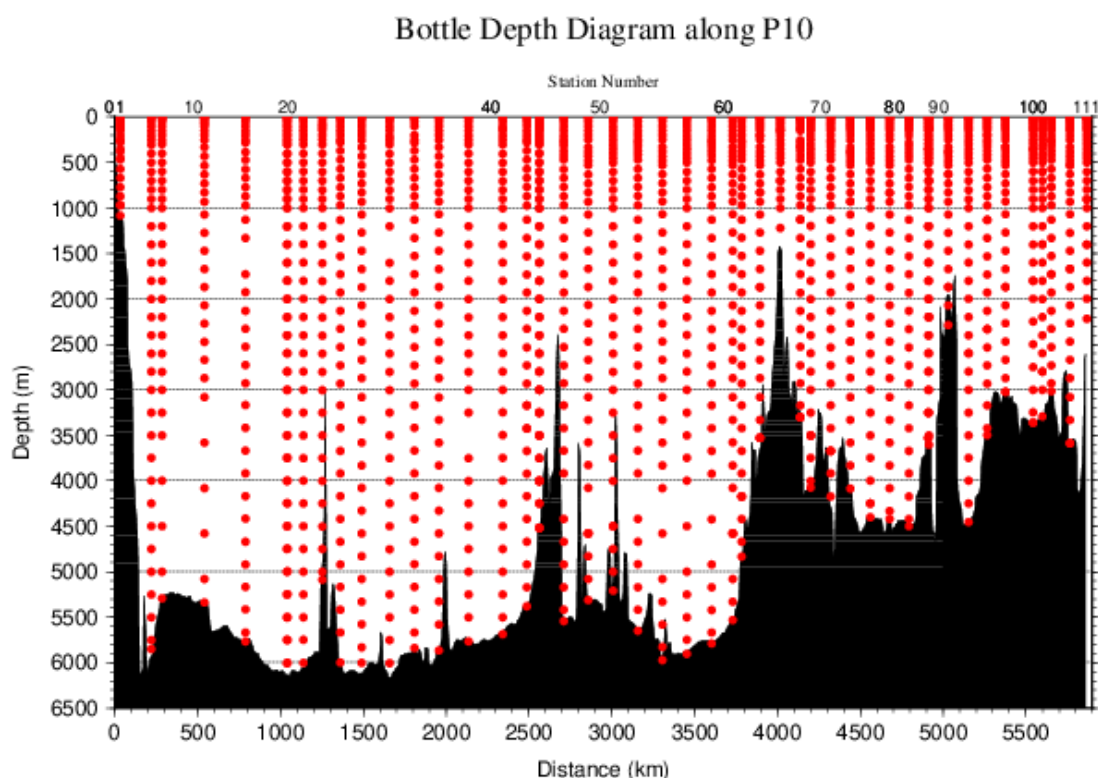


Figure C.6.2. Distance-depth distribution of sampling layers of DIC.

(3) Instrument

The measurement of DIC was carried out with DIC/TA analyzers (Nihon ANS Co. Ltd, Japan). We used two analyzers concurrently. These analyzers are designated as apparatus A and B.

(4) Sampling and measurement

Methods of seawater sampling, poisoning, measurement, and calculation of DIC concentrations were based on the Standard Operating Procedure (SOP) described in PICES Special Publication 3, SOP-2 (Dickson et al., 2007). DIC was determined by coulometric analysis (Johnson et al., 1985, 1987) using an automated CO₂ extraction unit and a coulometer. Details of sampling and measurement are shown in Appendix A1.

(5) Calibration

The concentration of DIC (C_T) in moles per kilogram (mol kg^{-1}) of seawater was calculated from the following equation:

$$C_T = N_S / (cV \cdot \rho_S) \quad (\text{C6.1})$$

where N_S is the counts of the coulometer (gC), cV is the calibration factor ($\text{gC (mol L}^{-1})^{-1}$), and ρ_S is density of seawater (kg L^{-1}), which is calculated from the salinity of the sample and the water temperature of the water-jacket for the sample pipette.

The values of cV were determined by measurements of Certified Reference Materials (CRMs) that were provided by Dr. Andrew G. Dickson of the Scripps Institution of Oceanography. Table C.6.1 provides information about the CRM batches used in this cruise.

Table C.6.1. Certified C_T and standard deviation of CRMs. Unit of C_T is $\mu\text{mol kg}^{-1}$. More information is available at the NOAA web site (https://www.ncei.noaa.gov/access/ocean-carbon-acidification-data-system/oceans/Dickson_CRM/batches.html).

Cruise	RF14-05	RF14-06, RF14-07
Batch number	134	137
C_T	2026.91±0.78	2031.90±0.32
Salinity	33.651	33.607

The CRM measurement was carried out at every station. After the cruise, a value of cV was assigned to each apparatus (A, B). Table C.6.2 summarizes the cV values. Figure C.6.3 shows details.

Table C.6.2. Assigned cV and its standard deviation for each apparatus during the cruise. Unit is $\text{gC (mol L}^{-1}\text{)}^{-1}$.

Apparatus	Cruise	cV
B	RF14-05	0.135116±0.000194 (N=33)
	RF14-06	0.135030±0.000179 (N=52)
A	RF14-07	0.189882±0.000254 (N=40)
B	RF14-07	0.196323±0.000175 (N=108)

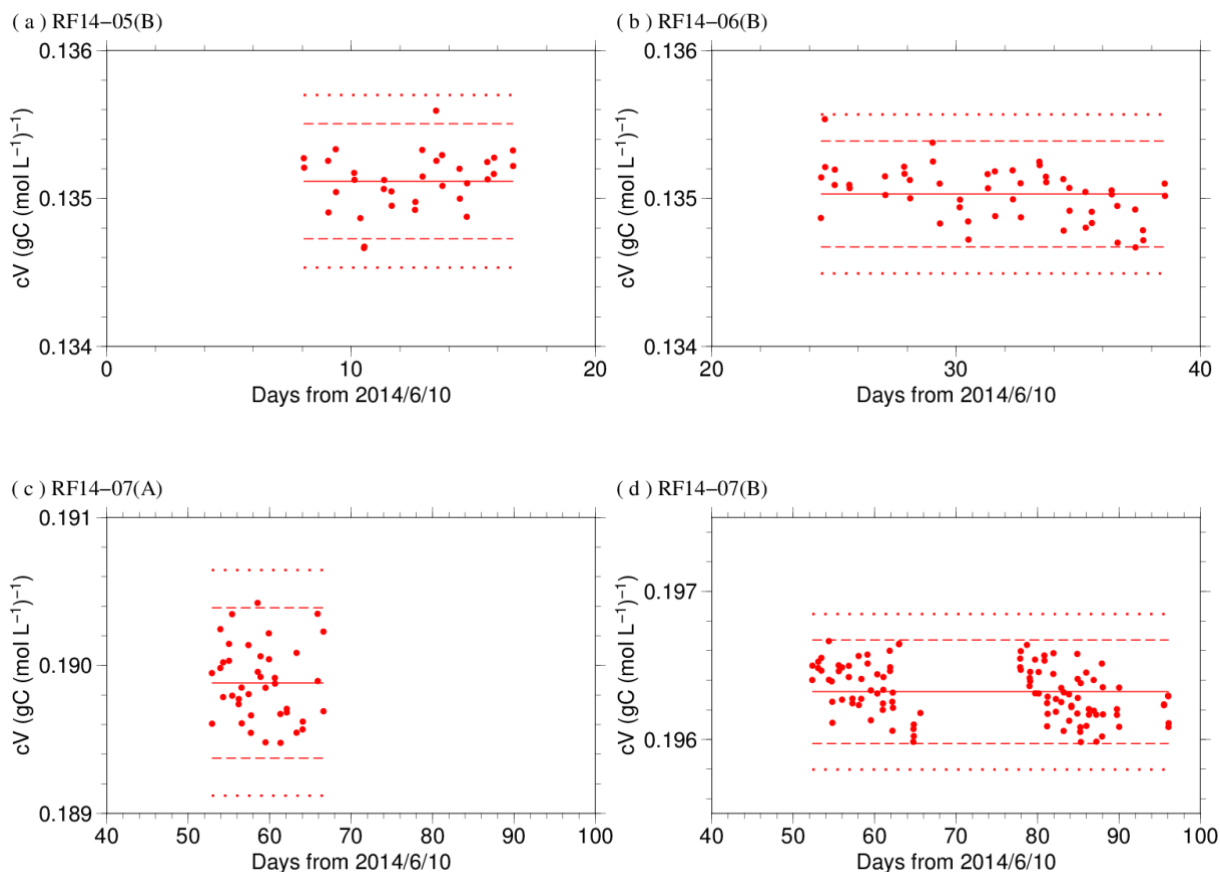


Figure C.6.3. Results of the cV at each station assigned for apparatus (a) B in RF14-05, (b) B in RF14-06, (c) A in RF14-07 and (d) B in RF14-07. The solid, dashed, and dotted lines denote the mean, the mean \pm twice the S.D., and the mean \pm thrice the S.D. for all measurements, respectively.

The precisions of the cV is equated to its coefficient of variation ($=$ S.D. / mean). They were 0.144 % for apparatus B in RF14-05, 0.133 % for apparatus B in RF14-06, 0.134 % for apparatus A in RF14-07 and 0.089 % for apparatus B in RF14-07. They correspond to $2.91 \mu\text{mol kg}^{-1}$, $2.69 \mu\text{mol kg}^{-1}$, $2.71 \mu\text{mol kg}^{-1}$ and $1.81 \mu\text{mol kg}^{-1}$ in C_T of CRM batch 134, respectively.

Finally, the value of C_T was multiplied by 1.00067 ($= 300.2 / 300.0$) to correct dilution effect induced by addition of 0.2 mL of mercury (II) chloride (HgCl_2) solution in a sampling bottle with a volume of ~ 300 mL.

(6) Quality Control

(6.1) Replicate and duplicate analyses

We took replicate (pair of water samples taken from a single Niskin bottle) and duplicate (pair of water samples taken from different Niskin bottles closed at the same depth) samples of DIC throughout the cruise. Table C.6.3 summarizes the results of the measurements with each

apparatus. Figures C.6.4–C.6.5 show details of the results. The calculation of the standard deviation from the difference of sets of measurements was based on a procedure (SOP 23) in DOE (1994).

Table C.6.3. Summary of replicate and duplicate measurements. Unit is $\mu\text{mol kg}^{-1}$.

Measurement	Apparatus A	Apparatus B
	Average magnitude of difference \pm S.D.	
Replicate	2.0 ± 1.9 (N=28)	1.5 ± 1.3 (N=112)
Duplicate	1.7 ± 1.5 (N=10)	1.5 ± 1.6 (N=54)

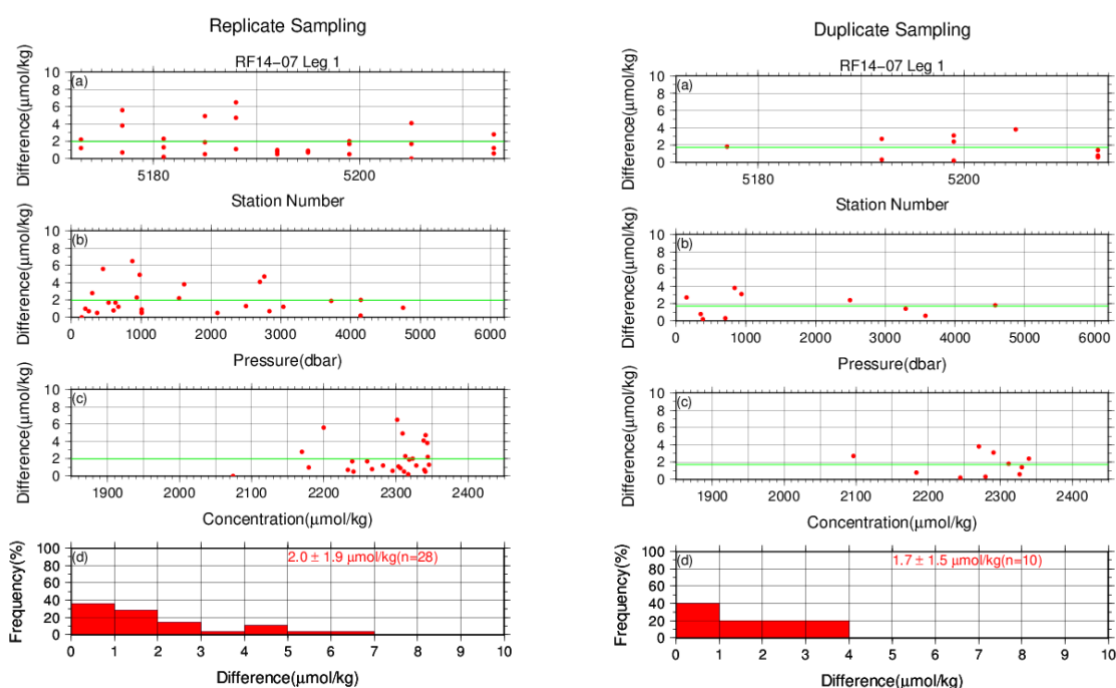


Figure C.6.4. Results of (left) replicate and (right) duplicate measurements during the cruise versus (a) station number, (b) pressure, and (c) C_T determined by apparatus A. The green lines denote the averages of the measurements. The bottom panels (d) show histograms of the measurements.

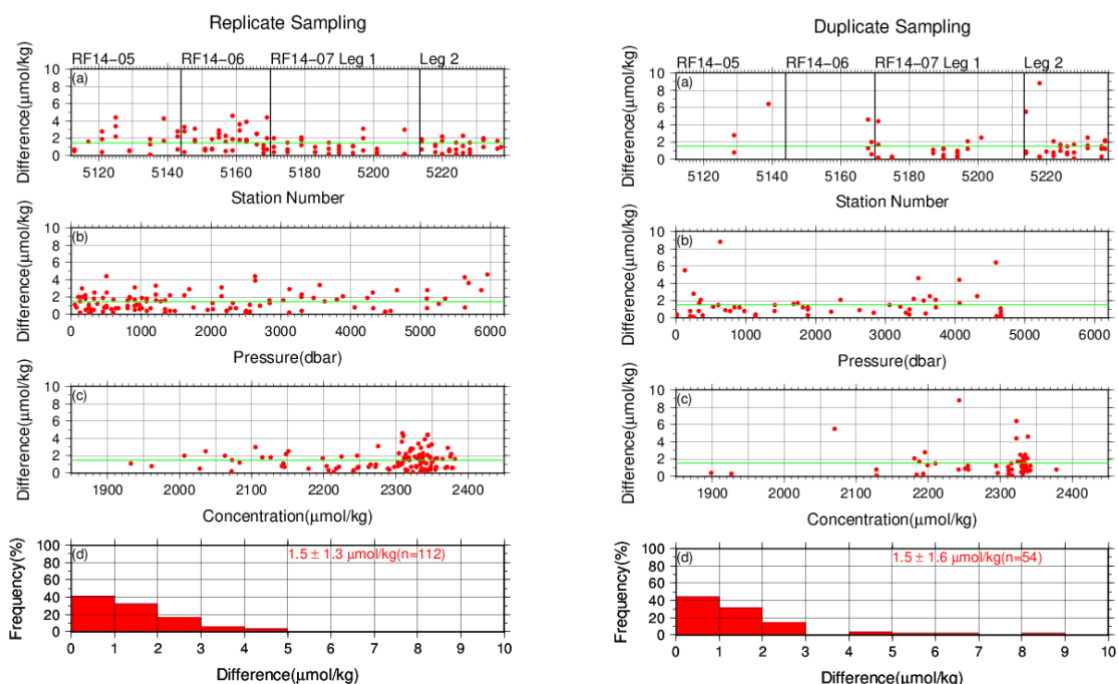


Figure C.6.5. Same as Figure C.6.4, but for apparatus B.

(6.2) Measurements of CRM and working reference materials

The precision of the measurements was monitored by using the CRMs and working reference materials bottled in our laboratory (Appendix A2). The CRM (batch 134 in RF14-05, 137 in RF14-06 and RF14-07) and working reference material measurements were carried out at every station. At the beginning of the measurement of each station, we measured a working reference material and a CRM. If the results of these measurements were confirmed to be good, measurements on seawater samples were begun. At the end of a sequence of measurements at a station, another CRM bottle was measured. A CRM measurement was repeated twice from the same bottle. Table C.6.4 summarizes the differences in the repeated measurements of the CRMs, the mean C_T of the CRM measurements, and the mean C_T of the working reference material measurements. Figures C.6.6–C.6.8 show detailed results.

Table C.6.4. Summary of difference and mean of C_T in the repeated measurements of CRM and the mean C_T of the working reference material. These data are based on good measurements. Unit is $\mu\text{mol kg}^{-1}$.

Cruise	RF14-05	RF14-06	RF14-07	
Apparatus	B	B	A	B
Average magnitude of difference \pm S.D. (CRM)	2.3 \pm 2.0 (N=16)	2.3 \pm 2.0 (N=26)	2.8 \pm 2.4 (N=20)	1.3 \pm 1.2 (N=52)
Mean Ave. \pm S.D. (CRM)	2027.0 \pm 2.6 (N=16)	2031.9 \pm 2.3 (N=26)	2031.9 \pm 2.1 (N=20)	2031.8 \pm 1.5 (N=52)
Mean Ave. \pm S.D. (Working reference material)	2035.5 \pm 2.6 (N=9)	2035.9 \pm 2.6 (N=18)	2035.3 \pm 2.2 (N=11)	2035.7 \pm 1.7 (N=27)

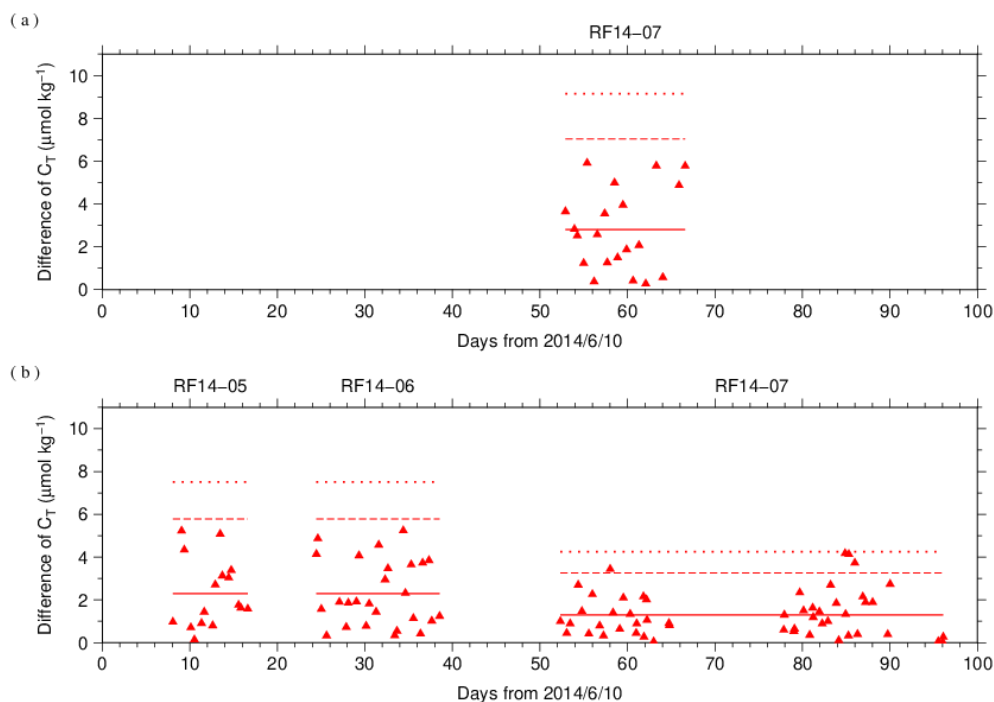


Figure C.6.6. The absolute difference (R) of C_T in repeated measurements of CRM determined by apparatus (a) A and (b) B. The solid line indicates the average of R (\bar{R}). The dashed and dotted lines denote the upper warning limit ($2.512\bar{R}$) and upper control limit ($3.267\bar{R}$), respectively (see Dickson et al., 2007).

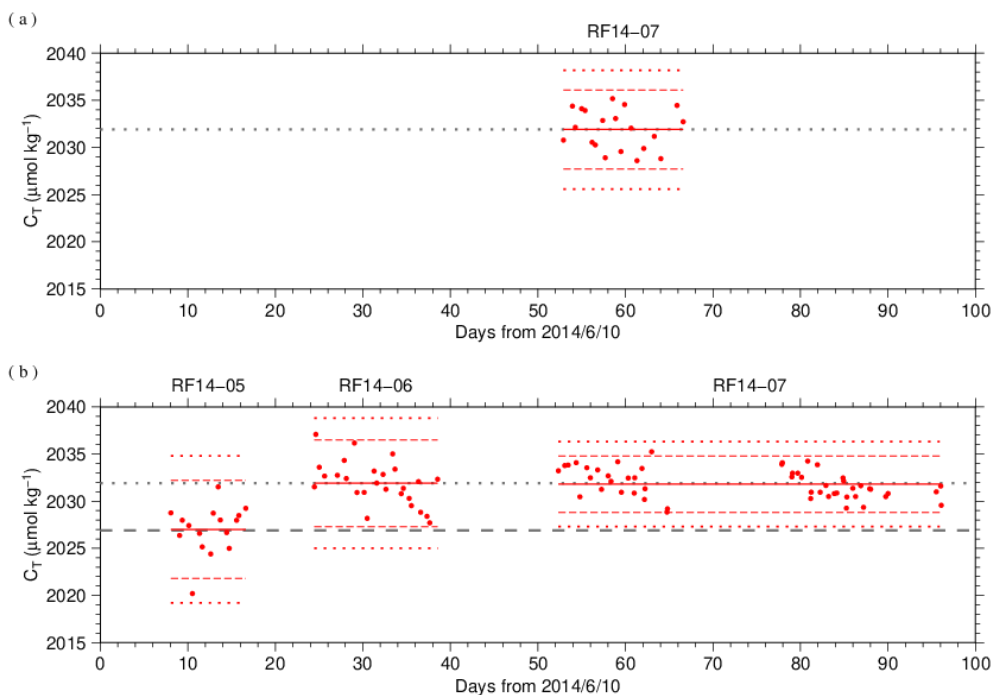


Figure C.6.7. The mean C_T of measurements of CRM. The panels show the results for apparatus (a) A and (b) B. The solid line indicates the mean of the measurements throughout the cruise. The dashed and dotted lines denote the upper/lower warning limit (mean \pm 2S.D.) and the upper/lower control limit (mean \pm 3S.D.), respectively. The gray dashed and dotted lines denote certified C_T of CRM batch 134 and 137.

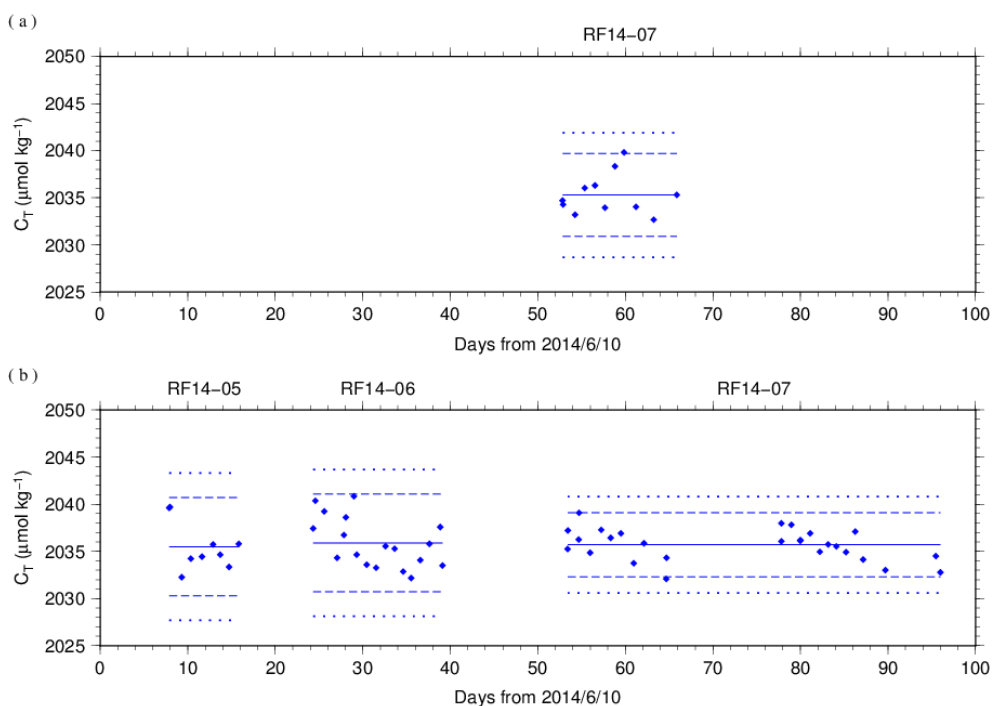


Figure C.6.8. Calculated C_T of working reference material measured by apparatus (a) A and (b) B. The solid, dashed and dotted lines are the same as in Figure C.6.7.

(6.3) Comparisons with other CRM batches

At every few stations, other CRM batches (132 in RF14-05, 129 in RF14-06, 134 in RF14-07) were measured to provide comparisons with batch 134 (in RF14-05) and 137 (in RF14-06 and RF14-07) to confirm the determination of C_T in our measurements. For these CRM measurements, C_T was calculated from the cV determined from batch 134 (in RF14-05) and 137 (in RF14-06 and RF14-07) measurements. Figures C.6.9 show the differences between the calculated and certified C_T .

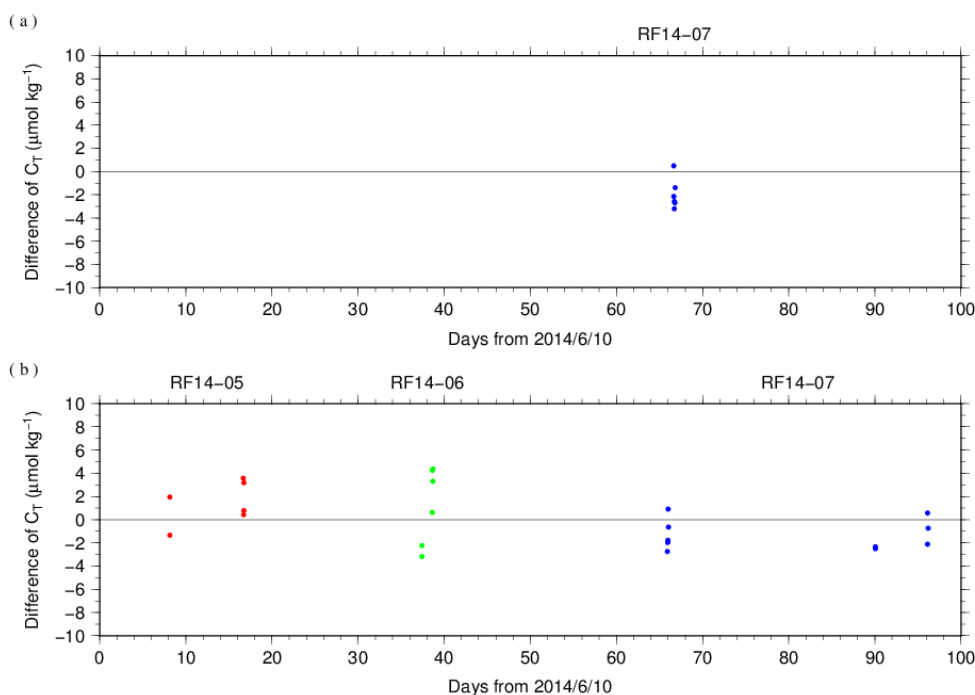


Figure C.6.9. The differences between the calculated C_T from batch 134 (in RF14-05) and 137 (in RF14-06 and RF14-07) measurements and the certified C_T . The panels show the results for apparatus (a) A and (b) B. Colors indicate CRM batches; red: 132, green: 129 and blue: 134.

(6.4) Quality control flag assignment

A quality control flag value was assigned to the DIC measurements (Table C.6.5) using the code defined in the IOCCP Report No.14 (Swift, 2010).

Table C.6.5. Summary of assigned quality control flags.

Flag	Definition	Number of samples
2	Good	1517
3	Questionable	34
4	Bad (Faulty)	6
5	Not reported	1
6	Replicate measurements	135
Total number of samples		1693

Appendix

A1. Methods

(A1.1) Seawater sampling

Seawater samples were collected from 10-liters Niskin bottles mounted on CTD-system and a stainless steel bucket for the surface. Samples for DIC/TA were transferred to Schott Duran[®] glass bottles using sample drawing tubes. Bottles were filled smoothly from the bottom after overflowing double a volume while taking care of not entraining any bubbles, and lid temporarily with ground glass stoppers.

After all sampling finished, 2 mL of sample is removed from each bottle to make a headspace to allow thermal expansion, and then samples were poisoned with 0.2 mL of saturated HgCl₂ solution and sealed with ground glass stoppers lubricated with Apiezon[®] grease (L).

(A1.2) Measurement

The unit for DIC measurement in the coupled DIC/TA analyzer consists of a coulometer with a quartz coulometric titration cell, a CO₂ extraction unit and a reference gas injection unit. The CO₂ extraction unit, which is connected to a bottle of 20 % v/v phosphoric acid and a carrier N₂ gas supply, includes a sample pipette (approx. 12 mL) and a CO₂ extraction chamber, two thermoelectric cooling units and switching valves. The coulometric titration cell and the sample pipette are water-jacketed and are connected to a thermostated (25 °C) water bath. The automated procedures of DIC analysis in seawater were as follows (Ishii et al., 1998):

- (a) Approximately 2 mL of 20 % v/v phosphoric acid was injected to an “extraction chamber”, *i.e.*, a glass tube with a coarse glass frit placed near the bottom. Purified N₂ was then allowed to flow through the extraction chamber to purge CO₂ and other volatile acids dissolved in the phosphoric acid.
- (b) A portion of sample seawater was delivered from the sample bottle into the sample pipette of CO₂ extraction unit by pressurizing the headspace in the sample bottle. After temperature of the pipette was recorded, the sample seawater was transferred into the extraction chamber and mixed with phosphoric acid to convert all carbonate species to CO₂ (aq).
- (c) The acidified sample seawater was then stripped of CO₂ with a stream of purified N₂. After being dehumidified in a series of two thermoelectric cooling units, the evolved CO₂ in the N₂ stream was introduced into the carbon cathode solution in the coulometric titration cell and then CO₂ was electrically titrated.

A2. Working reference material recipe

The surface seawater in the western North Pacific was taken until at least a half year ago. Seawater was firstly filtered by membrane filter (0.45 µm-mesh) using magnetic pump and transfer into large tank. After first filtration finished, corrected seawater in the tank was processed in cycle filtration again for 3 hours and agitated in clean condition air for 6 hours.

On the next day, agitated 5 minutes to remove small bubbles on the tank and transfer to Schott Duran® glass bottles as same method as samples (Appendix A1.1) except for overflowing a half of volume, not double. Created of headspace and poisoned with HgCl₂ was as same as samples, finally, sealed by ground glass stoppers lubricated with Apiezon® grease (L).

References

- Dickson, A. G., C. L. Sabine, and J. R. Christian (Eds.) (2007), Guide to best practices for ocean CO₂ measurements. *PICES Special Publication 3*, 191 pp.
- DOE (1994), Handbook of methods for the analysis of the various parameters of the carbon dioxide system in sea water; version 2. A. G. Dickson and C. Goyet (eds), *ORNL/CDIAC-74*.
- Ishii, M., H. Y. Inoue, H. Matsueda, and E. Tanoue (1998), Close coupling between seasonal biological production and dynamics of dissolved inorganic carbon in the Indian Ocean sector and the western Pacific Ocean sector of the Antarctic Ocean, *Deep Sea Res. Part I*, **45**, 1187–1209, doi:10.1016/S0967-0637(98)00010-7.
- Johnson, K. M., A. E. King and J. McN. Sieburth (1985), Coulometric TCO₂ analyses for marine studies; an introduction. *Marine Chemistry*, **16**, 61–82.
- Johnson, K. M., J. M. Sieburth, P. J. L. Williams and L. Brändström (1987), Coulometric total carbon dioxide analysis for marine studies: Automation and calibration. *Marine Chemistry*, **21**, 117–133.
- Swift, J. H. (2010): Reference-quality water sample data, Notes on acquisition, record keeping, and evaluation. *IOCCP Report No.14, ICPO Pub. 134*, 2010 ver.1.

7. *Total Alkalinity (TA)*

17 October 2023

(1) Personnel

ONO Etsuro	(RF14-05)
SAITO Shu	(RF14-05, RF14-07)
SAKAMOTO Naoaki	(RF14-05)
ENYO Kazutaka	(RF14-06, RF14-07)
HIRAISHI Naotaka	(RF14-06)
KAWAHARA Kyouichi	(RF14-06)
ONO Hisashi	(RF14-07)

(2) Station occupied

A total of 50 stations (RF14-05: 8, RF14-06: 12, RF14-07 Leg 1: 20, RF14-07 Leg 2: 10) were occupied for total alkalinity (TA). Station location and sampling layers of them are shown in Figures C.7.1 and C.7.2, respectively.

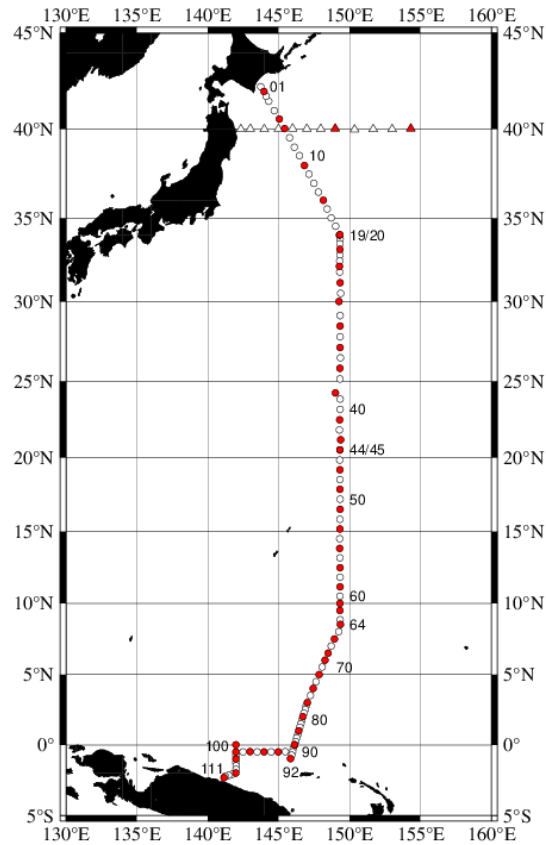


Figure C.7.1. Location of observation stations of TA. Closed and open circles indicate sampling and no-sampling stations, respectively. Triangles show sampling station which are not reported in the bottle data file, but the data at closed triangles are used for quality control of TA. These data are available from the JMA (https://www.data.jma.go.jp/gmd/kaiyou/db/vessel_obs/data-report/html/ship/ship_e.php?year=2014&season=spring).

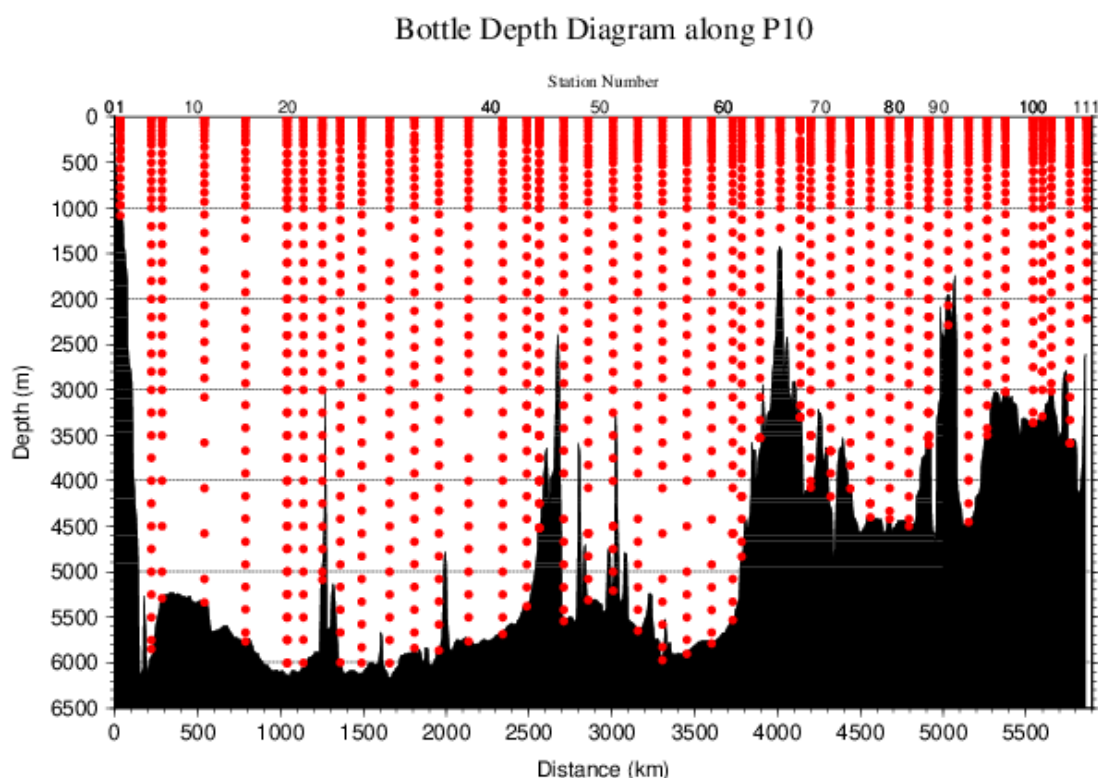


Figure C.7.2. Distance-depth distribution of sampling layers of TA.

(3) Instrument

The measurement of TA was carried out with DIC/TA analyzers (Nihon ANS Co. Ltd., Japan). The methodology that these analyzers use is based on an open titration cell. We used two analyzers concurrently. These analyzers are designated as apparatus A and B.

(4) Sampling and measurement

The procedure of seawater sampling of TA bottles and poisoning with mercury (II) chloride (HgCl_2) were based on the Standard Operating Procedure (SOP) described in PICES Special Publication 3 (Dickson et al., 2007). Details are shown in Appendix A1 in C.6.

TA measurement is based on a one-step volumetric addition of hydrochloric acid (HCl) to a known amount of sample seawater with prompt spectrophotometric measurement of excess acid using the sulfonephthalein indicator bromo cresol green sodium salt (BCG) (Breland and Byrne, 1993). We used a mixed solution of HCl, BCG, and sodium chloride (NaCl) as reagent. Details of measurement are shown in Appendix A1.

(5) Calculation

(5.1) Volume of sample seawater

The volumes of pipette V_s using in apparatus A and B was calibrated gravimetrically in our laboratory. Table C.7.1 shows the summary.

Table C.7.1. Summary of sample volumes of seawater V_S for TA measurements.

Apparatus	V_S / mL
A	42.7760
B	41.3393

(5.2) pH_T calculation in spectrophotometric measurement

The data of absorbance A and pipette temperature T (in °C) were processed to calculate pH_T (in total hydrogen ion scale; details shown in Appendix A1 in C.8) and the concentration of excess acid $[\text{H}^+]_T$ (mol kg^{-1}) in the following equations (C7.1)–(C7.3) (Yao and Byrne, 1998),

$$\begin{aligned} \text{pH}_T &= -\log_{10}([\text{H}^+]_T) \\ &= 4.2699 + 0.02578 \cdot (35 - S) + \log\{(R_{25} - 0.00131) / (2.3148 - 0.1299 \cdot R_{25})\} \\ &\quad - \log(1 - 0.001005 \cdot S) \end{aligned} \quad (\text{C7.1})$$

$$R_{25} = R_T \cdot \{1 + 0.00909 \cdot (25 - T)\} \quad (\text{C7.2})$$

$$R_T = (A_{616}^{\text{SA}} - A_{616}^{\text{S}} - A_{730}^{\text{SA}} + A_{730}^{\text{S}}) / (A_{444}^{\text{SA}} - A_{444}^{\text{S}} - A_{730}^{\text{SA}} + A_{730}^{\text{S}}). \quad (\text{C7.3})$$

In the equation (C7.1), R_T is absorbance ratio at temperature T , R_{25} is absorbance ratio at temperature 25 °C and S is salinity. A_{λ}^{S} and A_{λ}^{SA} denote absorbance of seawater before and after acidification, respectively, at wavelength λ nm.

(5.3) TA calculation

The calculated $[\text{H}^+]_T$ was then combined with the volume of sample seawater V_S , the volume of titrant V_A added to the sample, and molarity of hydrochloric acid HCl_A (in mmol L^{-1}) in the titrant to determine to TA concentration A_T (in $\mu\text{mol kg}^{-1}$) as follows:

$$A_T = (-[\text{H}^+]_T \cdot (V_S + V_A) \cdot \rho_{\text{SA}} + \text{HCl}_A \cdot V_A) / (V_S \cdot \rho_{\text{S}}) \quad (\text{C7.4})$$

ρ_{S} and ρ_{SA} denote the density of seawater sample before and after the addition of titrant, respectively. Here we assumed that ρ_{SA} is equal to ρ_{S} , since the density of titrant has been adjusted to that of seawater by adding NaCl and the volume of titrant (approx. 2.5 mL) is no more than approx. 6 % of seawater sample.

Finally, the value of A_T was multiplied by 1.00067 (= 300.2 / 300.0) to correct dilution effect in A_T induced by addition of HgCl_2 solution.

(6) Standardization of HCl reagent

HCl reagents were prepared in our laboratory (Appendix A2) and divided into bottles (HCl batches). HCl_A in the bottles were determined using measured CRMs provided by Dr. Andrew G. Dickson in Scripps Institution of Oceanography. Table C.7.2 provides information about the CRM batch used during this cruise.

Table C.7.2. Certified A_T and standard deviation of CRMs. Unit of A_T is $\mu\text{mol kg}^{-1}$. More information is available at the NOAA web site (https://www.ncei.noaa.gov/access/ocean-carbon-acidification-data-system/oceans/Dickson_CRM/batches.html).

Cruise	RF14-05	RF14-06, RF14-07
Batch number	134	137
A_T	2236.51±0.52	2231.59±0.62
Salinity	33.651	33.607

The CRM measurement was carried out at every station. The apparent HCl_A of the titrant was determined from CRM using equation (C7.4).

HCl_A was assigned for each HCl batches for each apparatus, as summarized in Table C.7.3 and detailed in Figure C.7.3.

Table C.7.3. Summary of assigned HCl_A for each HCl batches. The reported values are means and standard deviations. Unit is mmol L^{-1} .

Apparatus	Cruise	HCl Batch	HCl_A
B	RF14-05	B_1	50.6397±0.0456 (N=27)
		B_2	50.6196±0.0305 (N=24)
		B_3	50.7654±0.0260 (N=21)
	RF14-06	B_4	50.6903±0.0267 (N=32)
		B_5	50.7137±0.0248 (N=24)
A	RF14-07	A_1	49.4218±0.0243 (N=29)
		A_2	49.4308±0.0235 (N=30)
B	RF14-07	B_6	49.3946±0.0257 (N=31)
		B_7	49.4008±0.0390 (N=42)
		B_8	49.4311±0.0163 (N=15)
		B_9	49.3414±0.0217 (N=18)
		B_10	49.3624±0.0390 (N=51)

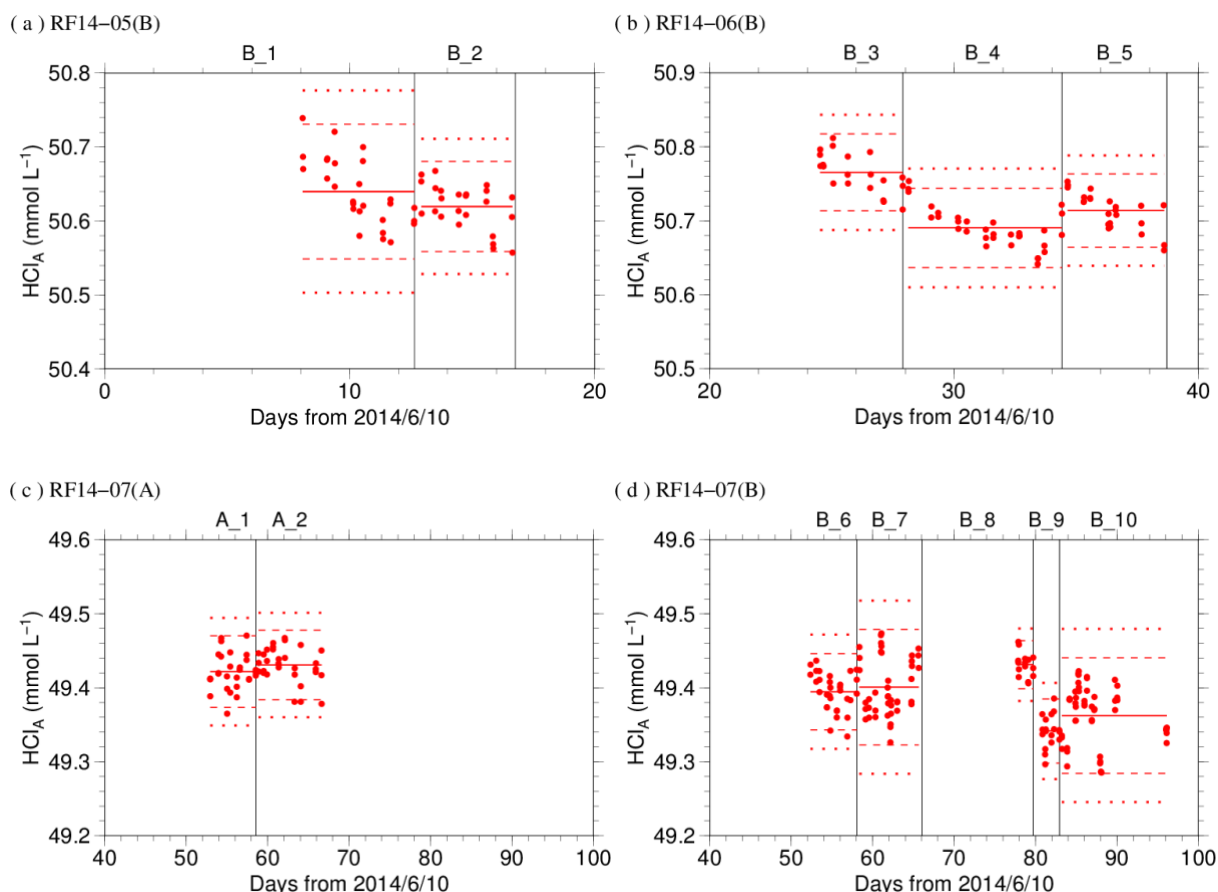


Figure C.7.3. Results of HCl_A measured by apparatus (a) B in RF14-05, (b) B in RF14-06, (c) A in RF14-07 and (d) B in RF14-07. The HCl batch names are indicated at the top of each graph, and vertical lines denote the day when the HCl batch was switched. The red solid, dashed, and dotted lines denote the mean and the mean \pm twice the S.D. and thrice the S.D. for each HCl batches, respectively.

The precisions of HCl_A , defined as the coefficient of variation ($= S.D. / \text{mean}$), were 0.0475–0.0492 % for apparatus A and 0.0330–0.0900 % for apparatus B. They correspond to 1.06–1.10 $\mu\text{mol kg}^{-1}$ and 0.74–2.01 $\mu\text{mol kg}^{-1}$ in A_T of CRM batch 134, respectively.

(7) Quality Control

(7.1) Replicate and duplicate analyses

We took replicate (pair of water samples taken from a single Niskin bottle) and duplicate (pair of water samples taken from different Niskin bottles closed at the same depth) samples of TA throughout the cruise. Table C.7.4 summarizes the results of the measurements with each apparatus. Figures C.7.4–C.7.5 show details of the results. The calculation of the standard deviation from the difference of sets of measurements was based on a procedure (SOP 23) in DOE (1994).

Table C.7.4. Summary of replicate and duplicate measurements. Unit is $\mu\text{mol kg}^{-1}$.

Measurement	Apparatus A	Apparatus B
	Average magnitude of difference \pm S.D.	
Replicate	1.1 ± 0.9 (N=29)	1.0 ± 0.9 (N=116)
Duplicate	0.6 ± 0.5 (N=14)	0.9 ± 0.8 (N=55)

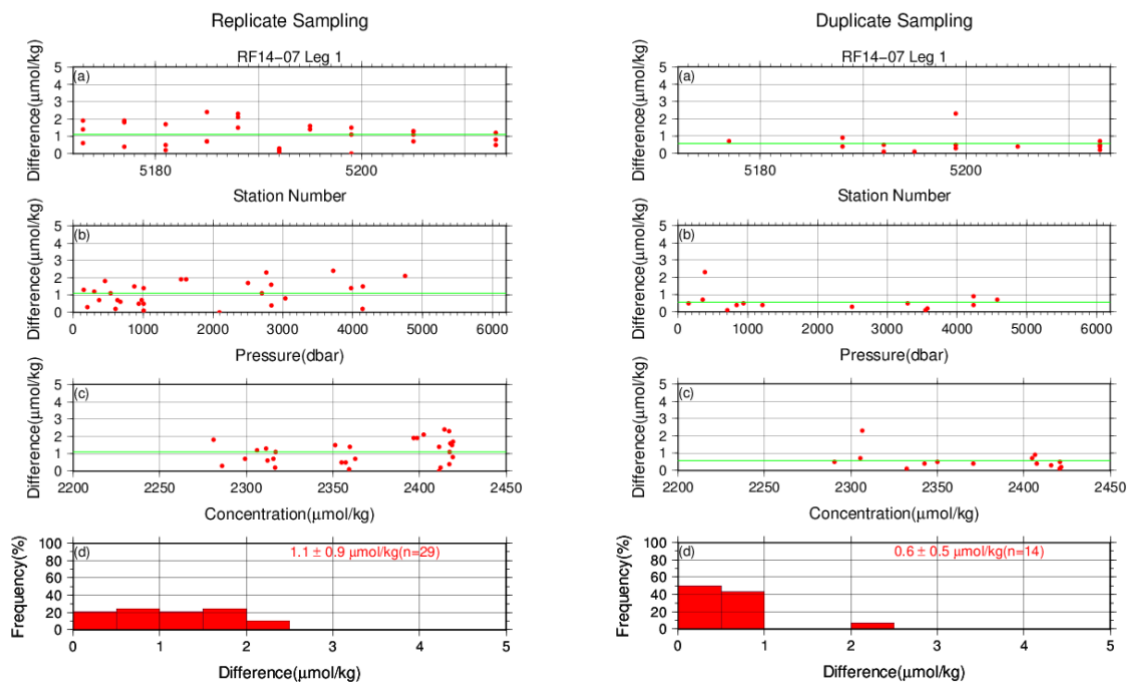


Figure C.7.4. Results of (left) replicate and (right) duplicate measurements during the cruise versus (a) station number, (b) pressure, and (c) A_T determined by apparatus A. The green lines denote the averages of the measurements. The bottom panels (d) show histograms of the measurements.

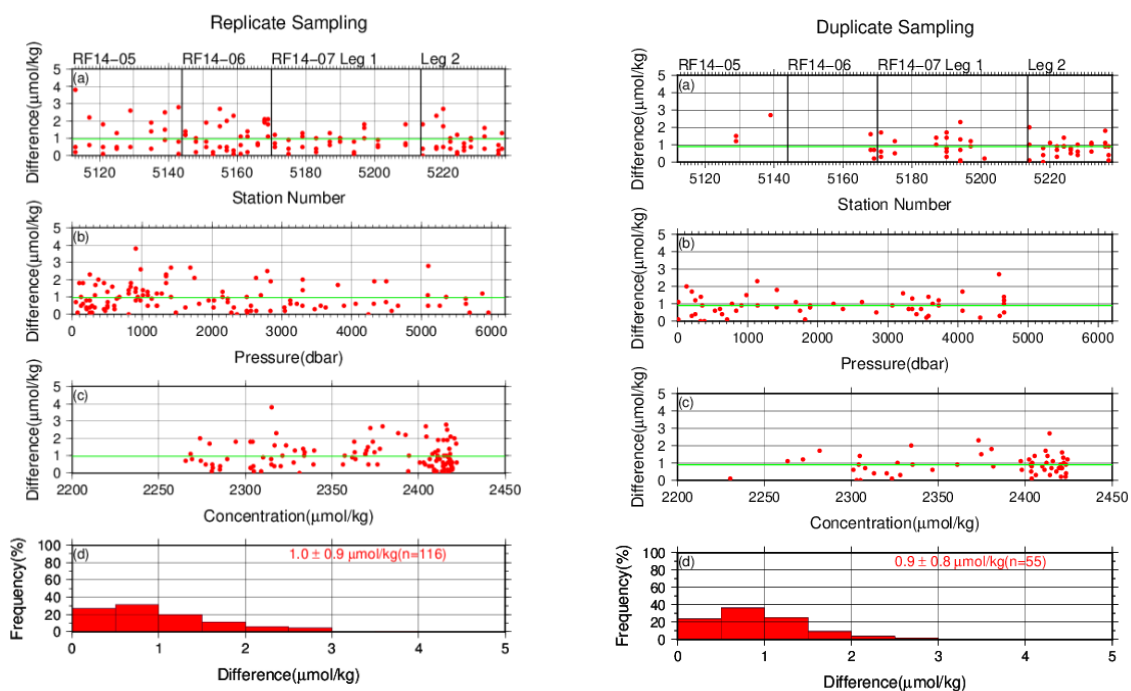


Figure C.7.5. Same as Figure C.7.4, but for apparatus B.

(7.2) Measurements of CRM and working reference materials

The precision of the measurements was monitored by using the CRMs and working reference materials bottled in our laboratory (Appendix A2 in C.6). The measurements of the CRMs and working reference materials were the same those used to measure DIC (see (6.2) in C.6), except that the CRM measurement was repeated 3 times from the same bottle. Table C.7.5 summarizes the differences in the repeated measurements of the CRMs, the mean A_T of the CRM measurements, and the mean A_T of the working reference material measurements. Figures C.7.6–C.7.8 show detailed results.

Table C.7.5. Summary of difference and mean of A_T in the repeated measurements of CRM and the mean A_T of the working reference material. These data are based on good measurements. Unit is $\mu\text{mol kg}^{-1}$.

Cruise	HCl Batch	Average magnitude of difference \pm S.D. (CRM)	Mean Ave. \pm S.D. (CRM)	Mean Ave. \pm S.D. (Working reference material)
RF14-05	B_1	1.5 \pm 1.2 (N=9)	2236.5 \pm 1.9 (N=9)	2269.8 \pm 1.7 (N=6)
	B_2	1.3 \pm 1.0 (N=8)	2236.5 \pm 1.2 (N=8)	2270.0 \pm 0.9 (N=5)
RF14-06	B_3	1.1 \pm 0.9 (N=7)	2231.6 \pm 0.9 (N=7)	2270.9 \pm 1.6 (N=5)
	B_4	0.6 \pm 0.5 (N=12)	2231.6 \pm 1.2 (N=12)	2269.0 \pm 2.4 (N=7)
	B_5	0.7 \pm 0.7 (N=8)	2231.6 \pm 1.0 (N=8)	2271.7 \pm 2.5 (N=6)
RF14-07	A_1	0.8 \pm 0.7 (N=10)	2231.6 \pm 1.0 (N=10)	2272.5 \pm 1.7 (N=8)
	A_2	1.1 \pm 0.9 (N=10)	2231.6 \pm 0.8 (N=10)	2272.1 \pm 1.7 (N=5)
RF14-07	B_6	1.0 \pm 0.8 (N=11)	2231.5 \pm 1.0 (N=11)	2269.7 \pm 1.3 (N=8)
	B_7	0.8 \pm 0.6 (N=14)	2231.6 \pm 1.8 (N=14)	2269.3 \pm 1.9 (N=6)
	B_8	0.9 \pm 0.7 (N=5)	2231.6 \pm 0.5 (N=5)	2269.7 \pm 1.4 (N=3)
	B_9	0.8 \pm 0.6 (N=6)	2231.6 \pm 0.9 (N=6)	2270.7 \pm 0.9 (N=5)
	B_10	0.6 \pm 0.5 (N=17)	2231.6 \pm 1.8 (N=17)	2270.8 \pm 1.5 (N=8)

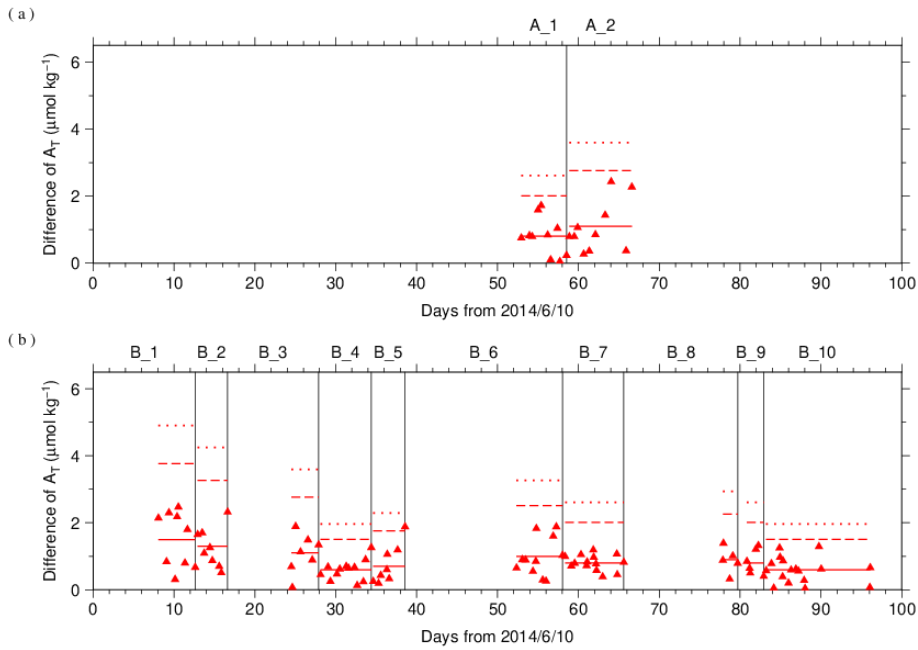


Figure C.7.6. The absolute difference (R) of A_T in repeated measurements of CRM determined by apparatus (a) A and (b) B. The solid line indicates the average of R (\bar{R}). The dashed and dotted lines denote the upper warning limit ($2.512\bar{R}$) and upper control limit ($3.267\bar{R}$), respectively (see Dickson et al., 2007).

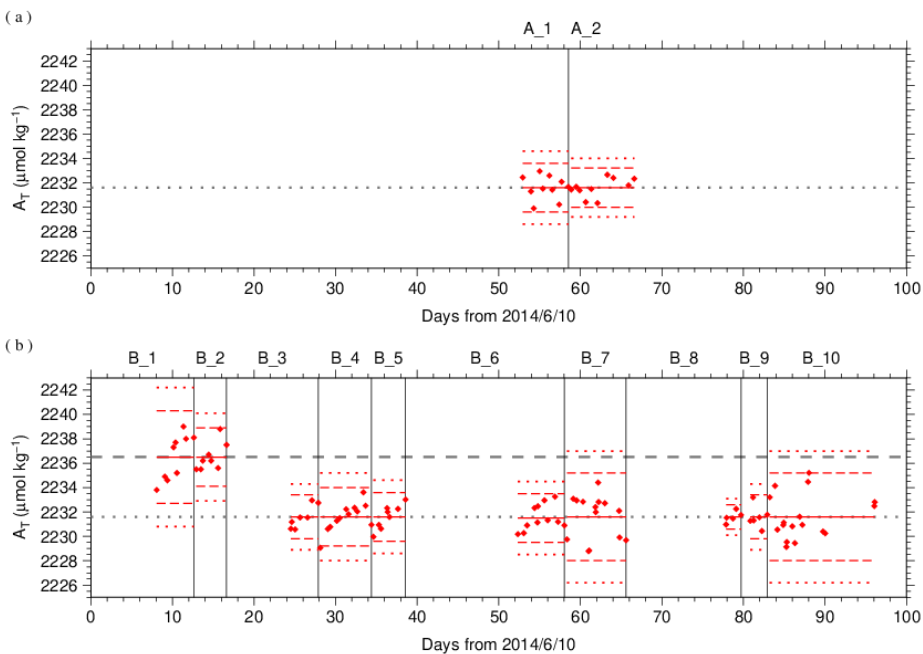


Figure C.7.7. The mean A_T of measurements of CRM. The panels show the results for apparatus (a) A and (b) B. The solid line indicates the mean of the measurements. The dashed and dotted lines denote the upper/lower warning limit ($\text{mean} \pm 2\text{S.D.}$) and the upper/lower control limit ($\text{mean} \pm 3\text{S.D.}$), respectively. The gray dashed and dotted lines denote certified A_T of CRM batch 134 and 137. The labels at the top of the graph and vertical lines have the same meaning as in Figure C.7.3.

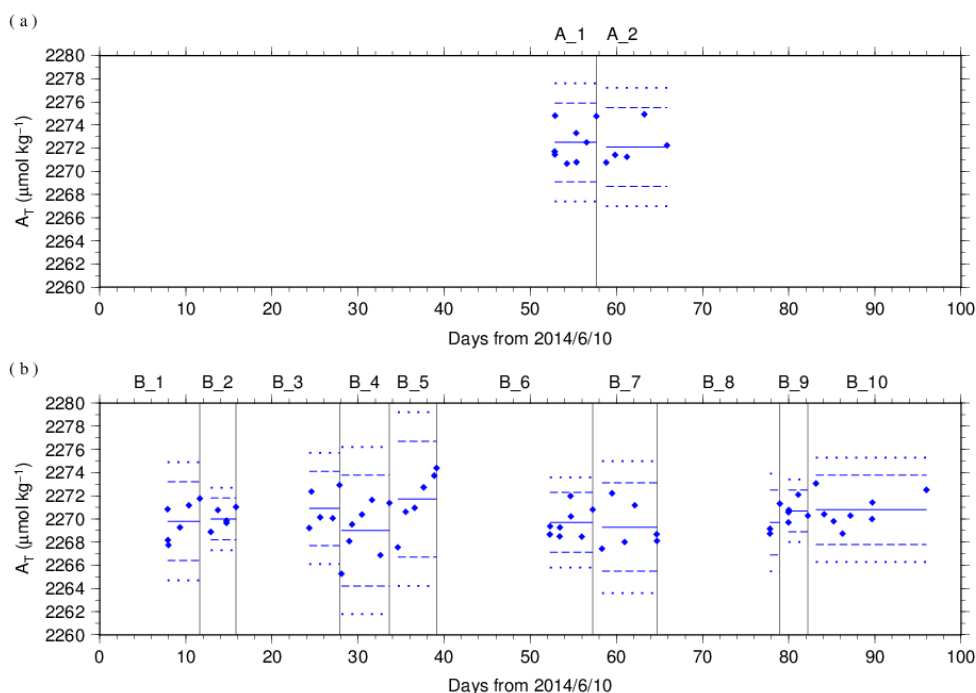


Figure C.7.8. Calculated A_T of working reference material measured by apparatus (a) A and (b) B. The solid, dashed and dotted lines have the same meaning as in Figure C.7.7. The labels at the top of the graph and vertical lines have the same meaning as in Figure C.7.3.

(7.3) Comparisons with other CRM batches

At every few stations, other CRM batches (132 in RF14-05, 129 in RF14-06, 134 in RF14-07) were measured to provide comparisons with batch 134 (in RF14-05) and 137 (in RF14-06 and RF14-07) to confirm the determination of A_T in our measurements. For these CRM measurements, A_T was calculated from HCl_A determined from batch 134 (in RF14-05) and 137 (in RF14-06 and RF14-07) measurements. Figures C.7.9 show the differences between the calculated and certified A_T .

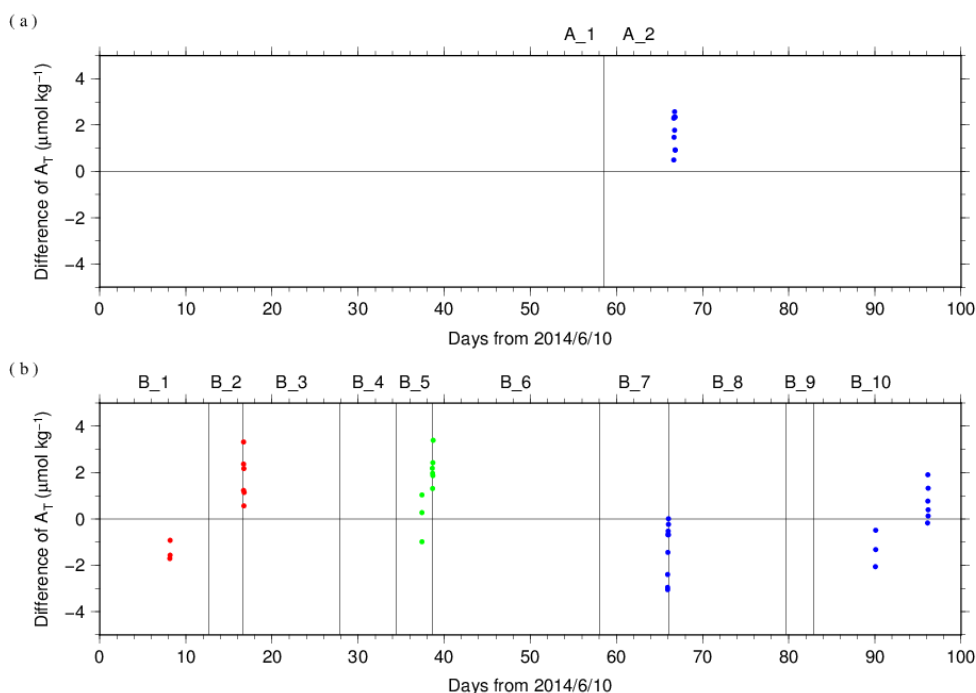


Figure C.7.9. The differences between the calculated A_T from batch 134 (in RF14-05) and 137 (in RF14-06 and RF14-07) measurements and the certified A_T . The panels show the results for apparatus (a) A and (b) B. The labels at the top of the graph and vertical lines have the same meaning as in Figure C.7.3. Colors indicate CRM batches; red: 132, green: 129 and blue: 134.

(7.4) Quality control flag assignment

A quality control flag value was assigned to the TA measurements (Table C.7.6) using the code defined in the IOCCP Report No.14 (Swift, 2010).

Table C.7.6. Summary of assigned quality control flags.

Flag	Definition	Number of samples
2	Good	1540
3	Questionable	7
4	Bad (Faulty)	6
5	Not reported	1
6	Replicate measurements	139
Total number of samples		1693

Appendix

A1. Methods

(A1.1) Measurement

The unit for TA measurements in the coupled DIC/TA analyzer consists of sample treatment unit with a calibrated sample pipette and an open titration cell that are water-jacketed and connected to a thermostated water bath (25 °C), an auto syringe connected to reagent bottle of titrant stored at 25 °C, and a double-beam spectrophotometric system with two CCD image sensor spectrometers combined with a high power Xenon lamp. The mixture of 0.05 N HCl and 40 $\mu\text{mol L}^{-1}$ BCG in 0.65 M NaCl solution was used as reagent to automatically titrate the sample as follows:

- (a) A portion of sample seawater was delivered into the sample pipette (approx. 42 mL) following sample delivery into the DIC unit for a measurement. After the temperature in the pipette was recorded, the sample was transferred into a cylindrical quartz cell.
- (b) An absorption spectrum of sample seawater in the visible light domain was then measured, and the absorbances were recorded at wavelengths of 444 nm, 509 nm, 616 nm, and 730 nm as well as the temperature in the cell.
- (c) The titrant that contains HCl was added to the sample seawater by the auto syringe so that pH of sample seawater altered in the range between 3.85 and 4.05.
- (d) While the acidified sample was being stirred, the evolved CO₂ was purged with the stream of purified N₂ bubbled into the sample at approx. 200 mL min⁻¹ for 5 minutes.
- (e) After the bubbled sample steadied down for 1 minute, the absorbance of BCG in the sample was measured in the same way as described in (b), and pH (in total hydrogen ion scale, pH_T) of the acidified seawater was precisely determined spectrophotometrically.

A2. HCl reagents recipes

0.05 N HCl and 40 $\mu\text{mol L}^{-1}$ BCG in 0.65 M NaCl solution

Dissolve 0.30 g of BCG and 190 g of NaCl in roughly 1.5 L of deionized water (DW) in a 5 L flask, and slowly add 200 mL concentrated HCl. After the powders completely dissolved, dilute with DW to a final volume of 5 L.

References

- Breland II, J. A. and R. H. Byrne (1993), Spectrophotometric procedures for determination of sea water alkalinity using bromocresol green, *Deep-Sea Res. I*, 470, 629–641.
- Dickson, A. G., C. L. Sabine, and J. R. Christian (Eds.) (2007), Guide to best practices for ocean CO₂ measurements. PICES Special Publication 3, 191 pp.
- DOE (1994), Handbook of methods for the analysis of the various parameters of the carbon dioxide system in sea water; version 2. A. G. Dickson and C. Goyet (eds), *ORNL/CDIAC-74*.
- Yao, W. and R. H. Byrne (1998), Simplified seawater alkalinity analysis: Use of linear array spectrometers. *Deep-Sea Res. I*, 45, 1383–1392.

Swift, J. H. (2010): Reference-quality water sample data, Notes on acquisition, record keeping, and evaluation. *IOCCP Report No.14, ICPO Pub. 134, 2010 ver.1.*

8. pH

17 October 2023

(1) Personnel

ONO Etsuro	(RF14-05)
SAITO Shu	(RF14-05, RF14-07)
SAKAMOTO Naoaki	(RF14-05)
ENYO Kazutaka	(RF14-06, RF14-07)
HIRAISHI Naotaka	(RF14-06)
KAWAHARA Kyouichi	(RF14-06)
ONO Hisashi	(RF14-07)

(2) Station occupied

A total of 50 stations (RF14-05: 8, RF14-06: 12, RF14-07 Leg 1: 20, RF14-07 Leg 2: 10) were occupied for pH. Station location and sampling layers of them are shown in Figures C.8.1 and C.8.2, respectively.

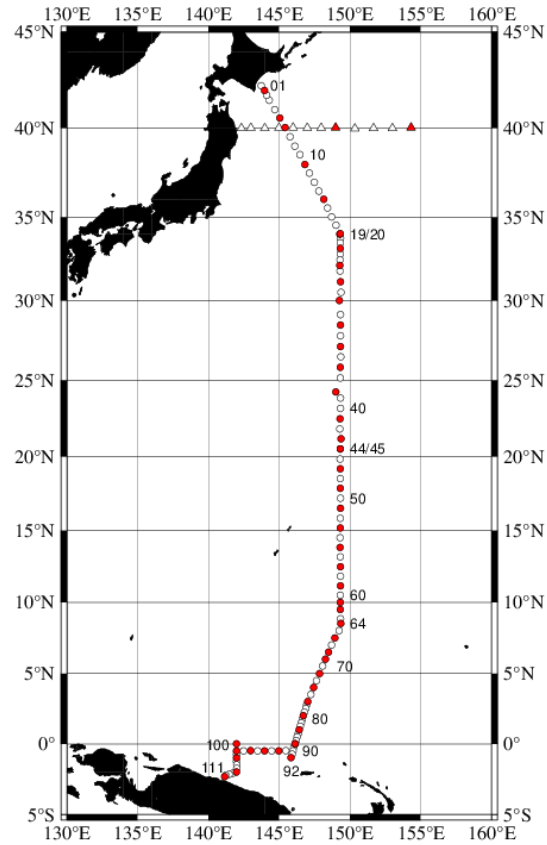


Figure C.8.1. Location of observation stations of pH. Closed and open circles indicate sampling and no-sampling stations, respectively. Triangles show sampling station which are not reported in the bottle data file, but the data at closed triangles are used for quality control of pH. These data are available from the JMA (https://www.data.jma.go.jp/gmd/kaiyou/db/vessel_obs/data-report/html/ship/ship_e.php?year=2014&season=spring).

Bottle Depth Diagram along P10

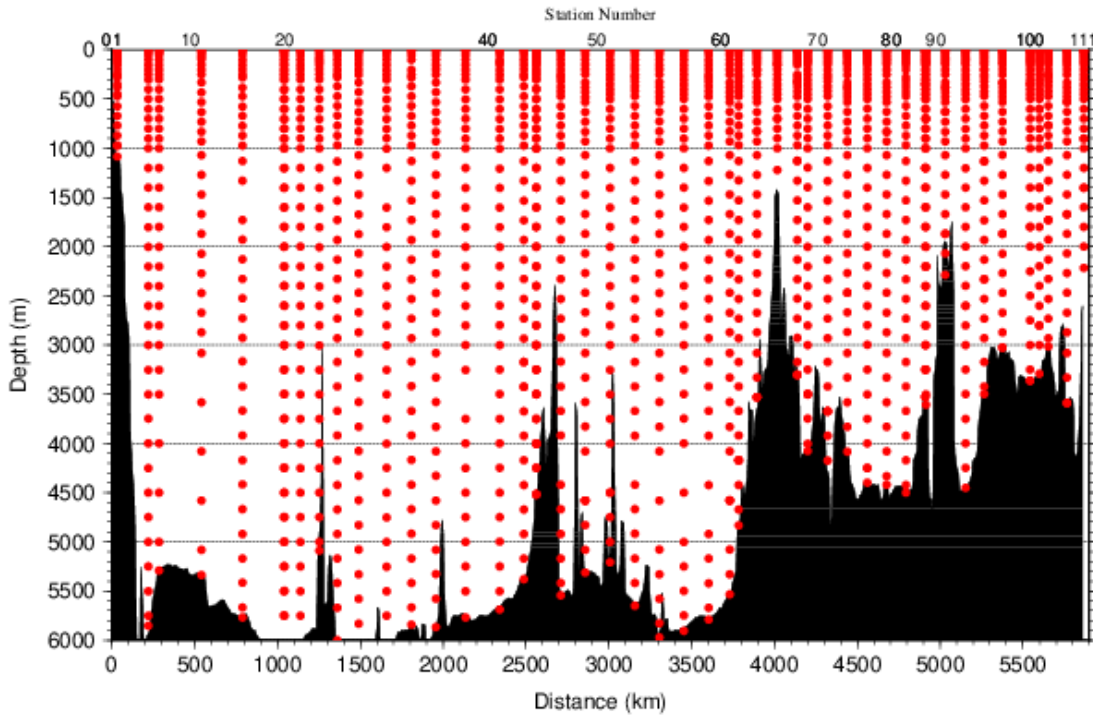


Figure C.8.2. Distance-depth distribution of sampling layers of pH.

(3) Instrument

The measurement of pH was carried out with a pH analyzer (Nihon ANS Co. Ltd, Japan).

(4) Sampling and measurement

Methods of seawater sampling, poisoning, spectrophotometric measurements using the indicator dye *m*-cresol purple (hereafter *m*CP) and calculation of pH_T (on the total hydrogen ion scale; Appendix A1) were based on Saito et al. (2008). The pH_T is calculated from absorbance ratio (R) with the following equations,

$$\text{pH}_T = \text{p}K_2 + \log_{10}\{(R - 0.0069)/(2.222 - 0.1331 \cdot R)\} \quad (\text{C8.1})$$

$$R = (A_{578}^{\text{SD}} - A_{578}^{\text{S}} - A_{730}^{\text{SD}} + A_{730}^{\text{S}})/(A_{434}^{\text{SD}} - A_{434}^{\text{S}} - A_{730}^{\text{SD}} + A_{730}^{\text{S}}) \quad (\text{C8.2})$$

where $\text{p}K_2$ is the acid dissociation constant of *m*CP,

$$\text{p}K_2 = 1245.69/T + 3.8322 + 0.00211 \cdot (35 - S) \quad (\text{C8.3})$$

(293 K \leq T \leq 303 K, 30 \leq S \leq 37).

A_{λ}^{S} and A_{λ}^{SD} in equation (C8.2) are absorbance of seawater itself and dye plus seawater, respectively, at wavelength λ (nm). The value of $\text{p}K_2$ in equation (C8.3) is expressed as a function of temperature T (in Kelvin) and salinity S (in psu). Finally, pH_T is reported as the value at temperature of 25 °C. Details are shown in Appendix A1.

(5) pH perturbation caused by addition of *m*-cresol purple solution

The *m*CP solution using as indicator dye was prepared in our laboratory (Appendix A2) and was subdivided into some bottles (*m*CP batches) that attached to the apparatus. The injection of *m*CP solution perturbs the sample pH_T slightly because the acid-base equilibrium of the seawater is disrupted by the addition of the dye acid-base pair (Dickson et al., 2007).

Before applying *R* to the equation (C8.1), the measured *R* in the sample was corrected to that value expected to be unperturbed by the addition of the dye (Dickson et al., 2007; Clayton and Byrne, 1993). The magnitude of the perturbation (ΔR) was calculated empirically from that by the second addition of the dye and absorbance ratio measurement as follows:

$$\Delta R = R_2 - R_1, \quad (\text{C8.4})$$

where R_1 and R_2 are the absorbance ratio after the initial addition of dye solution in the sample measurement and after the second addition in the experimental measurement, respectively.

Because the value of ΔR depends on the pH_T of sample, we expressed ΔR as a quadratic function of R_1 based on experimental ΔR measurement obtained at this cruise as follows:

$$\Delta R = C_2 \times R_1^2 + C_1 \times R_1 + C_0. \quad (\text{C8.5})$$

In each measurement for a station, ΔR was measured for about 10 samples from various depths to obtain wide range of R_1 and experimental ΔR data. For each *m*CP batch bottle, coefficients (C_0 , C_1 and C_2) were calculated by equation (C8.5), and ΔR was evaluated for each R_1 . The coefficients for each *m*CP batch are showed in Table C.8.1. The plots and function curves are illustrated in Figure C.8.3.

Table C.8.1. Summary of coefficients; C_2 , C_1 and C_0 in $\Delta R = C_2 \times R_1^2 + C_1 \times R_1 + C_0$.

Stations	<i>m</i> CP batch	C_2	C_1	C_0
2-19	1	-1.09651E-03	-9.11295E-03	1.17153E-02
20-44	2	-3.15643E-03	-9.75750E-03	1.39456E-02
45-111	3	-3.72846E-04	-1.46202E-02	1.34940E-02

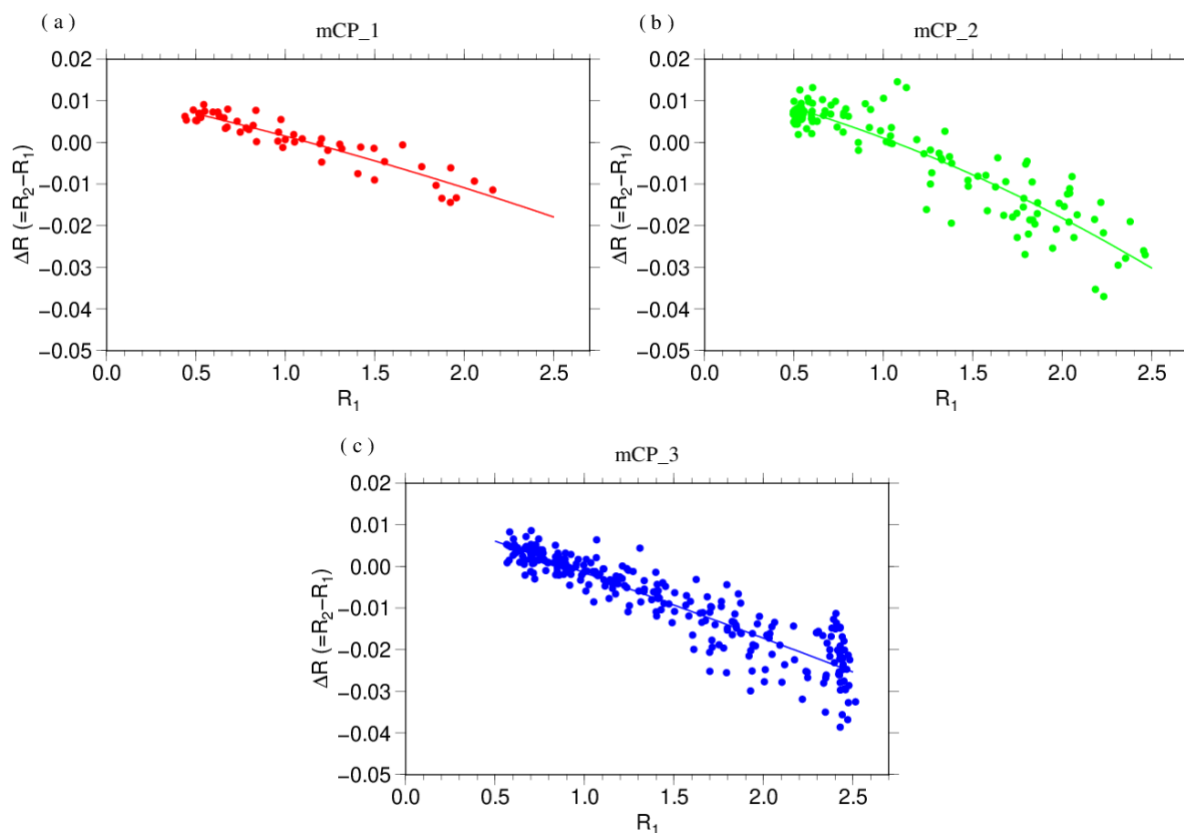


Figure C.8.3. The function curve of the $\Delta R (= R_2 - R_1)$ vs R_1 for (a) first, (b) second and (c) third *mCP* batch of solution shown in Table C.8.1.

(6) Quality Control

(6.1) Replicate and duplicate analyses

We took replicate (pair of water samples taken from a single Niskin bottle) and duplicate (pair of water samples taken from different Niskin bottles closed at the same depth) samples for pH_T determination throughout the cruise. Table C.8.2 summarizes the results of the measurements. Figure C.8.4 shows details of the results. The calculation of the standard deviation from the difference of sets of measurements was based on a procedure (SOP 23) in DOE (1994).

Table C.8.2. Summary of replicate and duplicate measurements of pH_T .

Measurement	Average magnitude of difference \pm S.D.
Replicate	0.0022 \pm 0.0023 (N=143)
Duplicate	0.0025 \pm 0.0027 (N=68)

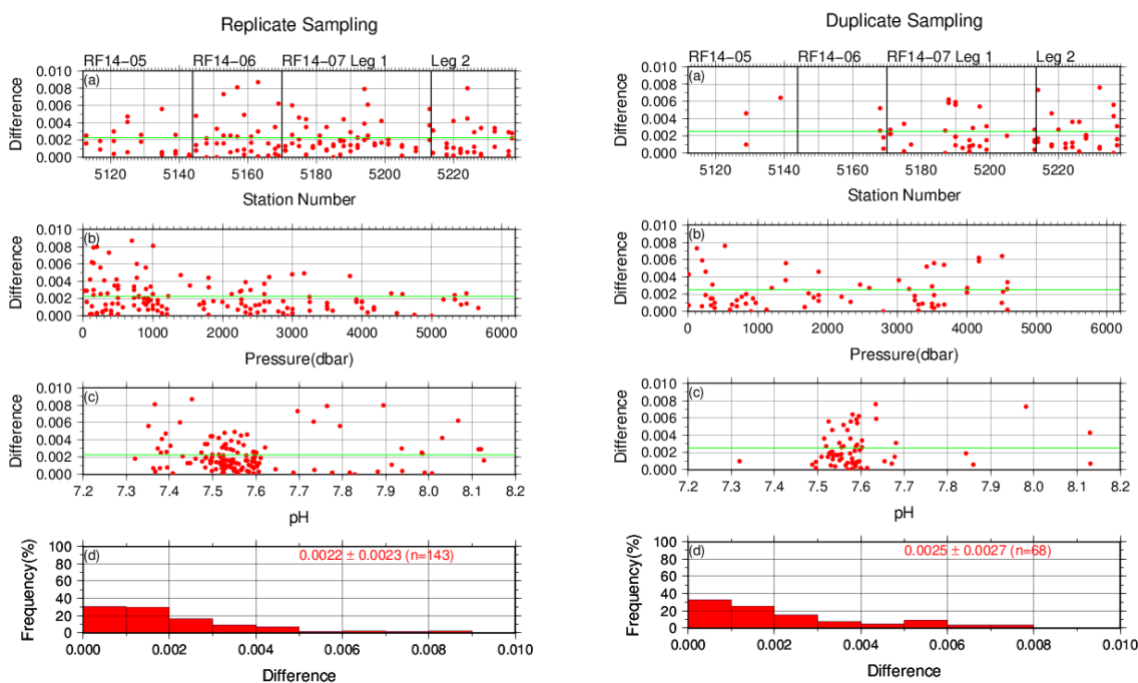


Figure C.8.4. Results of (left) replicate and (right) duplicate measurements during the cruise versus (a) station number, (b) pressure and (c) pH_T . The green lines denote the averages of the measurements. The bottom panels (d) show histograms of the measurements.

(6.2) Measurements of CRM and working reference materials

The precision of the measurements was monitored by using the CRMs and working reference materials bottled in our laboratory (Appendix A2 in C.6). Although the pH_T value of the CRM was not assigned, it could be calculated from certified parameters of DIC and TA (https://www.ncei.noaa.gov/access/ocean-carbon-acidification-data-system/oceans/Dickson_CRM/batches.html) based on the chemical equilibrium of the carbonate system (Lueker et al., 2000). The pH_T of the CRMs (batch 134 and 137) were calculated to be 7.9013 and 7.8820. Working reference material measurements were carried out first at every station. If the results of the measurements were confirmed to be good, measurements on seawater samples were begun. CRM (batch 134 in RF14-05, 137 in RF14-06 and RF14-07) measurements were done at every few (about 3) stations. The measurement for seawater sample and working reference material was made once for a single bottle, and that for CRM was made twice. Table C.8.3 summarizes the means of difference of pH_T between two measurements and pH_T values for a CRM bottle and the means of the pH_T value for a working reference material for each *mCP* batch. Figures C.8.5–C.8.7 show detailed results.

Table C.8.3. Summary of difference and means of the pH_T values for two measurements for a CRM bottle, and mean of pH_T for a working reference material, which was calculated with data with good measurements.

Cruise	<i>mCP</i> Batch	Magnitude of difference Ave. \pm S.D. (CRM)	Mean Ave. \pm S.D. (CRM)	Mean Ave. \pm S.D. (Working reference material)
RF14-05	1	0.0005 \pm 0.0005 (N=4)	7.8969 \pm 0.0014 (N=4)	7.9350 \pm 0.0032 (N=11)
RF14-06	2	0.0013 \pm 0.0011 (N=7)	7.8805 \pm 0.0027 (N=7)	7.9357 \pm 0.0032 (N=16)
RF14-07	3	0.0014 \pm 0.0013 (N=13)	7.8826 \pm 0.0021 (N=13)	7.9365 \pm 0.0029 (N=33)

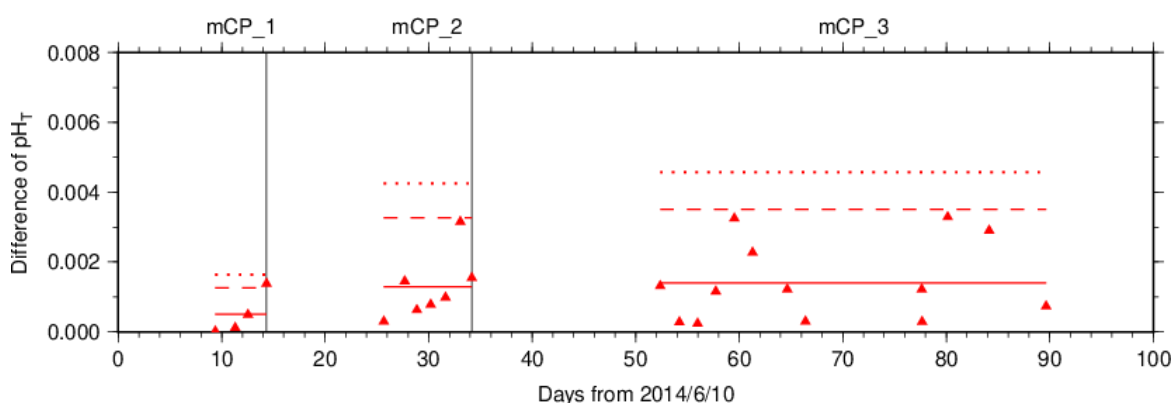


Figure C.8.5. The absolute difference (R) of pH_T between two measurements of a CRM bottle. The *mCP* batch names are shown above the graph, and vertical lines denote the day *mCP* batches were changed. The solid, dashed and dotted lines denote the average range (\bar{R}), upper warning limit ($2.512\bar{R}$) and upper control limit ($3.267\bar{R}$) for each *mCP* batch bottle, respectively (see Dickson et al., 2007).

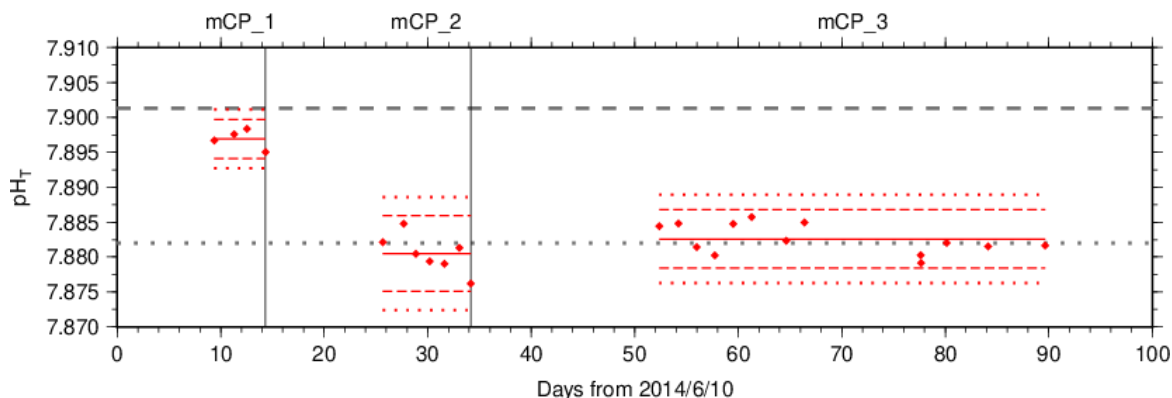


Figure C.8.6. The mean of pH_T values between two measurements of a CRM bottle. The *mCP* batch names are shown above the graph, and vertical lines denote the day when the *mCP* batch was changed. The solid, dashed, and dotted lines denote the mean of measurements, upper/lower warning limit (mean \pm 2S.D.), and upper/lower control limit (mean \pm 3S.D.) for each *mCP* batch bottle, respectively (see Dickson et al., 2007). The gray dashed and dotted lines denote pH_T of CRM batch 134 and 137 calculated from certified parameters.

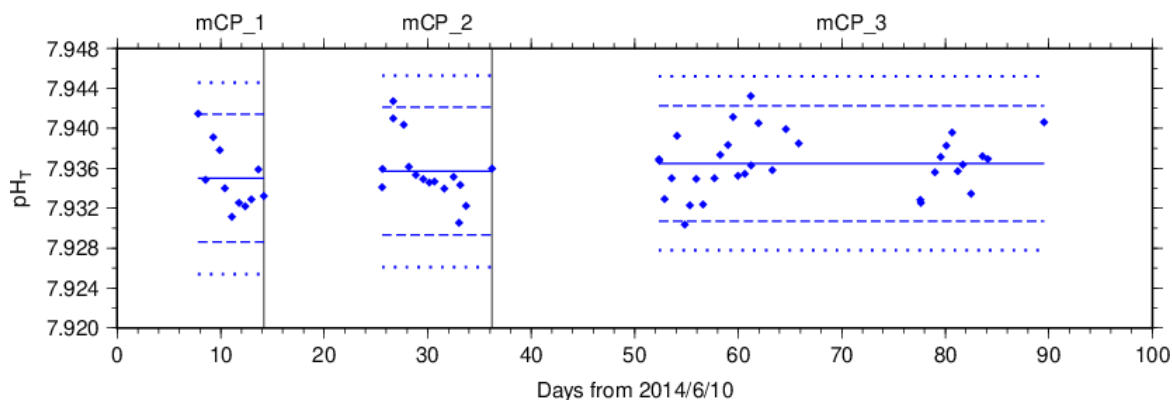


Figure C.8.7. Same as C.8.6, but for working reference material.

(6.3) Quality control flag assignment

A quality control flag value was assigned to the pH measurements (Table C.8.4) using the code defined in the IOCCP Report No.14 (Swift, 2010).

Table C.8.4. Summary of assigned quality control flags.

Flag	Definition	Number of samples
2	Good	1528
3	Questionable	22
4	Bad (Faulty)	6
5	Not reported	0
6	Replicate measurements	137
Total number of samples		1693

(6.4) Comparison at cross-stations during the cruise

There were cross-stations during the cruise located at $34^{\circ}\text{N}/149^{\circ}-20'\text{E}$ (Stn.19 in RF14-05 and Stn.20 in RF14-06), $20^{\circ}-30'\text{N}/149^{\circ}-20'\text{E}$ (Stn.44 in RF14-06 and Stn.45 in RF14-07) and $0^{\circ}\text{N}/146^{\circ}\text{E}$ (Stn.87 and Stn.88 in RF14-07). At these points, hydrocast sampling for pH_{T} was conducted two times at interval of 23 days (Stn.19 and Stn.20), 19 days (Stn.44 and Stn.45) and 12 days (Stn.87 and Stn.88), respectively. These profiles are shown in Figure C.8.8.

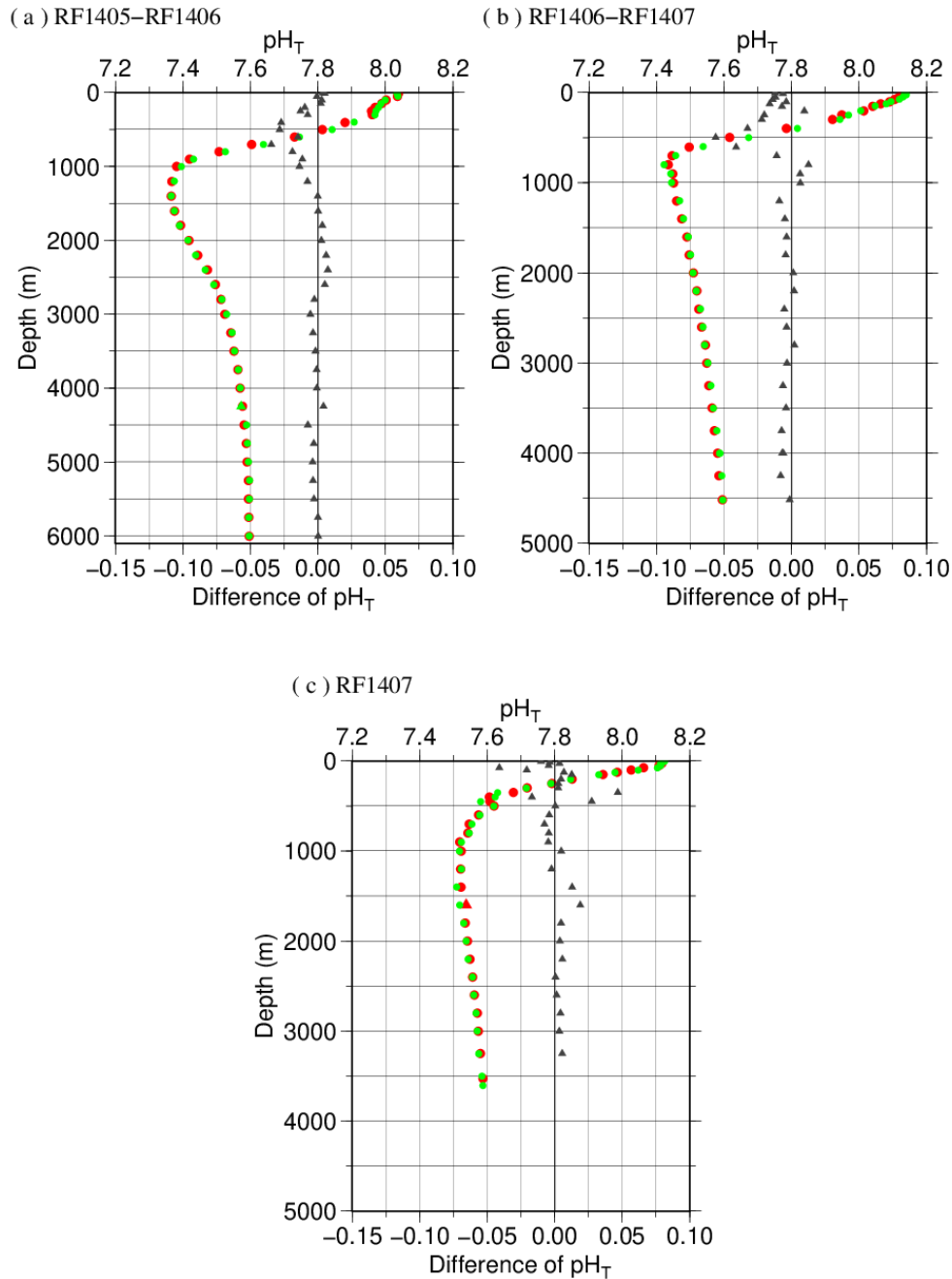


Figure C.8.8. Comparison of pH_{T} observed at same location in different legs of the cruise: (a) $34^{\circ}\text{N}/149^{\circ}-20'\text{E}$ (RF14-05 and RF14-06), (b) $20^{\circ}-30'\text{N}/149^{\circ}-20'\text{E}$ (RF14-06 and RF14-07) and (c) $0^{\circ}\text{N}/146^{\circ}\text{E}$ (RF14-07). The red and green circles denote former (Stns.19, 44 and 87) and latter

(Stns.20, 45 and 88) stations, respectively. Triangles denote the difference in pH_T measured at same depth in different legs.

(6.5) Comparison at cross-stations of WHP cruises

We compared pH_T data of this cruise and other WHP cruises by JMA, Japan Agency for Marine-Earth Science and Technology (JAMSTEC), Scripps Institution of Oceanography (SIO) and Tohoku National Fisheries Research Institute (TNFRI) at cross points. Summary of the comparisons are shown in Figure C.8.9(a) for cross point with WHP-P4 line (around 9°N/149°E), Figure C.8.9(b) for cross point with WHP-P3 line (around 24°N/149°E), Figure C.8.9(c) for cross point with WHP-P2 line (around 30°N/149°E) and Figure C.8.9(d) for cross point with WHP-40N line (around 40°N/145°E). Data of other cruises are downloaded from the CCHDO web site (<https://cchdo.ucsd.edu>).

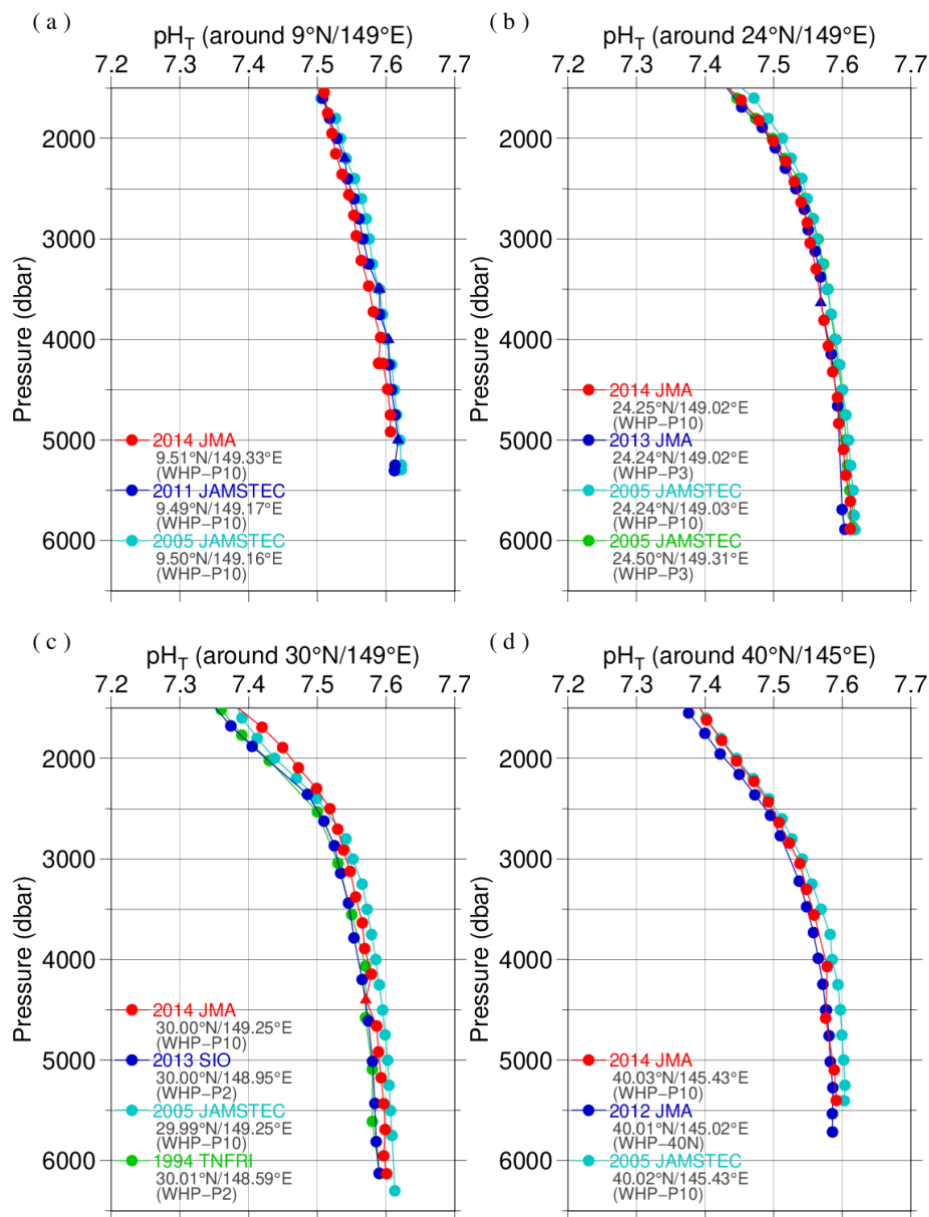


Figure C.8.9. Comparison of pH_T profiles at (a) $9^\circ\text{N}/149^\circ\text{E}$ (cross point with WHP-P4 line), (b) $24^\circ\text{N}/149^\circ\text{E}$ (cross point with WHP-P3 line), (c) $30^\circ\text{N}/149^\circ\text{E}$ (cross point with WHP-P2 line) and (d) $40^\circ\text{N}/145^\circ\text{E}$ (cross point with WHP-40N line). Circles and triangles denote good and questionable values, respectively. The red ones show this cruise.

Appendix

A1. Methods

(A1.1) Seawater sampling

Seawater samples were collected from 10-liters Niskin bottles mounted on CTD-system and a stainless steel bucket for the surface. Samples for pH were transferred to Schott Duran® glass bottles using sample drawing tubes. Bottles were filled smoothly from the bottom after overflowing double a volume while taking care of not entraining any bubbles, and lid temporarily with ground glass stoppers.

After all sampling finished, 2 mL of sample is removed from each bottle to make a headspace to allow thermal expansion. Although the procedure is differed from Standard Operating Procedure (SOP) described in PICES Special Publication 3, SOP-2 (Dickson, 2007), poisoned with 0.2 mL of saturated HgCl₂ solution to prevent change in pH_T caused by biological activity. Finally, samples were sealed with ground glass stoppers lubricated with Apiezon® grease (L).

(A1.2) Measurement

Custom-made pH analyzer (2009 model; Nihon ANS) was prepared and operated in the cruise. The analyzer comprised of a sample dispensing unit, a pre-treatment unit combined with an automated syringe, and two (sample and reference) spectrophotometers combined with a high power xenon light source. Spectrophotometric cell was made of quartz tube that has figure of “U”. This cell was covered with stainless bellows tube to keep the external surface dry and for total light to reflect in the tube. The temperature of the cell was regulated to 25.0 ± 0.1 °C by means of immersing the cell into the thermostat bath, where the both ends of bellows tube located above the water surface of the bath. Spectrophotometer, cell and light source were connected with optical fiber.

The analysis procedure was as follows:

- a) Seawater was ejected from a sample loop.
- b) A portion of sample was introduced into a sample loop including spectrophotometric cell. The spectrophotometric cell was flushed two times with sample in order to remove air bubbles.
- c) An absorption spectrum of seawater in the visible light range was measured. Absorbance at wavelengths of 434 nm, 488 nm, 578 nm and 730 nm as well as cell temperature were recorded. To eject air bubbles from the cell, the sample was moved four times and the absorbance was recorded at each stop.
- d) 10 µl of indicator *mCP* was injected to the loop.
- e) Circulating 2 minutes 40 seconds through the loop tube, seawater sample and indicator dye was mixed together.
- f) Absorbance of *mCP* plus seawater was measured in the same way described above (c).

(A1.3) Calculation

In order to state clearly the scale of pH, we mention “pH_T” that is defined by equation (C8.A1.3.1),

$$\text{pH}_T = -\log_{10}([\text{H}^+]_T/C^0) \quad (\text{C8.A1.3.1})$$

where $[\text{H}^+]_T$ denotes the concentration of hydrogen ion expressed in the total hydrogen ion scale. $[\text{H}^+]_T = [\text{H}^+]_F(1 + [\text{SO}_4]_T/K_{\text{HSO}_4^-})$, where $[\text{H}^+]_F$ is the concentration of free hydrogen ion, $[\text{SO}_4]_T$ is the total concentration of sulphate ion and $K_{\text{HSO}_4^-}$ is acid dissociation constant of hydrogen sulphate ion (Dickson, 1990). C^0 is the standard value of concentration (1 mole per kilogram of seawater, mol kg⁻¹). The pH_T was reported as the value at temperature of 25 °C in “total hydrogen ion scale”.

pH_T was calculated from the measured absorbance (A) based on the following equations (C8.A1.3.2) and (C8.A1.3.3), which are the same as (C8.1) and (C8.2), respectively.

$$\begin{aligned} \text{pH}_T &= \text{p}K_2 + \log_{10}([\text{I}^{2-}]/[\text{HI}^-]) \\ &= \text{p}K_2 + \log_{10}\{(R - 0.0069)/(2.222 - 0.1331 \cdot R)\} \end{aligned} \quad (\text{C8.A1.3.2})$$

$$R = (A_{578}^{\text{SD}} - A_{578}^{\text{S}} - A_{730}^{\text{SD}} + A_{730}^{\text{S}})/(A_{434}^{\text{SD}} - A_{434}^{\text{S}} - A_{730}^{\text{SD}} + A_{730}^{\text{S}}) \quad (\text{C8.A1.3.3})$$

where $\text{p}K_2$ is the acid dissociation constant of $m\text{CP}$. $[\text{I}^{2-}]/[\text{HI}^-]$ is the ratio of $m\text{CP}$ base form (I^{2-}) concentration over acid form (HI^-) concentration which is calculated from the corrected absorbance ratio (R) shown in the section 8(5) and the ratios of extinction coefficients (Clayton and Byrne, 1993). A_{λ}^{S} and A_{λ}^{SD} in equation (C8.A1.3.3) are absorbance of seawater itself and dye plus seawater, respectively, at wavelength λ (nm). The value of $\text{p}K_2$ ($= -\log_{10}(K_2/k^0)$, $k^0 = 1$ mol kg⁻¹) had also been expressed as a function of temperature T (in Kelvin) and salinity S (in psu) by Clayton and Byrne (1993), but the calculated value has been subsequently corrected by 0.0047 on the basis of a reported pH_T value accounting for “tris” buffer (DeValls and Dickson, 1998):

$$\begin{aligned} \text{p}K_2 &= \text{p}K_2(\text{Clayton \& Byrne, 1993}) + 0.0047 \\ &= 1245.69/T + 3.8322 + 0.00211 \cdot (35 - S). \end{aligned} \quad (\text{C8.A1.3.4})$$

(293 K ≤ T ≤ 303 K, 30 ≤ S ≤ 37)

Finally, pH_T determined at a temperature t (pH_T(t), with t in °C) was corrected to the pH_T at 25.00 °C (pH_T(25)) with the following equation (Saito et al., 2008).

$$\begin{aligned} &(\text{pH}_T(t) - \text{pH}_T(25))/(t - 25.00) \\ &= (2.00170 - 0.735594 \cdot \text{pH}_T(25) + 0.0896112 \cdot \text{pH}_T(25)^2 - 0.00364656 \cdot \text{pH}_T(25)^3). \end{aligned} \quad (\text{C8.A1.3.5})$$

A2. pH indicator

Indicator m -cresol purple ($m\text{CP}$) solution

Add 0.67 g $m\text{CP}$ to 500 mL deionized water (DW) in a borosilicate glass flask. Pour DW slowly into flask to weight of 1 kg ($m\text{CP} + \text{DW}$), and mix well to dissolve $m\text{CP}$. Regulate the pH (free hydrogen ion scale) of indicator solution to 7.9±0.1 by small amount of diluted NaOH solution (approx. 0.25 mol L⁻¹) if the pH was out of the range. The pH of indicator solution was monitored using glass electrode pH meter. The reagent had not been refining.

References

- Clayton T.D. and R.H. Byrne 1993. Spectrophotometric seawater pH measurements: total hydrogen ion concentration scale calibration of m-cresol purple and at-sea results. *Deep-Sea Res. I*, **40**, 2115–2129.
- DelValls, T. A and A. G. Dickson, 1998. The pH of buffers based on 2-amino-2-hydroxymethyl-1,3-propanediol ('tris') in synthetic sea water. *Deep-Sea Res. I*, **45**, 1541-1554.
- Dickson, A.G. 1990. Standard potential of the reaction: $\text{AgCl(s)} + 1/2 \text{H}_2(\text{g}) = \text{Ag(s)} + \text{HCl(aq)}$, and the standard acidity constant of the ion HSO_4^- in synthetic sea water from 273.15 to 318.15 K. *J. Chem. Thermodynamics*, **22**, 113–127.
- Dickson, A.G., Sabine, C.L. and Christian, J.R. (Eds.) 2007. Guide to best practices for ocean CO_2 measurements. *PICES Special Publication 3*, 191 pp.
- Lueker, T.J, A.G. Dickson and C.D. Keeling, 2000. Ocean $p\text{CO}_2$ calculated from dissolved inorganic carbon, alkalinity, and equations for K_1 and K_2 : validation based on laboratory measurements of CO_2 in gas and seawater at equilibrium. *Marine Chem.*, **70**, 105-119.
- Saito, S., M. Ishii, T. Midorikawa and H.Y. Inoue 2008. Precise Spectrophotometric Measurement of Seawater pH_T with an Automated Apparatus using a Flow Cell in a Closed Circuit. *Technical Reports of Meteorological Research Institute*, **57**, 1–28.
- Swift, J. H. (2010): Reference-quality water sample data, Notes on acquisition, record keeping, and evaluation. *IOCCP Report No.14, ICPO Pub. 134, 2010 ver.1*